

Development of User-Friendly Tablet Sensors for Detection of Copper and Nitrite

Maryam Mansouri

A Thesis

In the Department of
Chemical and Materials Engineering

Presented in partial fulfillment
of the requirements for the degree
Master of Applied Science (Chemical Engineering) at
Concordia University
Montreal, Quebec, Canada

April 2025

© Maryam Mansouri, 2025

CONCORDIA UNIVERSITY

School of Graduate Studies

This is to certify that the thesis is prepared,

By: **Maryam Mansouri**

Entitled: **Development of User-Friendly Tablet Sensors for Detection of Copper and Nitrite**

And submitted in partial fulfillment of the requirements for the degree of

Master of Applied Science in (Chemical Engineering)

Complies with the regulations of the University and meets the accepted standards concerning originality and quality.

Signed by the Final Examination Committee:

_____ Chair

Dr. Patricia Comeau

_____ Examiner 1

Dr. Patricia Comeau

_____ Supervisor

Dr. Sana Jahanshashi Anbuhi

Approved by: _____

Dr. Zhibin Ye

Graduate Program Director

Date: 2025 _____ Dean of Faculty

Dean Mourad Debbabi

Abstract

Development of User-Friendly Tablet Sensors for Detection of Copper and Nitrite

Maryam Mansouri

The development of portable, easy-to-use, and reliable analytical tools is essential for environmental monitoring of contaminants, particularly in settings with limited access to laboratory infrastructure. In diagnostics area, recent advancements in tablet-based sensing technologies have shown the promise for enabling simple, rapid and user-friendly detection with minimal preparation. Motivated by the need to support and improve public health, this thesis is dedicated to the development of tablet-based sensors that enable rapid, user-friendly, and affordable detection of environmental contaminants. In this context, this research focuses on the development of innovative tablet-based sensors for on-site detection of (1) **copper in water** and (2) **nitrite in soil**, which provide precise reagent dosages, enhanced portability, and reliable performance in resources with limited facilities.

In the case of copper detection, the sensor utilizes an auto-mixing tablet that simplifies the process by incorporating all necessary reagents into a single solid form. This ensures precise dosing, offering a simple, quick, and user-friendly alternative in compare with traditional methods such as including inductively coupled plasma detector, atomic absorption spectroscopy, surface plasmon resonance detector and X-ray fluorescence spectrometry. Copper detection is vital as excessive copper levels in drinking water and natural water bodies can pose serious health risks, including gastrointestinal distress, liver or kidney damage, and neurodegenerative diseases, also contribute to environmental pollution. The tablet initiates a colourimetric reaction with 2,2'-biquinoline-4,4'-dicarboxylic acid (bichinonic acid) within two minutes, producing a measurable color change indicative of copper concentration. Unlike conventional tablets that require manual mixing, the effervescence and auto-mixing feature enhances reagent dissolution and improves usability. The sensor demonstrated working range of 0 to 2.5 ppm, with a detection limit of 0.3 ppm, which are adequate for monitoring copper contamination considering that The World Health Organization (WHO) has set the permissible limit for copper ions (Cu^{2+}) in drinking water at 2.0 mg/L (2 ppm). However, Cu^{2+} concentrations in some local water sources exceed this threshold. Therefore, there is an urgent need to develop highly sensitive and selective methods for Cu^{2+} detection.

Interference tests confirmed the sensor's selectivity for copper. The sensor's selectivity complements its sensitivity, providing reliable detection of copper at low concentrations with minimal influence from other potential contaminants. While analyses of real water samples validated its accuracy and practical applicability. Stability assessments over three months of room temperature showed consistent performance, highlighting the sensor's long-term usability. The tablet format provides a portable, pre-measured detection system that eliminates the need for laboratory preparation, making it an effective solution for real-time copper monitoring, particularly in regions with restricted access to analytical tools.

In the case of nitrite detection, this study presents two tablet-based sensors: (1) a Dual Reagent Tablet, which contains separate sulfanilamide (SUL) and N-(1-naphthyl)ethylenediamine (NED) reagents in two distinct tablets; and (2) an All-in-One Integrated Reagent Tablet, which combines all necessary reagents into a single tablet, simplifying the detection procedure. Nitrite contamination harms ecosystems by reducing oxygen levels, disrupting biodiversity, and producing toxic compounds such as nitrosamines, while posing human health risks such as methemoglobinemia, neurological disorders, and increased cancer risk. Therefore, effective soil monitoring is crucial for pollution control and sustainable agriculture. Both utilize a pullulan matrix to encapsulate reagents in solid form, enhancing stability and practicality. Each sensor enables rapid soil nitrite measurements within 2 minutes through a colourimetric reaction, producing a pink/purple azo dye as an indicator. Furthermore, unlike traditional methods requiring manual pH adjustment, these tablet sensors incorporate a buffering system to maintain optimal acidic conditions for the reaction, ensuring reliable performance across diverse sample environments without external acidification. The tablets also ensure consistent reagent dosages, removing the need for laboratory preparation and providing a portable, pre-measured platform for on-site nitrite detection in complex soil matrices. The Dual Reagent Tablet demonstrated a detection limit of 3 μM , while the All-in-One Tablet achieved a detection limit of 5 μM , both with a working range up to 400 μM . Interference experiments confirmed selectivity for nitrite, and analyses of real soil samples validated the method's accuracy and applicability. Stability assessments over six weeks at room temperature showed consistent performance, demonstrating the long-term usability of these sensors.

Acknowledgments

First and foremost, I would like to express my gratitude to my supervisor, Dr. Sana Jahanshahi-Anbuhi, for her unwavering guidance, continuous support, and for fostering a warm and inspiring research environment. I am genuinely appreciative of the opportunity to be part of such a collaborative and motivating team. Working in this lab not only expanded my knowledge but also taught me many valuable lessons in life.

I am truly thankful to my wonderful colleagues, Hamid Safiabadi-Tali, for his consistent support and encouragement, and Zubi Sadiq, who consistently extended a helping hand when needed. Working alongside such colleagues has been a privilege and a source of inspiration.

I wish to thank my partner, Yannis, for believing in me and supporting me throughout this journey, even during the most challenging times. I also want to express my deepest appreciation to my parents, Arezou and Mahmoud, for their endless love and support, and to my sister, Agrin, and my brother, Sam, who have always been there for me whenever I needed them. I miss them deeply and could not have reached this point without their constant support, encouragement, and unconditional love.

I would like to thank Dr. Rafik Naccache and his student, Gianluca Fuoco, for their valuable help and collaboration on a part of my project. Also, special thanks to Mr. Arash (Ahmad) Dehdast for his sincere encouragement, valuable knowledge and for believing in my potential. I also wish to thank Harriet Laryea and Kerri Warbanski for their invaluable help and time.

I would also like to thank my friends, Mahshad, Shahrzad, and Ali for their constant presence, understanding, and encouragement, as well as all the others of my friends who helped me along the way.

And finally, heartfelt thanks to all my little students, who brought me energy, joy, and inspiration.

Table of contents

Abstract	iii
Acknowledgments	v
Table of contents	vi
List of figures	ix
List of tables	xv
Abbreviations	xvi
Chapter 1: Introduction and objective	1
1.1 Background.....	1
1.2 Thesis objectives.....	3
1.3 Thesis organization.....	5
1.4 List of publications and conference contributions	6
Chapter 2: Literature review	8
2.1. Introduction	8
2.1.1 Copper.....	9
2.1.2 Nitrite	9
2.2 Copper detection techniques.....	11
2.2.1 Electrochemical sensor	11
2.2.2 Fluorescence sensor	12
2.2.3 Colourimetric sensor.....	13
2.3 Nitrite detection techniques	15
2.3.1 Catalytic-spectrophotometric	15
2.3.2 Chromatographic.....	16
2.3.3 Griess assay-based (colourimetric)	17
2.3.4 Capillary electrophoresis.....	19
2.3.5 Electrochemical.....	19
2.3.6 Fluorescence	20
2.4 Development of tablet-based sensors	21
2.4.1 Polysaccharide encapsulation process	22
2.4.2 Compression method	23
2.4.2.1 Auto-mixing tablets.....	24

Chapter 3: Copper detection.....	26
3.1 Introduction	27
3.2 Chemicals and materials	30
3.3 Auto-mixing tablet fabrication	30
3.4 Detection Procedure	31
3.5 Result and Discussion.....	31
3.5.1 Characterization	32
3.5.2 Detection of copper with tablets	36
3.5.3 Analytical performance.....	37
3.5.4 Real water sample	37
3.5.5 Selectivity analysis for copper detection with eff-tablets	39
3.5.6 Stability tests: over period of time	40
3.7 Conclusion	42
Chapter 4: Nitrite detection	43
4.1 Introduction	44
4.2 Chemical and material	46
4.3 Tablet fabrication.....	46
4.6 Detection of nitrite by tablets	47
4.5 Real samples	48
4.6 Results and discussion	49
4.7.1 Analytical performance.....	51
4.7.2 Real samples	53
4.7.3 Selectivity tests	54
4.7.4 Stability tests: over period of time	55
4.7 Conclusion	57
Chapter 5: Conclusions and future direction	58
Future direction	60
References	61
Appendices	88
APPENDIX A. Supplementary information for Chapter 3	88
APPENDIX B. Supplementary information for Chapter 4	88
APPENDIX C. Development of portable fluorescent sensors for heavy metal detection in water	92

C.1 Introduction to carbon dots	92
C.2 Detection heavy metals by CDs	93
C.3 Synthesis of graphene quantum dots	94
C.4 Synthesis of pentaethylenhexamine (PH6-CDs)	95
C.5 Heavy metal quenching assays.....	96
C.6 Fluorescence portable platforms; QDs paper-based plate and QDs tablet-based	99

List of figures

Figure 1.	A. It shows how neurons regulate copper and its link to Alzheimer's. Copper enters through Ctr1, is transported to enzymes, and released by ATP7A in synapses, increasing A β production. Excess copper and A β form toxic complexes, generating H ₂ O ₂ , causing oxidative stress and amyloid plaque formation, contributing to Alzheimer's (adapted from [29]). B. The nitrogen cycle in soil. This involves nitrification, denitrification, and nitrogen fixation, with bacteria regulating nitrogen transformations. Nitrification inhibitors (NIs) reduce nitrogen loss, lower greenhouse gas emissions, and improve soil fertility, supporting plant growth (adapted from [65])	11
Figure 2.	A. Basic concepts of electrochemical sensors (adapted from [75]). B. Scheme of the designed gold nanoelectrodes and GHK-ligand, along with the proposed mechanism for in vitro/in vivo detection of Cu ²⁺ (adapted from [79])	12
Figure 3.	A. Mechanism of colourimetric detection of Cu ²⁺ with silver/dopamine nanoparticles (adapted from [90]). B. Images and absorbance measurements of Ag/AuNPs after adding Cu ²⁺ (adapted from [93]).....	15
Figure 4.	Classification and characteristics of nitrite detection methods. Reproduced from Zhang et al., <i>Applied Sciences</i> 2024, 14(19), 9027, under the terms of the Creative Commons CC BY 4.0 license [38].....	15
Figure 5.	Interaction between DAN and nitrite for NAT production (adapted from [106])	17
Figure 6.	A. Schematic representation of the basic principle of Griess assay (adapted from [98]). B. Schematic illustration of mechanism of colourimetric and fluorescent dual-readout sensor for the detection of nitrite (adapted from [116]).....	19
Figure 7.	A. The graphical diagram for preparation of Cu/Ag/MWNTs modified electrode, adapted from [134]) . B. Strategies for fluorescent probes for NO ₂ (adapted from [135]).....	21
Figure 8.	A. All-inclusive pullulan tablets production for ATP detection (adapted from [150]). B. It shows the process of creating compressed tablets (adapted from [154])	24
Figure 9.	Graphical abstract illustrating a on-site detection of copper in water using auto-mixing tablet sensor	27
Figure 10.	A colourimetric reaction of 2,2'-biquinoline-4,4'-dicarboxylic acid (bicinchoninic acid) with Cu ⁺	30
Figure 11.	A. Fabrication tablet-based sensor for copper detection. Initially, all powders were measured and mixed in a weighting paper. Then, the mixture was transferred into tablet mold and pressed at force of 2 tf (19613.3 N) for 30 seconds, resulting in solid tablets. B. The detection procedure of copper in water samples. First, 5 ml of the water sample were collected, and a single eff-	

tablet is added to a glass vial. After 1.5-2 minutes of incubation, if the water sample contains copper, the purple-colored complex of bicinchoninic acid and Cu^{1+} is created. Then, the reaction between citric acid and bicarbonate will accelerate solution rate mixing. 32

Figure 12. **A.** Tablet performance and dissolution behavior **A.** Image showing a powder-based kit during activation, where powder disperses due to electrostatic forces, leading to material loss despite careful handling. **B.** Comparison of the remained amount (%) between tablets and powder packs across three individual samples of tablets and powder packs. Tablets retained nearly their full initial mass with a mean of 99.36% (SD = 0.52%), while powder packs exhibited significant mass loss due to dispersion, with a lower mean of 59.68% (SD = 18.13%). The difference in retention between the two forms was statistically significant (unpaired t-test, $P \leq 0.05$) **C.** The performance of the auto-mixing tablets was compared with that of the traditional tablets in detecting copper (2 ppm). The auto-mixing tablet gave a uniform solution after 2 minutes, while the traditional tablet was not completely mixed even after 15 minutes. **D.** Comparison of premeasured unit dose reagents stored in different solid forms (auto-mixing tablets, traditional tablets and powder pillow, and liquid solution) ready to use in detection assays: Performance across key aspects. 34

Figure 13. The stability of the weight of the tablets. Weight stability of tablets (n=6) over 30 days, with RSD less than 2%, indicating robust structural integrity. One-way ANOVA showed no statistically significant difference in weights over time ($p > 0.09$), supporting the structural stability and consistent formulation of the tablets. 35

Figure 14. CO_2 content expressed as a percentage of total tablet weight over a 30-day storage period (n = 3). RSD remained below 0.1%, across all time points, demonstrating excellent consistency. One-way ANOVA confirmed no statistically significant difference in CO_2 content over time ($p > 0.9$), indicating chemical stability of the effervescent components throughout storage. Error bars are not visible in the plot as they are hidden by the size of the data markers due to minimal variation. 36

Figure 15. **A.** Analytical performance of the assay. The relationship between copper concentration and color intensity in the tablet colourimetric detection system, creates the calibration curve. The curve demonstrates a high degree of fit, with an R^2 value of 0.9953, with a linear range of 0.3-2 ppm. The LoD is marked at 0.3 ppm, and the working range of 0.3-3 ppm. **B.** Comparison between the results of auto-mixing tablets and standard method for the different spiked amounts of copper in real water samples (n=3). The results obtained with our auto-mixing tablets were consistent with the total copper content determined using the standard method with RSD% less than 6.9, confirming the tablets' effectiveness in accurately detecting copper concentrations in real-world. 38

Figure 16. Potential Interference of copper was tested among common water ions Mg^{2+} , Ca^{2+} , Zn^{2+} , Co^{2+} , Fe^{3+} at 50 mg/l concentrations. While the working solution remained colorless for all other ions, a copper sample of 1.5 ppm was able to turn the solution purple, indicating the sensor's specificity for copper detection. One-way ANOVA, $p < 0.0001$, confirmed a statistically significant difference in color intensity among ions.	39
Figure 17. Stability of the auto-mixing tablets over an 8-week storage period ($n = 3$). The average color intensity at week 8 retained 96.29 ± 2.14 % of the original color intensity at week 1. RSD remained below 3%, confirming high reproducibility and consistent detection performance during storage	41
Figure 18. Graphical abstract illustrating a tablet-based sensor for user-friendly detection of nitrite in soil samples through a colourimetric reaction using SUL and NED reagents.	43
Figure 19. The actual images of the tablet systems used for nitrite detection: Dual-Tablet, and All-in-One Tablet. These tablets contain 5% w/v pullulan, giving uniform circular shape and a firm, easy-to-handle physical structure	47
Figure 20. The schematic represents the Griess assay used for nitrite detection, which involves a two-step reaction. First, sulfanilamide reacts with nitrite ions, producing a diazonium cation. This cation then reacts with N-(1-naphthyl)ethylenediamine dihydrochloride, resulting in the formation of a purple-pink azo dye.....	48
Figure 21. A. Sample preparation for detection of nitrite in soil samples: First, 5 mL of compressed soil samples were added to a tube and diluted with water to a total volume of 15 mL. The mixture was shaken thoroughly and allowed to settle. The supernatant was then collected and used as the test sample. B. Detection procedure of nitrite in soil samples: Two tablets (NED and SUL tablets) were added to a pre-loaded buffer test tube. Then the sample solution was added to the mixture. In the presence of nitrite, an azo dye forms, indicating the presence or absence of nitrite in the sample.	49
Figure 22. Color intensity increased with buffer concentration (0.2–1 M, $n = 3$). One-way ANOVA ($p < 0.0001$) indicated a highly significant effect of buffer concentration on color intensity. Tukey's HSD confirmed that 0.5–1 M buffers gave significantly higher and more consistent signals than concentrations ≤ 0.4 M ($p < 0.001$). B. Compatibility tests were conducted at 0.5 M, 0.8 M, and 1 M buffer concentrations ($n = 3$) under acidic, neutral, and basic pH.. Two-way ANOVA showed significant effects of buffer ($p < 0.0001$), pH ($p < 0.05$), and their interaction ($p < 0.001$). Among these, the 1 M buffer provided the most consistent results across all tested pH conditions. One-way ANOVA and Tukey's HSD, ($p > 0.9$).....	50
Figure 23. The kinetic study of nitrite detection using NED and SUL tablets at a concentration of 50 μM nitrite indicates that the reaction is complete in less than 20 seconds.....	51

Figure 24. The calibration curve of nitrite detection with NED and SUL tablets. The calibration curve was found to follow the Michaelis–Menten equation with an R^2 value of 0.9971, confirming the compatibility of data with standard saturation model. The three samples of soil (Berri St. ■, NDG ◆, and Downtown ▲) were collected in Montreal, Canada as specified in experimental Section and analyzed for their nitrite level. Each sample was tested with three replicates	52
Figure 25. Comparison between the results of SUL, NED tablets and standard method for the nitrite detection in real soil samples (n=3). Paired t-tests showed no significant differences between methods ($p > 0.05$, $p = 0.50$ for Berri St., $p = 0.54$ for NDG, and $p = 0.12$ for Downtown), confirming that tablet results agree with UV-Vis measurements.	54
Figure 26. Potential interference of nitrite was tested with three replicates among common ions (nitrate, cobalt, mercury, copper, magnesium, calcium, lead, sodium, iron and zinc) at 1mM concentrations. While the working solution remained colorless for all three ions, a nitrite sample of 20µM was able to turn the solution purple, confirming the sensor’s selectivity for nitrite detection. One-way ANOVA, $p < 0.0001$, confirmed a statistically significant difference in color intensity among ions.	55
Figure 27. The stability of the tablets over six weeks (n=3). The average color intensity at week 6 recorded $102.3 \pm 1.81\%$ of the original color intensity recorded at week 1. RSD remained below 5.5%, confirming high reproducibility and consistent performance during storage.....	56
Figure A 1. Different percentages of pullulan (3%, 4%, and 5% w/v) were tested for preparing solid tablets. The solutions were pipetted to prepare polysaccharide-encapsulated tablets. Each N-(1-naphthyl)ethylenediamine dihydrochloride (NED) and sulfanilamide (SUL) solution was dispensed onto a carbon-steel tray and dried at room temperature in a dark environment for 24 hours. Compared to 5% tablets, lower percentages were not physically stable and did not maintain a spherical shape. Conversely, increasing the pullulan percentage prolonged the dissolving time during tests. Thus, the 5% composition was optimized and chosen for subsequent experiments	89
Figure A 2. The kinetic study of all-in-one tablets in concentration of 50 µM nitrite (n=3). The time-dependent light absorbance of the nitrite samples was measured using a UV-Vis spectrometer. To account for background color intensity, in readings we added a control sample which did not contain the nitrite. The absorbance at 548 nm was recorded at 15-seconds intervals over a total time duration of 20 minutes. The results showed that, similar to the kinetics of SUL and NED tablets the sensor had rapid increase in absorbance response, stabilizing and saturating within the first minute. Since the all-in-one tablet has a pinkish color due to the reaction between the reagents during the drying process, it showed a higher absorbance level in both 50 µM nitrite and background color intensity compared to the SUL and NED tablets.....	90

- Figure A 3.** The calibration curve for nitrite detection using all-in-one tablets was developed. The color intensity of the solution correlated with nitrite concentration, and the Michaelis–Menten equation was used to plot the relationship. The calibration curve had an R^2 value of 0.9965, and a LoD of 5 μM was calculated in the buffer medium ($n=3$)..... 90
- Figure A 4.** The stability of all-in-one tablets was assessed over six weeks. Tablets were stored at room temperature (22°C) in a glass vial containing silica gel pack and wrapped in aluminum foil. Tablets were tested in 50 μM nitrite solution in citrate-phosphate buffer. Results were normalized such that the percentage on day 0 represented 100% activity. According to the standard Griess assay protocol [1], liquid reagent mixtures have limited stability, requiring use within 8 hours due to NED's sensitivity to air and light. In contrast, the tablets exhibited high stability, comparable to SUL and NED tablets ($n=3$) 91
- Figure A 5.** Nitrite detection was performed using standard UV-Vis tests following the ThermoFisher Scientific protocol ($n=3$) [1]. The reagent solutions were prepared by dissolving 1 mg/ml of NED in deionized water and 10 mg/ml of SUL in 5% phosphoric acid. In the next step, a mixture of 1:1 ratio of the NED and SUL solutions was prepared for use in the tests before measurements. For the test, 20 μL of the Griess reagent mixture was added to one well of a 96-well plate, followed by the addition of 150 μL of the sample and 130 μL of deionized water. After that, the solution was shaken for 30 minutes on a microplate vortex mixer (Fisherbrand, USA) before reading the results at room temperature with a UV-Vis instrument at 540 nm (Cytation 5, Agilent Technologies, USA). Nitrite concentrations of 1-200 μM were prepared in deionized water and tested with the UV-Vis method to obtain the calibration curve 82
- Figure A 6.** Optical properties of functionalized graphene quantum dots. **A.** The UV-Vis absorbance was measured using a UV-Vis spectrophotometer (BioTek Cytation 5, imaging reader) with a 1 cm quartz cuvette. The absorption spectra were recorded over a range of 298–800 nm. **B.** Fluorescence spectra. All fluorescence data were collected at an excitation wavelength (λ_{ex}) of 365 nm, with emissions measured from 230 to 800 nm at 1 nm intervals. Data were processed using Excel..... 95
- Figure A 7.** Optical properties of amine-passivated CDs. **A.** The UV-Vis absorbance of the PH6-CDs was measured using a UV-Vis spectrophotometer (BioTek Cytation 5, imaging reader) with a 1 cm quartz cuvette. The absorption spectra were recorded over a range of 230–800 nm. **B.** Fluorescence spectra of the PH6-CDs were obtained by setting the excitation wavelength (λ_{ex}) to 350 nm, with emissions measured from 230 to 800 nm at 1 nm intervals. Data was processed using Excel..... 96

- Figure A 8.** Heavy metal monitoring using 10 $\mu\text{g}/\text{mL}$ dispersion of PH6-CDs. **A.** A concentration of 100 nM of Pb^{3+} , Cu^{2+} , Fe^{3+} , Co^{2+} , Hg^{2+} , and Ca^{2+} was added to the cuvette and measured for fluorescence intensity. Fluorescence data were collected at an excitation wavelength (λ_{ex}) of 350 nm at 1 nm intervals. **B.** Endpoint fluorescence results were recorded for Pb^{3+} , Cu^{2+} , Hg^{2+} , and Ca^{2+} (100 nM) at $\lambda_{\text{ex}} = 350$ nm and $\lambda_{\text{em}} = 455$ nm..... 97
- Figure A 9.** Quantitation of Cu^{+2} through fluorescence spectroscopy in the range 0-95 μM using a 10 $\mu\text{g}/\text{mL}$ dispersion of PH6-CDs. Fluorescence data were collected at an excitation wavelength (λ_{ex}) of 350 nm at 1 nm intervals..... 98
- Figure A 10.** The figures compare the effect of adding different types of polymers on heavy metal detection using functionalized graphene quantum dots (**A**). Polymers, including dextran(**B**) pullulan(**C**), and polyvinyl alcohol (PVA) (**D**), were added at a concentration of 5% w/v to the quantum dot solution. The solutions were then added to the cuvette, and fluorescence intensity was measured. Fluorescence data were collected at an λ_{ex} of 365 nm at 1 nm intervals. Data was processed using Excel. As shown, the addition of polymers interfered with metal ion detection. 98
- Figure A 11.** 2% pullulan solution was used to mix with QDs and investigate their physical characteristics on a tablet platform containing QDs. The polysaccharide was freshly mixed with a CD solution. The mixture was then thoroughly mixed, and 100 μL was pipetted onto the tray and left to dry at room temperature. 99
- Figure A 12.** Creating paper-plate. To analyze the potential of using carbon dots (CDs) in a paper-plate platform sensor, the platform was first designed using inkscape software then they were fabricated via the PHLC method by first laminating the filter papers by thermal bonding of Parafilm in an oven and then laser ablation of the patterns on the paper side. In order to get a robust bonding and uniform lamination, we optimized the process in terms of temperature (80–140 $^{\circ}\text{C}$), duration of heating (5–60 minutes), and cooling (at room temperature or slow cooling in the oven). We found 90 $^{\circ}\text{C}$ and 30 minutes with cooling at room temperature (~ 2 minutes) gave proper lamination. 99
- Figure A 13.** Testing acetone percentages on paper-based plate embedded with dried QDs on paper. (**A**) 10 μL of solution was added to each well and left to dry at room temperature. Different percentages of acetone (0-100%) were added to the dried QDs on paper, and the photo was captured immediately, before drying (**A**) and after acetone dried (**B**)..... 100

List of tables

Table 1. Comparison of the proposed auto-mixing tablet sensor with some commercial copper kits in terms of mixing efficiency and user-friendliness. A ✓ indicates the feature is present, while a ✗ indicates a challenge or limitation.....	41
Table 2. Comparison between the performance of the tablet sensors in this study with other reported POC assays.	56
Table A 1. Analytical Performance Comparison of Dual (SUL, NED) Tablet, All-in-One Tablet, and UV-Vis Method.	91

Abbreviations

Ag/AuNPs	Silver-Coated Gold Nanoparticles
AgNP	Silver Nanoparticle
ATP	Adenosine Triphosphate
AuNP	Gold Nanoparticle
CE	Count Electrode
CFP	Carbon Fiber Paper
DAN	2,3-Diaminonaphthalene
DI	De-ionized Water
E2Zn2SOD	Superoxide Dismutase
FIA	Flow-Injection Analysis
g	Gram
HM	Heavy Metals
HPLC	High-Performance Liquid Chromatography
IC	Ion Chromatography
L	Litre
LoD	Limit of Detection
mg	Milligram
min	Minutes
mL	Milliliter
mM	Millimolar
MOFs	Metal–Organic Frameworks
MS	Mass Spectrometry
NaCl	Sodium Chloride

NaOH	Sodium Hydroxide
NAT	2,3-Naphthotriazole
NED or NEDA	N-(1-naphthyl)ethylenediamine
NPs	Nanoparticles
OCI ⁻	Hypochlorite
OT-CEC	Open-Tubular Capillary Electrochromatography
PADs	Paper-based Analytical Devices
POC	Point-of-Care
RE	Reference Electrode
SD	Standard Deviation
sec	Second
SUL	Sulfanilamide
UV-Vis	Ultraviolet Light Visible
WE	Working Electrode
WHO	World Health Organization
w/v	Weight per Volume
°C	Degree of Celsius
μM	Micromolar
R%	Recovery Percentage
RSD%	Relative Standard Deviation Percentages

Chapter 1: Introduction and objective

In this chapter, there is a brief introduction to the research, outlining the background of copper and nitrite detection, as well as the use of tablet-based sensing platforms. This section continues with the objectives of this research project and ends up with the thesis organization.

1.1 Background

Point-of-use methods have revolutionized environmental monitoring and human health by providing rapid, portable, and user-friendly solutions to address the limitations of traditional techniques, which are often expensive, complex, and lack portability [2]. Proteins [3,4], nucleic acids [5,6], human cells [7], microbes and pathogens [8,9], and a variety of metabolites [10] have been targeted by point-of-care (POC) techniques. POC and point-of-use devices have numerous applications in environmental monitoring [11]. POC techniques are typically used in clinical or diagnostic settings to test human samples, while point-of-use methods refer more broadly to environmental or field applications for on-site contaminant detection without laboratory testing. Different environmental pollutants such as heavy metals (HM) are [12] and nitrite ions [13] were targeted for detection.

Different detection techniques, such as electrochemical biosensors [14], colourimetric methods [15] and fluorescent methods [16] have been used for detection of pollutants. On the other hand, several innovative detection platforms have been developed over time based on variations in size and sensing capabilities, including microfluidic devices [17] and paper-based analytical devices (PADs) [18]. However, these platforms still face certain challenges; for example, microfluidic lateral flow paper-based assays experience issues with reagent instability, sample interaction with materials, sample leakage, and limited sensitivity [19,20]. Therefore, there is a need to develop novel sensors that overcome the existing challenges of point-of-care devices while still adhering to the ASSURED (Affordable, Sensitive, Specific, User-friendly, Rapid and Robust, Equipment-free or environmentally friendly, and Deliverable to end-users) criteria set by the World Health Organization (WHO) [21–24]. The tablet-based sensors developed in this thesis aim to meet several aspects of the ASSURED criteria, particularly affordability, selectivity, being user-friendly, rapid and robust, and make detection simple for field delivery. Recently, different platforms have been explored for analyte detection using solution-based sensors. It is well established that detection in the solution phase provides greater sensitivity compared to solid-

supported systems. Tablet-based sensors enable rapid detection in the solution phase by releasing the reagents during testing [25]. This approach not only enhances the sensitivity and stability of reagents but also combines the benefits of point-of-use analytical devices. One approach to creating tablet sensors utilizes polysaccharide encapsulation, where polysaccharides like pullulan and dextran are added to a reagent solution and formed into the tablet [24]. Alternatively, powder compression involves mixing powdered reagents, weighing them, and then compressing the mixture into tablet form [26].

In this context, copper has been detected by POC sensors in water without the need for complex lab equipment or trained personnel. This makes them practical for field applications, especially in resource-limited settings where rapid, on-site monitoring is critical. While copper is essential in small amounts, excessive exposure can cause serious health problems in humans and harm ecosystems [27–30]. In the context of this thesis, copper concentrations exceeding 2.0 mg/L (2 ppm), the maximum permissible limit set by the WHO are considered excessive. Different types of sensors mostly including electrochemical and optical (colourimetric and fluorescence-based systems) offer different advantages depending on the application. Colourimetric tests offer a low-cost solution by changing color in the presence of copper ions [31], while electrodes provide accurate measurements by detecting electrical signals related to copper concentration [32]. Biosensors typically use biological elements like enzymes, antibodies, or whole cells, combined with physical or chemical transducers, to detect copper ions in water [33,34]. Integration with microfluidics and nanomaterials has further improved their performance, sensitivity and portability [35]. However, traditional copper detection methods often suffer from challenges such as high costs, complex fabrication processes, lack of stability in field conditions, and the need for laboratory equipment.

Nitrite has been focused in detection field due to its high toxicity in soil, water and food, linked to health issues like methemoglobinemia and cancer [36,37]. For the purposes of this study, nitrite concentrations exceeding 1 mg/L (approximately 22 μ M), based on environmental and drinking water safety standards, are considered excessive. In this aim, researchers have developed improved detection methods, including smartphone-assisted spectrophotometry, colourimetric sensors, fluorescence-based systems and electrochemical sensors integrated with nanomaterials and POC platforms. These offer better portability, faster response times, and eco-friendlier

alternatives to traditional methods [38]. Electrochemical sensors use oxidation/reduction reactions with materials like gold, copper, or zinc oxide, and can be miniaturized or integrated with smartphones for real-time monitoring [39]. Fluorescent probes offer high sensitivity, rapid response, and strong selectivity, specially combined with paper-based sensors and hydrogels even in complex samples [40]. Color-based detection is typically based on azo-coupling, diazotization-hydrolysis, nitrosation, and nanoparticle-based methods, allowing for simple, fast, and often instrument-free identification of nitrite [41]. However, traditional nitrite detection techniques remain expensive, complex, and dependent on specialized facilities and skilled personnel. Also, different POC platforms such as paper-based devices, despite offering improved portability, often suffer from complex fabrication processes and reagent instability.

1.2 Thesis objectives

The aim of this thesis is to develop tablet-based sensors for the rapid, user-friendly, and cost-effective detection of environmental contaminants to enhance public health. To achieve this goal, two types of tablet sensors were developed. The first objective is to create a novel tablet-based sensor for rapid, on-site copper detection in water, while the second focuses on point-of-use, user-friendly detection of nitrite in soil samples. These innovative approaches address the limitations of existing detection methods, such as high costs, complexity, and reliance on laboratory settings. By leveraging colourimetric detection principles and using a solid-phase platform, the sensors aim to provide a cost-effective, portable, and user-friendly solution, adhering to the ASSURED criteria.

The research aims to develop a tablet-based sensor as a portable point-of-use detection platform for water, particularly for field-based, immediate copper detection. Existing point-of-use techniques for copper detection include commercial powders and tablet-based sensors. However, this objective involves integrating various materials into all-in-one solid auto-mixing tablets, minimizing the risk of spillage, enhancing ease of use, and improving automation compared to both powdered and conventional tablet forms. The goal is to improve water quality monitoring by offering an efficient, reliable, non-invasive, and practical solution for detecting copper contamination in various water sources.

Furthermore, the study aims to design a novel tablet-based sensor for rapid, cost-effective nitrite detection in soil samples. This tablet sensor is intended to simplify point-of-use soil analysis, and

ensure user-friendliness, selectivity, and long-term storage stability, enhance accessibility of nitrite measurement, particularly in resource-limited settings.

1.3 Thesis organization

This thesis is organized into five chapters, each playing a significant role in explaining the research as follows:

- Chapter 1 provides an introduction that covers background of development of POC techniques and tablet-based sensors, with a focus on detecting copper and nitrite. It outlines the objectives and overall framework of the study and includes a summary of the author's publications and research contributions.
- Chapter 2 undertakes a thorough review of the relevant literature related to heavy metal detection techniques with a focus on copper as well as nitrite detection techniques. Then it introduces the development of tablet-based sensors, specifically for detecting copper and nitrite, utilizing polysaccharide encapsulation and compression methods.
- Chapter 3 describes an auto-mixing tablet for the on-site and user-friendly detection of copper in water. The chapter details the preparation of reagents, experimental procedures, and fabrication of the tablet-based sensor. The chapter also presents results from copper detection tests, demonstrating the tablet's performance and effectiveness.
- Chapter 4 describes a novel tablet-based sensor using pullulan encapsulation for user-friendly detection of nitrite in soil samples. the methods and experiments carried out for nitrite detection, along with the experiments and results of detecting nitrite in real soil samples. It also examines analytical performance, interference studies, and stability tests, offering an overview of the research findings.
- Chapter 5 provides a conclusion on the research work and future recommendations.

1.4 List of publications and conference contributions

The following list of publications and conference proceedings shows my contribution to the annals of research in the course of this thesis.

Peer-reviewed journal articles

- **Maryam Mansouri**, Seyed Hamid Safiabadi Tali, Zubi Sadiq, Sana Jahanshahi-Anbuhi*, "User-friendly detection of nitrite in soil samples with tablet-based sensor", **2025**. (revision request).
- **Maryam Mansouri**, Seyed Hamid Safiabadi Tali, Sana Jahanshahi-Anbuhi*, "Instant Auto-Mixing Tablets for On-Site Detection of Copper in Water", **2025**. (submitted)
- Seyed Hamid Safiabadi Tali, Muna Al-Kassawneh, **Maryam Mansouri**, Zubi Sadiq, Sana Jahanshahi-Anbuhi¹*, "All-in-one reagent tablet with rapid auto-mixing for point-of-care diagnostic". *ASC Sensors*, **2025**. DOI: [10.1021/acssensors.4c03726](https://doi.org/10.1021/acssensors.4c03726)
- Zubi Sadiq, Seyed Hamid Safiabadi Tali, **Maryam Mansouri**, Sana Jahanshahi-Anbuhi*, "Dual-functional nanogold tablet as a plasmonic and nanozyme sensor for point-of-care applications", *RSC Nanoscale Advances*, **2025**. DOI: [10.1039/D5NA00082C](https://doi.org/10.1039/D5NA00082C)

Conferences

- **Maryam Mansouri**, Seyed Hamid Safiabadi Tali, Zubi Sadiq, Sana Jahanshahi-Anbuhi* , "User-friendly detection of nitrite in soil samples with tablet-based sensor". Chemical Engineering Research Day, Montreal, Canada, March **2025**.

*** This work was recognized with the Best Poster Presentation Prize in the Student Poster Presentation Competition category.

- **Maryam Mansouri**, Seyed Hamid Safiabadi Tali, Sana Jahanshahi-Anbuhi*, "On-site and rapid detection of copper in water with low-cost tablet-based sensor". Chemical Engineering Research Day, Montreal, Canada, March **2024**.

*** This work was recognized with the Sustainability Prize in the Student Presentation Competition category.

- Seyed Hamid Safiabadi Tali, Muna Al-Kassawneh, **Maryam Mansouri**, Zubi Sadiq, Sana Jahanshahi-Anbuhi*, "All-in-one reagent tablet with rapid auto-mixing for point-of-care diagnostic". Chemical Engineering Research Day, Montreal, Canada, March **2024**.

Chapter 2: Literature review

This chapter discusses the environmental and health risks posed by pollutants like heavy metals and nitrite. It reviews various detection methods for copper and nitrite, focusing on electrochemical, fluorescence, and colourimetric techniques. Then it introduces the development of tablet-based sensors, specifically for detecting copper and nitrite, utilizing polysaccharide encapsulation and compression methods. It highlights the innovation of auto-mixing tablets and nitrite tablets. The goal is to create portable, cost-effective, and reliable point-of-care devices for environmental and health monitoring.

2.1. Introduction

Heavy metal pollution is one of the most serious issues. Heavy metals are defined as naturally occurring metals with an atomic number greater than 20 and a density more than 5 g cm^{-3} [42]. It means they are defined as elements with high density and weight. Among all the pollutants in environment heavy metals are under supreme attention as they have toxic properties [43]. The indiscriminate release of heavy metals without adequate treatment into the systems such as soil and water poses a significant global health threat [44]. Heavy metals are non-biodegradable and widely present in the environment, presenting human health and ecosystems with long-lasting and significant risks [45,46]. The excess amount of them in the biosphere leads to their entry into the food chain, where they cause considerable harm to human health [47,48]. They can enter through water, food, air or absorbance from the skin in contact stemming from manufacturing sources, agricultural, residential and pharmaceutical. The toxicity of these metals depends on factors such as the type of organism, the duration of exposure, the specific properties of the metal, and its role in biological processes. As heavy metals accumulate and spread through the food chain, they pose risks to all living organisms, with particularly harmful effect on human health [43]. Some living organisms require small quantities of certain heavy metals like iron, cobalt, zinc, copper, manganese, etc., but at higher concentrations these elements lead to toxic effects [49]. However, the rising levels of various metals in soil and water, due to growth of industrialization, have resulted in a concerning situation for both human health and aquatic life [44]. On the other hand, some metals like cadmium, lead, mercury and some others are regarded as hazardous substances. They have the potential to cause serious health and environmental risks even at low concentrations by accumulation in living organisms [50,51].

2.1.1 Copper

Copper (II) is one of the most common substances in the environment among heavy metals. It has a role in biological processes such as chlorophyll synthesis, photosynthesis, cell wall development, and respiratory electron transport pathways. It acts as an essential element for various biological functions within the human body, serving as a crucial cofactor and structural component in numerous enzymes, participating in vital metabolic processes [52–54]. Copper-based enzymes play important roles in various physiological processes, including pigmentation (tyrosinase), epigenetic modification (lysyl oxidase-like 2), respiration (cytochrome c oxidase), iron uptake (ceruloplasmin), antioxidant defense (Cu/Zn superoxide dismutase), neurotransmitter synthesis, and metabolism (dopamine β -hydroxylase) [55]. It maintains the normal functioning of the brain and nervous system, elasticity of blood vessels, supports the formation of collagen and elastin, and regulates hemoglobin levels [56]. However, various human activities contribute to copper contamination in the environment. These include the use of agricultural fertilizers and pesticides, mining, and industrial production processes in the chemical, pharmaceutical, and paper industries [57]. Exceeding the optimal levels of copper intake can lead to detrimental consequences. Elevated copper concentrations has been linked to gastrointestinal issues, liver and kidney damage, and the predominance of neurodegenerative diseases such as Menkes, Wilson's, and Alzheimer's [27–30]. Additionally, an excess of copper endangers the survival of aquatic organisms and reduces the self-purification capacity of natural water systems [58,59]. Therefore, an adequate intake of copper from food and drinking water is extremely crucial for living organisms. The World Health Organization (WHO) has defined permissible limits for copper ion concentrations at 2.0 mg/L in drinking water [60]. However, the concentration of copper ion in certain local water areas is still much higher than this tolerance limit. Hence, there is an urgent need to develop highly sensitive and selective methods for copper ion detection.

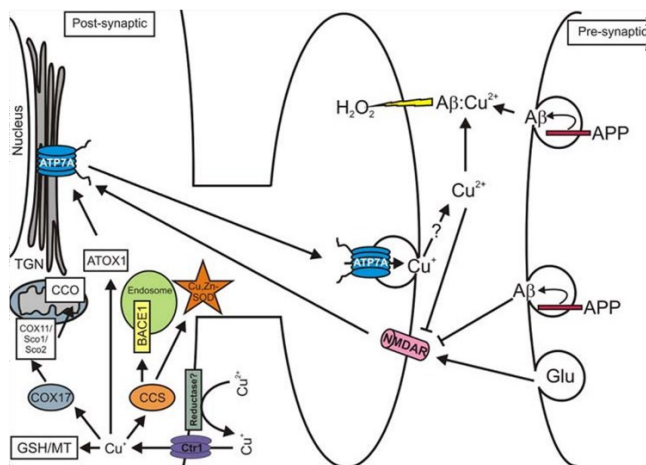
2.1.2 Nitrite

Nitrite has been widely utilized in food industry and environmental fields, such as for preserving food and enhancing flavor of meat products [61]. Nitrite is also found in water distribution systems, including groundwater, lakes, and oceans [36]. As a result, it accumulates in vegetables, fruits, processed meats, and drinking water, making it a common component of our daily consumption and one of the most widespread pollutants in both food and the environment [62]. Nitrite also plays a crucial role in the plant nitrogen cycle [63], acting as an essential nutrient that helps make

nitrogen available to plants. The nitrification process, which transforms ammonium into nitrite and then into nitrate, is primarily driven by ammonium-oxidizing bacteria such as *Nitrosomonas* and *Nitrobacter* in the soil [64–67]. As food demand rising over recent decades, many countries have excessively used inorganic fertilizers, often containing nitrite, to boost agricultural productivity. This overuse contributes to increased nitrification and nitrogen leakage into the environment. Accumulated nitrite in soil can lead to overloading and nitrate leaching, contaminating various water sources. This contamination can encourage the growth of toxic algae, including harmful algal blooms that reduce oxygen levels in water and harm biodiversity. Excessive nitrite levels in food and water can pose serious health hazards. In the acidic environment of the stomach, nitrite can form carcinogenic nitrosamines. It also reduces the blood's ability to carry oxygen by converting hemoglobin into methemoglobin[36,37]. By and large, the high incidence of medical issues such as gastric and esophageal cancers, central nervous system abnormalities, and neonatal methemoglobinemia commonly referred to as "blue baby syndrome" can stem from excessive nitrite ingestion [68–70].

To address these risks, the World Health Organization (WHO) has established a limit of 3.0 mg/L (65.2 μ M) for in drinking water and for the protection of wildlife, while the U.S. Environmental Protection Agency (EPA) determines a Contaminant Level (MCL) of 1.0 mg/L (21 μ M) [71,72]. Therefore, the evaluation of nitrites became a very important issue in environmental fields.

A



B

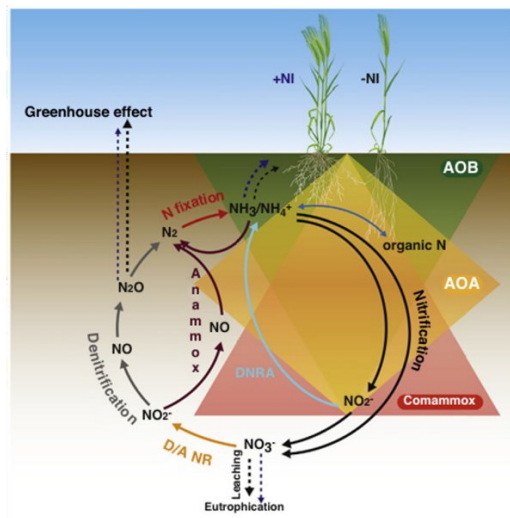


Figure 1. A. It shows how neurons regulate copper and its link to Alzheimer's. Copper enters through Ctr1, is transported to enzymes, and released by ATP7A in synapses, increasing A β production. Excess copper and A β form toxic complexes, generating H₂O₂, causing oxidative stress and amyloid plaque formation, contributing to Alzheimer's (adapted from [29]). **B.** The nitrogen cycle in soil. This involves nitrification, denitrification, and nitrogen fixation, with bacteria regulating nitrogen transformations. Nitrification inhibitors (NIs) reduce nitrogen loss, lower greenhouse gas emissions, and improve soil fertility, supporting plant growth (adapted from [65]).

2.2 Copper detection techniques

Various conventional methods have been developed for this purpose, ranging from inductively coupled plasma detectors, atomic absorption spectroscopy, and electrochemical sensors to surface plasmon resonance detectors, X-ray fluorescence spectrometry, neutron activation analysis, and plasma-optical emission spectrometry [73,74].

2.2.1 Electrochemical sensor

Electrochemical sensors comprise three-electrode systems which contain a working electrode (WE), a reference electrode (RE) and a count electrode (CE) [75]. The WE can be modified with various materials to enable selective detection and enhanced concentration of metal ions. The detection of metal ions is based on the observable variations in electrochemical properties. The analysis of these changes leads to accurately identify the specific metal ions in a sample [76]. The working mechanism of these sensors is related to utilizing electrodes through electrochemical technologies, such as anodic stripping voltammetry, to measure heavy metals. Recent advances in materials increase the sensitivity of these sensors, which categorized in inorganic, organic, and biomaterial modified electrodes for electrochemical detection of heavy metal ions. These materials demonstrate high sensitivity and selectivity which could enhance selectivity, stability, and sensitivity, of detection heavy metal ions. As an example using gold nano- material for detecting Cu²⁺ in wastewater which has investigated by [77]. Similarity, Romero-Cano et al. in 2019 explored the application of carbon paste electrodes made from grapefruit peel bio-template for functionalized with carboxyl groups electrochemical detection of Cu²⁺ ions in water [78]. In 2024 Timoshenko et al. [79] presented a highly selective electrochemical sensor for detecting Cu²⁺ ions in both in vitro and in vivo, demonstrated enhanced sensitivity and selectivity due to the

modification of gold nanoelectrodes with a conjugate of the Gly-His-Lys (GHK) tripeptide and lipoic acid, which improved Cu^{2+} binding affinity.

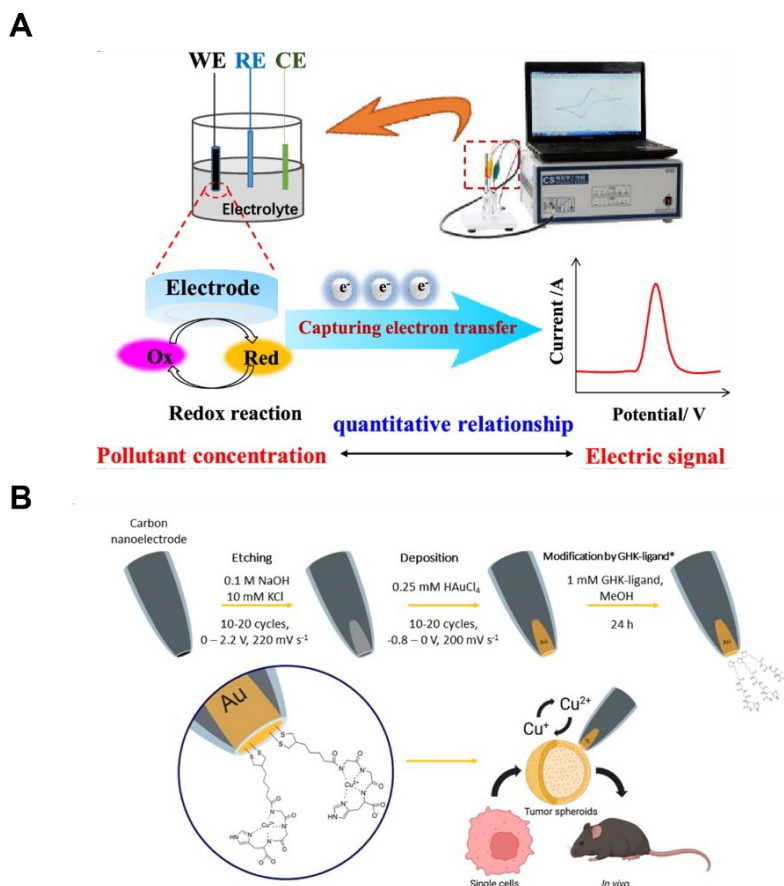


Figure 2. **A.** Basic concepts of electrochemical sensors (adapted from [75]). **B.** Scheme of the designed gold nanoelectrodes and GHK-ligand, along with the proposed mechanism for in vitro/in vivo detection of Cu^{2+} (adapted from [79]).

The main advantages of electrochemical sensors include their cost effectiveness, sensitivity, and ease of operation. However, they face challenges in reproducibility and stability, particularly in complex systems and large-scale production. For example, this technique needed controlled environments like buffer solutions, with limitations on practical usage. Therefore, further investigation is needed in this regard [80].

2.2.2 Fluorescence sensor

Fluorescence sensors measuring the change of wavelength of electromagnetic radiation emission by a substance change after it absorbs light [81]. These sensors are highly sensitive and selective

for sensing Cu^{2+} ions. There are two mechanisms for detecting Cu^{2+} ions using fluorescence; first one is because of paramagnetic nature of the Cu^{2+} ions the binding of a fluorophore with the metal ion, can led to a "turn-off" signal and quenching. The second one, is through generating a "turn-on" signal when the Cu^{2+} with the fluorophore make complex [82]. In recent years, different types of detection probes for Cu^{2+} ions have also been developed due to their unique properties such as nanoparticles (NPs), because of their unique electronic, optical and catalytic properties for sensitive detection minimal material usage, metal–organic frameworks (MOFs) which are effective for selective detection in various solution and quantum dots, which is mostly studied because of luminescence abilities [83]. For example, Liu et al. created a highly sensitive fluorescence sensor for detecting Cu^{2+} ions. the silica-coated CdSe quantum dots were used and Cu^{2+} ion nanoclusters were attached to them. The color change from yellow-green to red was observed when different levels of Cu^{2+} ions were released (with a detection limit of 8.9 nM.) [84]. In 2021, Niu et al. developed a switch fluorescence sensor using gold nanoclusters stabilized with bovine serum albumin for detecting cysteine and copper ions ("on" state when cysteine is present, and then "off" state when copper ions are introduced.). In living samples tests , the sensor proved to be fast, chemical stable and sensitive, which indicate it had potential for early Alzheimer's disease diagnosis [85]. Patir et al. developed a fluorescence sensor using nitrogen-doped carbon dot for detecting Cu^{2+} ions with the detection limit of 2.3 nM. The sensors were also incorporated into a low-cost, paper-based microfluidic device, which is easy for on-site detection in real-world samples like tap water [86].

2.2.3 Colourimetric sensor

Colourimetric sensors are designed to measure the modification in reactive sensing components. This color change is observed by the naked eyes. The main function of colourimetric sensors is showing how the target substance is visually affected by different factors like pH, temperature changes, or stress. These sensors have been remarkably emphasized owing to their simplicity, aptitude for on-site observation, short-time analysis and selectivity [87,88]. The three examples of sensors are highlighted as gold nanoparticles, silver-coated gold nanoparticles, and microfluidic systems. Gold and silver nanoparticles have been crucial in various fields, including chemistry, biology, and environmental science, because of their simplicity, sensitivity, and excellent biocompatibility. Gangapuram et al. developed a gold nanoparticle (AuNP)-modified colourimetric sensor specifically designed for the selective and sensitive detection of Cu^{2+} ions.

They used AuNPs@ carboxymethyl gum karaya, showed a significant color change from red to blue upon interaction with Cu^{2+} ions ranging from 10 to 1000 nM [89]. In other project Ma et al. emphasized on using silver nanoparticles (AgNPs) made with dopamine for detecting Cu^{2+} . By impact of dopamine silver ions reduced into AgNPs. Which can bind with Cu^{2+} , causing the particles to clump together and change color. This is one step, creation, modification, and detection of Cu^{2+} . After adding silver nitrate, the color of the solution turns yellow, and the speed of reaction is based on adjusting the pH with NaOH [90].

in 2014 Park et al. developed a receptor specifically for detecting Cu^{2+} . In this work color changed from yellow to purple, by interaction of Cu^{2+} to receptor. The mechanism is selective to Cu^{2+} among 18 different cations tested [91]. Similarly, Deng and colleagues created a gold nanoparticle-based colourimetric sensor for Cu^{2+} detection, where the presence of Cu^{2+} caused the color to shift from red to purple-blue, with a detection limit of 0.04 μM using UV-Vis spectrometry and 2 μM visible to the naked eye [92]. Xei et al. also developed a microfluidic system combined with a colourimetric sensor for detecting Cu ions. In this project the color intensity in the microfluidic channels reduced in a linear fashion within the 0–30 mg/L range as Cu^{2+} presence increased (detection limit of 0.096 mg/L) in tap water tests [31]. Also, Lou et al. measured Cu^{2+} in water with silver-coated gold nanoparticles (Ag/AuNPs) by detecting decrease in surface plasmon resonance absorption [93].

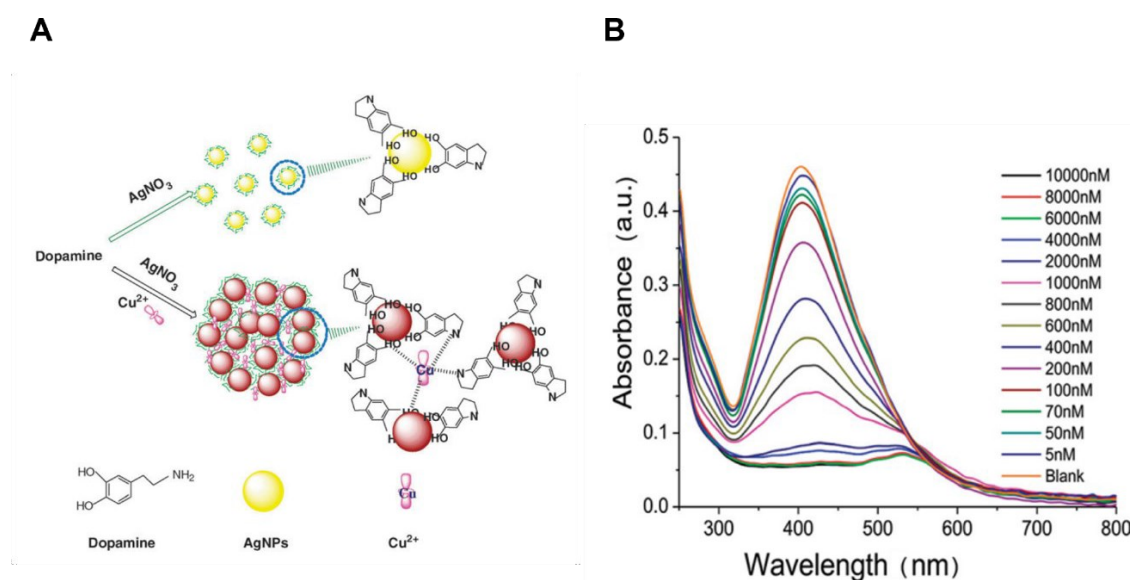


Figure 3. A. Mechanism of colourimetric detection of Cu^{2+} with silver/dopamine nanoparticles (adapted from [90]). **B.** Images and absorbance measurements of Ag/AuNPs after adding Cu^{2+} (adapted from [93]).

2.3 Nitrite detection techniques

Various conventional methods have been explored for nitrite detection, ranging from spectrophotometry including UV/Vis spectroscopy, catalytic-spectrophotometric, raman spectroscopy, IR and FTIR spectroscopy, atomic absorption spectroscopy (AAS), fluorescence spectroscopy, chemiluminescence, mass spectroscopy, to different chromatography methods [38,61,94].

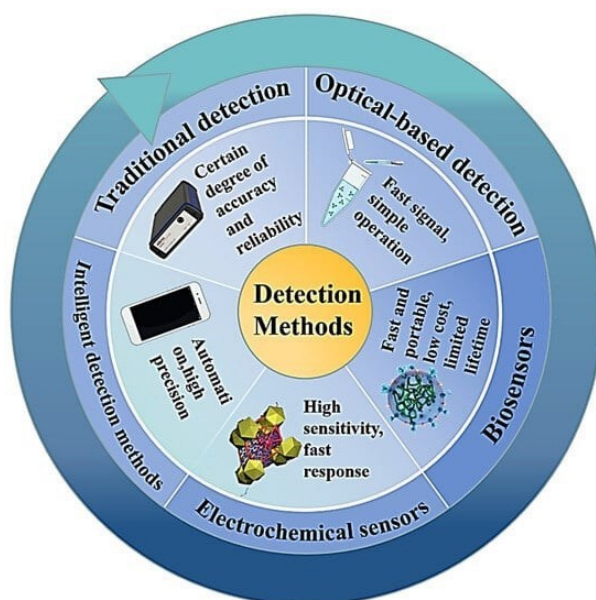


Figure 4. Classification and characteristics of nitrite detection methods. Reproduced from Zhang et al., *Applied Sciences* 2024, 14(19), 9027, under the terms of the Creative Commons CC BY 4.0 license [38].

2.3.1 Catalytic-spectrophotometric

There are different types of spectrophotometric methods for detecting nitrite. One of these techniques is catalytic-spectrophotometric. The different catalytic-spectrophotometric techniques are based on the catalytic effect of nitrite on a specific reaction. In these methods, nitrite reacts

with an oxidizing agent and changes the color of the indicator. The intensity of the color is measured by a spectrophotometer at specific wavelength. This technique extensively applied for the detection of nitrate and nitrite in food, water, and biological samples. Substituted phenothiazine derivatives [95], triarylmethane alkaline [96] and acidic dyes, azo dyes [97], and similar compounds have been used as indicator species. Meanwhile, oxidizing agents such as potassium bromate [95] and hydrogen peroxide [98] have been commonly employed. Flow-injection analysis (FIA) to catalytic-spectrophotometric methods improves their efficiency. Ensafi and Kazemzadeh in 1999 used flow-injection analysis for simultaneous determination of nitrite and nitrate, with nitrate reduced to nitrite using copperized-cadmium columns. Nitrite catalyzed the oxidation of galloxyaniline as an indicator. They applied to food and water samples [99]. Stopped-flow technique was used for the reaction rate method for nitrite measurement by Pettas et al. (1998). They developed a method using thymol blue as an indicator and potassium bromate as an oxidizing agent. Nitrite catalyzed the reaction between thymol blue and bromate in acidic media [100]. In other study researchers developed a catalytic-spectrophotometric method for the simultaneous detection of nitrite and nitrate. They used crystal violet as the indicator dye and potassium bromate as the oxidizing agent, with catalytic effect of nitrite on the redox reaction in a phosphoric acid medium. This method demonstrated high sensitivity, with detection limits of 0.3 ng/mL for nitrite and 1.0 ng/mL for nitrate [96].

2.3.2 Chromatographic

Another technique to detect nitrite is using chromatography. high-performance liquid chromatography (HPLC) and ion chromatography are used mainly for direct sample analysis of nitrite. As an example, ion chromatography (IC) was used for determination of nitrite in human saliva with high recovery rates (95%-101%), excellent linearity ($r^2 = 0.9991$). This technique provides direct, selective, and interference-free analysis with minimal sample preparation [101]. The reversed-phase high-performance liquid chromatography method with fluorescence detection was used for the rapid detection of nitrite in cell culture media, plasma, and urine. The method is based on the derivatization of nitrite with 2,3-diaminonaphthalene (DAN) under acidic conditions, forming the highly fluorescent compound 2,3-naphthotriazole (NAT) [102]. In recent years, as there is need for precise detection, ion chromatography is rarely used alone and studies focus on frequently combined this method with other instruments or techniques to enhance the detection of target substances. For instant, IC combined with mass spectrometry (MS) to detect trace levels of

nitrite in microcrystalline cellulose. Ion chromatography was used to separate nitrite from other anions, while mass spectrometry improved sensitivity by targeting a specific mass-to-charge ratio [103]. In another study HPLC-UV-Vis method was applied for enhance sensitivity of nitrite detection in biological and vegetal samples. It used pre-column derivatization with the Griess reaction to enhance nitrite detection while directly detecting nitrate via UV absorbance [104]. HPLC and IC could be combined to increase selectivity and sensitivity of nitrite detection. While HPLC component identified nitroaromatic compounds using UV detection, IC quantified anions with conductivity detection [105].

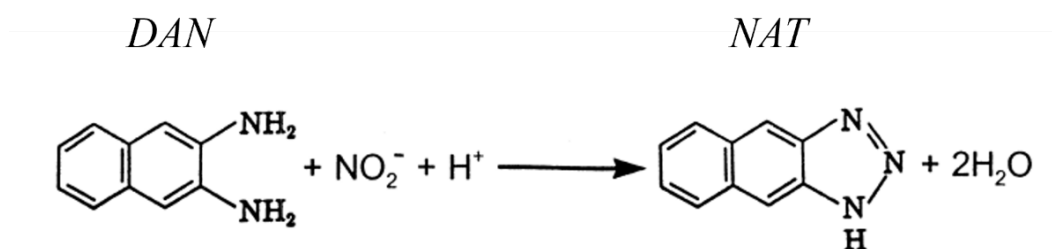


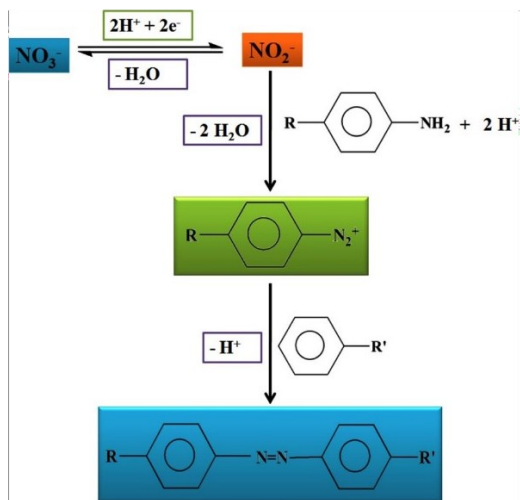
Figure 5. Interaction between DAN and nitrite for NAT production (adapted from [102]).

2.3.3 Griess assay-based (colourimetric)

The Griess reaction, originally introduced by Johann Peter Griess in 1879 [106], for nitrate detection in saliva through a diazotization process. First, nitrite reacts with sulfanilic acid under acidic condition to form a diazonium cation. Then, this cation couples with 1-naphthylamine, resulting in the formation of water-soluble azo dye, a red-violet, with a maximum absorption wavelength of approximately 540 nm [94,107]. Over time, this reaction has been widely applied for detection of bacterial infections in the urogenital tract, by identifying nitrite, which is formed through the bacterial reduction of nitrate. Nitrite is the main nitrogen oxide anion present in human urine [108]. The Griess reaction is selective for nitrite. To analyze nitrate using this method, it requires chemical or enzymatic reduction to nitrite. To enhance the assay's performance and minimize interferences, this reaction has been continuously modified. The original Griess reaction is based on a diazotization process. While originally, sulfanilic acid and α -naphthylamine were commonly used as Griess reagents, Bratton and Marshall proposed N-(1-naphthyl)ethylenediamine (NED or NEDA) as new coupling components for sulfanilamide [109]. The Griess assay is a simple, cost-effective, and practical technique for detection nitrite. The Griess

reaction has been integrated with HPLC and FIA systems, enabling the analysis of nitrite in complex samples such as food and biological fluids. In the HPLC combined with Griess method, nitrite and nitrate are first separated chromatographically, making detection easier in challenging matrices. Researchers modified colourimetric Griess method for nitrate determination in soil and plant extracts, by removing barium sulfate and using sulfanilamide and NED in a diazotization reaction. It simplifies the procedure by replacing centrifugation with filtration for color development and measurement [110]. Wang et al. in 1998, used diazotization-coupling reaction between sulfanilamide and sodium 1-naphthol-4-sulfonate in a hydrochloric acid medium which led to analyzed nitrate and nitrite in water and fruit samples by using a column preconcentration method [111]. Wu et al. developed a dual-readout sensor combining fluorescent and colourimetric detection for nitrite in real food samples based on the Griess reaction. The sensor uses acid-resistant carbon quantum dots and 3-aminophenol in an acidic environment. A yellow-colored azo compound was produced for colourimetric detection by diazotization-coupling reaction [112].

A



B

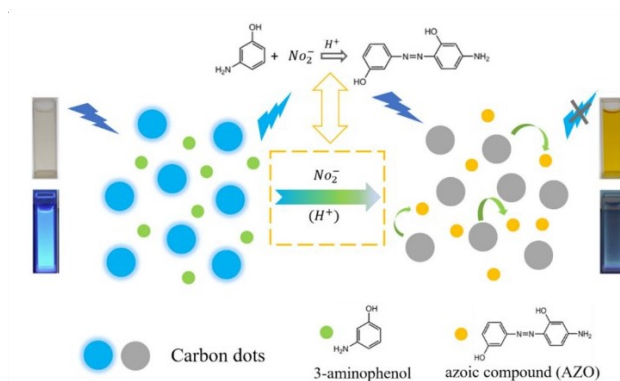


Figure 6. A. Schematic representation of the basic principle of Griess assay (adapted from [94]).

B. Schematic illustration of mechanism of colourimetric and fluorescent dual-readout sensor for the detection of nitrite (adapted from [112]).

2.3.4 Capillary electrophoresis

Capillary electrophoresis (CE) is a versatile technique which can be used to analyze cationic, anionic and neutral compounds. This technique is an efficient analytical method for detecting nitrite and nitrate in biological samples as it is highly sensitive, has short time runs, separate compounds effectively, and has wide applicability for analysis a variety of anions. This method requires only a small sample volume, relies on inexpensive reagents, and involves a simple operational process. Nitrite was detected by capillary zone electrophoresis with transient isotachopheresis in seawater [113] and in human plasma [114]. It was measured also by capillary zone electrophoresis technique in saliva, while direct UV detection at 214 nm was applied [115]. In another study researchers explored using microchip capillary electrophoresis, the microchip was made of quartz and nitrite detected by UV detection at 214 nm. The method utilizes a specially formulated running buffer based on human serum components to improve separation efficiency [116]. Zhang et. al used modified open-tubular capillary electrochromatography (OT-CEC). A nano-latex coated capillary was used to improve separation efficiency and enhance sensitivity in plasma and urine samples [117].

2.3.5 Electrochemical

Electrochemical techniques, such as voltametric [118,119], potentiometric [120–122] and impedimetric electrodes [123,124], detect nitrite ions by converting them into measurable electrical responses, including current signals, potential differences, and impedance, respectively. While voltametric measures the current generated by a chemical reaction on the electrode surface while applying voltage, potentiometric creates a voltage difference between two electrodes, no current flows and substances are contributed during detection. This technique detects nitrite using a membrane that selectively binds to ions. Measures the resistance of the electrode, which increases with nitrite concentration. In impedimetric electrodes a voltage or current signal is applied, and the response is recorded to determine nitrite levels. The partially oxidized state of nitrogen in nitrite enables its detection by both oxidation and reduction methods [125]. Electrochemical oxidation of nitrite leads to production of nitrate and remains unaffected by dissolved oxygen. Both oxidation

and reduction mechanisms have been investigated using enzymatic and non-enzymatic strategies for nitrite electrochemical assays [126,127]. Yang et al. worked on ion-selective polymeric membrane electrodes using a cobalt(III) corrole complex for nitrite and nitrate detection [121]. Zhu et al. used air-annealed carbon fiber paper (CFP) to enhance electrochemical nitrite sensing, improving its wettability, surface roughness, and catalytic activity. They demonstrated that the oxidized carbon fiber paper exhibited high sensitivity, a wide detection range and a rapid response time for nitrite detection. They tested it in real food samples, including mineral water and sausage [128]. Baciú et al. developed a composite electrode for the simultaneous detection of ammonium and nitrite in groundwater. They decorated carbon nanotubes with silver nanoparticles to enhance electrocatalytic activity [129]. Zhang et al. detected nitrite by modified glassy carbon electrode. The electrode was modified by electrodeposition method with Ag/Cu nanoclusters and multiwalled carbon nanotubes. They tested sensors in lake water, drinking water, and seawater [130].

2.3.6 Fluorescence

Fluorescence probes have been widely used for nitrite detection. These sensors work by producing a fluorescence signal when the probe reacts specifically with nitrite, allowing for its detection. Fluorescent probes for detecting nitrite are designed using different strategies. The most common method is the diazotization reaction, where diazotized is produced by reaction of compounds like aniline or naphthylamine with nitrite, enabling fluorescent detection. The other approach is the nitration reaction, where nitrite modifies the probe's structure, leading to fluorescence changes for selective detection. The third strategy is based on nitrite binding to metal ions. The probes with coordination groups like pyridine form complexes with nitrite⁻, which changes fluorescence intensity [131]. A colourimetric and near-infrared fluorescent probe, TBM, was used by Wu et al. for detecting nitrite on water and food samples. The probe reacts with nitrite, resulting in a visible color change from red to colorless and a decrease in fluorescence intensity. It also used in *Escherichia coli* for fluorescence imaging of nitrite [132]. Nüssler et al. designed a fluorometric assay to measure nitrite and nitrate by using 2,3-diaminonaphthalene (DAN). They tested nitrite detection in biological fluids such as serum and urine [133]. Zhu et al. utilized a fluorescence-based sensor using an anthracene carboxyimide derivative for nitrite detection, by "turn-on" fluorescence mechanism in real food samples [134]. A spectrofluorimetric method for nitrite detection was used in food products in a study. Researchers designed a method based on the

reaction between nitrite and a dihydropyridine derivative, forming a highly fluorescent pyridine compound, applied on food samples [135].

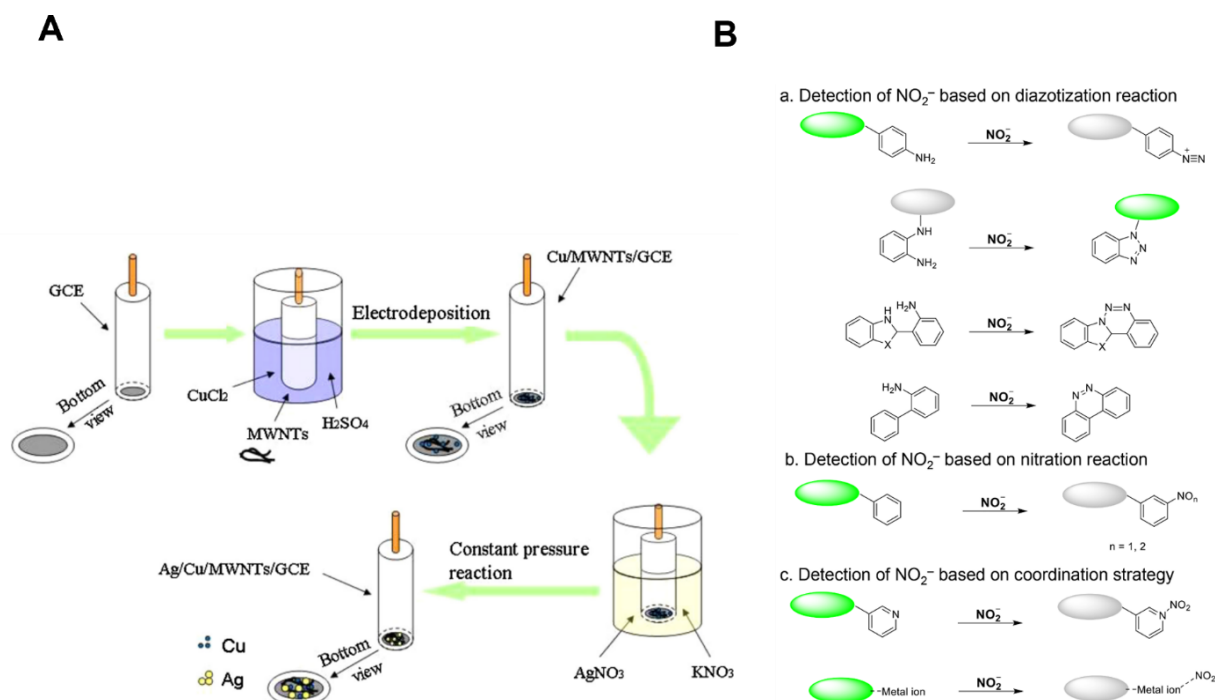


Figure 7. A. The graphical diagram for preparation of Cu/Ag/MWNTs modified electrode, (adapted from [130]) . **B.** Strategies for fluorescent probes for NO_2 (adapted from [131]).

2.4 Development of tablet-based sensors

Tablet-based bioassays are remarkable advances in POC detection which offers solution-based detection, with pre-measured quantities of reagents, long-term solid-phase platform stability and portability. Solid tablets offer a versatile solution for simplifying and enhancing diagnostic processes. They improve assay reproducibility by providing premeasured quantities. Due to their inexpensive production system, user-friendly handling, and heightened reagent stability, they elevate the efficiency of complex tests. Reagent tablets were first utilized for POC applications in the early 1940s for detecting reducing substances in urine [136]. However, recent developments have led to re-popularized tablet-based devices, particularly after publications by Jahanshahi-Anbuhi et al. starting in 2014 [137,138]. So far, two major methods have been employed to create tablet-based devices, namely polysaccharide encapsulation of reagents and powder compression.

2.4.1 Polysaccharide encapsulation process

In the polysaccharide encapsulation process, the polysaccharides like pullulan and dextran are combined with a reagent solution and then shaped into tablets. In 2014, pullulan, a non-ionic polysaccharide, has been highlighted by Jahanshahi-Anbuhi et al. as a potential material for stabilizing sensitive bioreagents. Due to pullulan's capacity to form films during the drying process, when mixed with bioreagents such as enzymes, it can encapsulate them and maintain their stability for extended periods at room temperature, overcoming challenges like the need for cold storage and shipping. The pullulan encapsulation could preserve enzyme activity and allowed assays to be performed as a point of care method for limited facilities regions [137]. In addition, in 2016, this method got extended to create all-inclusive bioassay tablets for detecting adenosine triphosphate (ATP). It simplified the assay by gathering all the reagents into one tablet, make it applicable for user friendly and or field diagnostics. In this project pullulan stabilized labile enzymes and substrates, luciferase and luciferin. The tablets enhanced enzymes stability at high temperatures by restricting their molecular motion as well as protecting them from oxidation. Despite all the advantages, there were some challenges during tablet production, such as ensuring the stability of sensitive components like enzymes. the formulation required optimization to ensure the tablets worked well and quickly dissolve [138].

Recently glucose oxidase and horseradish peroxidase got capsulated with dextran to form enzyme tablets for glucose detection in urine. Dextran is a biocompatible and biodegradable polysaccharide that enhances the stability and performance of enzymes under harsh conditions, such as high temperatures. However, some enzyme activity was lost under extreme thermal stress and some high concentrations of dextran posed challenges due to increased viscosity. These tablets could detect glucose with in both artificial and real human urine with limit of detection of 0.013 mM [139]. In other study, gold nanoparticle coated with dextran were used for detecting hypochlorite (OCl^-) in swimming water. The gold nanoparticles were synthesized through green chemical process and used for different range of hypochlorite concentrations, with the results showing high sensitivity and selectivity compared with solution phase sensors. Optimizing dextran percentage is crucial as the higher concentrations of dextran could led to lower sensitivity [140]. In similar study gold nanoparticles were stabilized by pullulan and formed into tablets for detecting cysteamine. The tablets exhibited strong peroxidase-mimicking catalytic activity. The detection mechanism relies on the inhibition of this activity by cysteamine [141].

2.4.2 Compression method

There are different techniques for creating reagent tablets, including powder compression and polysaccharide encapsulation of reagents. The compression method for creating tablets involves weighing and mixing the reagents, then compressing the mixture into tablets. In 2017, Udugama et al. [142] developed a method to create color-coded tablets which could simplify and thermally stabilize diagnostic assays. They used freeze-drying to remove moisture and encapsulate bioreagent with trehalose and compress reagents to form tablets. This approach allows reagents to be pre-measured, stored without refrigeration, and easily transported for point-of-care applications, especially in resource-limited regions. The tablets were tested on various diagnostic assays, including genetic and protein-based tests. Unfortunately, this approach has some challenges including keeping reagents long term stable in different conditions, especially in high humidity and requiring costly manufacturing equipment for tablet production. In addition, the procedure needs an optimization process for some sensitive reagents like enzymes and antibodies during compression as only specific quantities are needed for each assay.

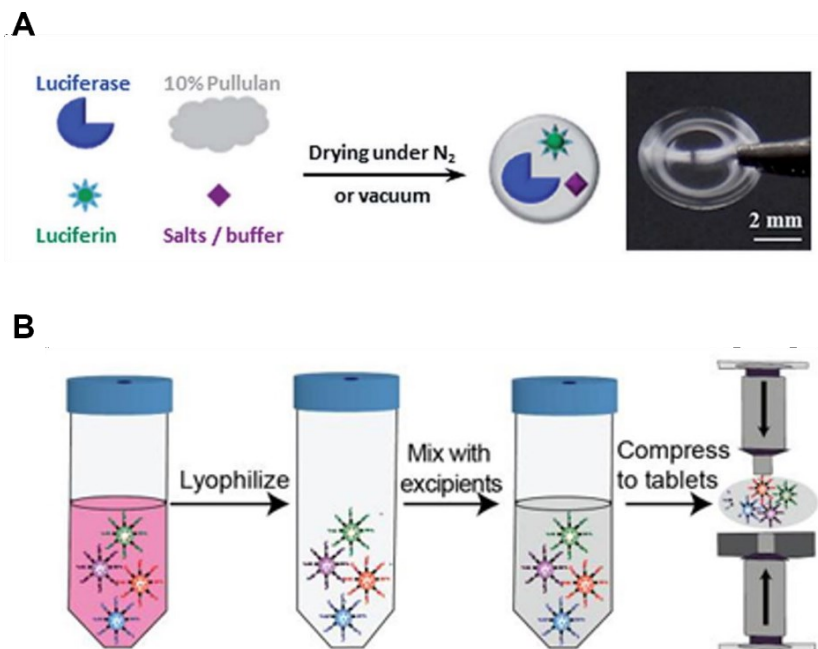


Figure 8. A. All-inclusive pullulan tablets production for ATP detection (adapted from [138]). **B.** It shows the process of creating compressed tablets (adapted from [142]).

In other study Li et al. [143] developed a special multilayer tablet that releases different chemicals at specific times. The tablets are made of cellulose-grade polymers and used for two assays: nucleic acid detection and nitrite ion detection. The design of tablets let them to be used friendly, ease of use, and low cost. The layers dissolved one by one, releasing the chemicals at the correct time for the test. However, as the time of each release was determined by compression force applied during tablet formation or altering the chemical mature of each layer, it could be difficult to control these factors and subsequently time releasing for more complex tests. Besides, the tablets have particular formulation which limit their flexibility to use for different essays.

2.4.2.1 Auto-mixing tablets

One challenge for the compressed tablets is they often require shaking to fully mix and release the reagents and create a uniform solution. To overcome this issue, some studies have used effervescence materials such as citric acid and sodium bicarbonate in the formulation. These auto-mixing tablets are indeed formed using the compression method. After these materials combined in contact with water, they led to release of carbon dioxide gas, which creates bubbles, and helps

to accelerate the dissolution in solution. This effervescent reaction is what makes the tablets “auto-mixing,” as it eliminates the need for external shaking or stirring.

For example, in the study has done by Li et al. they combined sodium bicarbonate and citric acid in the core layer of the multilayered tablets to facilitate the rapid mixing and release of reagents. Auto-mixing tablets or fast-dissolving tablets have been widely used in the pharmaceutical industry because of their rapid dissolution, practicality and ease-of-use with aim of enhancing taste and drug absorption [143]. Aslani et al. used auto-mixing tablets for different therapeutic purposes. For example, in one study they utilized these tablets to deliver the potassium citrate. This study targeted patients suffering from kidney stones, as potassium citrate helps prevent the formation of calcium oxalate and urate stones [144]. In another example the amoxicillin auto-mixing tablets were developed with aim of making simple and stable medicine for treating bacterial infections, especially in children [145]. In our group’s recent approach for overcoming the barriers of solubility of tablets in different mediums is expanding the application of “auto-mixing” tablet assays in POC testing and developing the first tablet “biosensor” with auto-mixing capability with showing their applicability for challenging media such as viscous fluids (i.e., saliva) [146]. As a result, the solid auto-mixing tablets act as a portable easy-to-use detection platform that can be inserted into the sample medium and readily dissolve to initiate the assay procedure.

Chapter 3: Copper detection

This chapter presents the development of auto-mixing tablets for rapid copper detection in water. It explains the tablet fabrication process, testing method, and performance evaluation. The tablets are simple, portable, and user-friendly, offering accurate results with minimal equipment. The chapter includes results on sensitivity, selectivity, real water sample testing, and tablet stability over time. This chapter is based on a submitted journal manuscript titled "On-site detection of copper in water using auto-mixing tablet sensor", Maryam Mansouri, Seyed Hamid Safiabadi Tali, and Sana Jahanshahi-Anbuhi. (Submitted, 2025)

Additionally, here are links to two videos providing visual insight for this chapter: 1- A comparison of the format of traditional and auto-mixing tablets. [Video 1: [Link](#)]. 2-A demonstration of the challenges encountered with the powder formulation. [Video 2: [Link](#)]

Author Contributions: MM: conceptualization, investigation, methodology, formal analysis, validation, prepared figures, software, validation, visualization, writing – original draft, review and editing; SHST: conceptualization, visualization, methodology, validation, formal analysis; SA: conceptualization, project administration, validation, supervision, reviewing & editing, funding acquisition, resources.

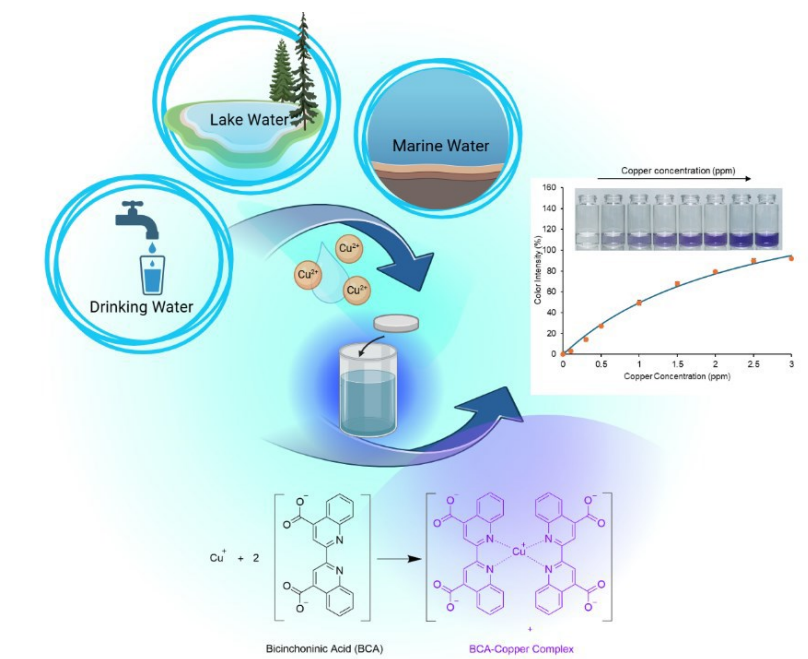


Figure 9. Graphical abstract illustrating a on-site detection of copper in water using auto-mixing tablet sensor.

3.1 Introduction

In the human body, copper (Cu) acts as a crucial cofactor and structural component in numerous enzymes, participating in vital metabolic processes [52–54]. It supports the normal functioning of the brain and nervous system, maintains the elasticity of blood vessels, aids in the formation of collagen and elastin, and regulates hemoglobin levels [56]. However, excessive copper intake can have harmful effects. Elevated copper levels have been linked to gastrointestinal issues, liver and kidney damage, and neurodegenerative diseases such as Menkes, Wilson’s, and Alzheimer’s [27–30]. Additionally, excessive copper endangers the survival of aquatic organisms and reduces the self-purification capacity of natural water systems [58,59]. Therefore, adequate copper intake from food and drinking water is crucial for living organisms. The World Health Organization (WHO) has set the permissible limit for copper ions (Cu^{2+}) in drinking water at 2.0 mg/L [60]. However, Cu^{2+} concentrations in some local water sources exceed this threshold. Therefore, there is an urgent need to develop highly sensitive and selective methods for Cu^{2+} detection.

Various conventional methods have been developed for this purpose, including inductively coupled plasma detectors [147,148], atomic absorption spectroscopy [149], surface plasmon resonance detectors [150,151], X-ray fluorescence spectrometry [152], neutron activation analysis [153,154] and plasma-optical emission spectrometry [155–157]. While these methods have been validated for accuracy and sensitivity, their application for on-site Cu^{2+} detection is constrained due to their time-consuming nature, complexity, and high equipment costs [158]. Considering these limitations, researchers have focused on developing easy-to-use, rapid, and inexpensive detection methods for Cu^{2+} . Among the available detection techniques, colourimetric sensors have gained particular attention due to their simplicity and suitability for on-site analysis [159,160]. Therefore, in developing and underdeveloped countries, there is still a critical need for simple, rapid, and cost-effective detection methods for diagnostics and environmental monitoring to support sustainable public health [161]. Limited availability of experts, laboratories, transportation options, and financial resources often leads to delayed analyses, exacerbating the risks associated with contamination. To achieve this, point-of-use devices offer compact, portable, and user-friendly solutions ideal for practical on-site determination of various elements [162–164].

POC devices are used mainly in healthcare to test patients, while point-of-use devices are used in the field to test environmental samples. Recent studies in point-of-use and point-of-care (POC) diagnostics have explored various detection methods in liquid environments, including microfluidic paper-based microfluidic devices [165–167], powder-based kits [168–170] and, more recently, tablet-based systems [137,138,171,172]. These approaches often involve releasing pre-loaded reagents during the assay to enhance detection sensitivity and achieve uniform color development, while integrating the key advantages of POC platforms. Powder-based kits offer portable, pre-measured detection; however, they often present challenges such as the dispersal of powder during handling, which requires extra attention to avoid contamination and ensure accurate dosing. Additionally, inconsistent reagent dosage and the need for manual shaking or mixing to achieve complete dissolution can compromise test reliability. Tablet-based sensors have emerged as promising alternatives, offering pre-measured dosages, improved assay repeatability, ease of handling, and enhanced reagent stability [139,173–175]. However, traditional tablet-based copper detection kits often require physical crushing or stirring to dissolve fully, limiting their development and standardization [171,172].

To address these challenges, we developed a novel copper-sensing platform based on solid auto-mixing tablets. By incorporating optimized quantities of effervescent agents specifically citric acid and sodium bicarbonate, into the tablet matrix, we enabled a self-mixing mechanism. When in contact with water, these agents generate carbon dioxide (CO_2), creating vortices that enhance the dissolution of tablet contents. Gas-generating formulations have previously been in drug delivery systems [176,177], pharmaceutical industry [143,144], cleaning product [178] and extraction and detection [179,180]. We demonstrate their applicability in environmental sensing by formulating an auto-mixing tablet compatible with copper-detection bioreagents, which does not require complex detection procedures such as UV-Vis spectrophotometry, or centrifugation used in other effervescence tablet studies for copper [181]. The assay employed 2,2'-biquinoline-4,4'-dicarboxylic acid (bicinchoninic acid) for the qualitative detection of Cu^{2+} ions by forming a purple-colored complex with Cu^{1+} , resulting in a visible color change [182,183]. The tablet formulation integrates all necessary components into a compact form that ensures fixed reagent dosage, reduces the risk of contamination and spillage, and offers reliable performance compared to powders and conventional tablet forms.

Here, we present a compact self-activating tablet sensor designed for the on-site detection of copper in water. These tablets integrate pre-measured reagents into a stable matrix that dissolves quickly, eliminating the need for complex sample preparation. By combining this approach with colourimetric analysis, we demonstrate a method that is both user-friendly and effective for environmental monitoring.

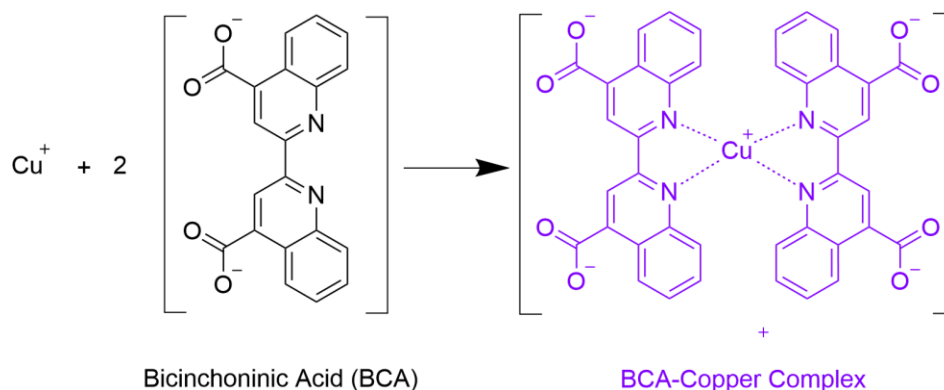


Figure 10. A colourimetric reaction of 2,2'-biquinoline-4,4'-dicarboxylic acid (bicinchoninic acid) with Cu^+ .

3.2 Chemicals and materials

All chemicals and materials were used as received. Polyvinylpyrrolidone (PVP, Cat. No. 81420), sodium bicarbonate (NaHCO_3 , Cat. No. S6014, $\geq 99.7\%$), citric acid ($\text{C}_6\text{H}_8\text{O}_7$, Cat. No. C1909, $\geq 99\%$), polyethylene glycol (PEG, Cat. No. 8.07491, Lot. S7901391), copper (II) sulfate pentahydrate ($\text{CuSO}_4 \cdot 5\text{H}_2\text{O}$, Cat. No. 209198, $\geq 98\%$), zinc sulfate heptahydrate ($\text{ZnSO}_4 \cdot 7\text{H}_2\text{O}$, Cat. No. Z4750), magnesium sulfate (MgO_4S , Cat. No. 208094, $\geq 97\%$), iron (III) chloride (FeCl_3 , Cat. No. 451649) were acquired from Sigma-Aldrich, Oakville, ON, Canada. Calcium chloride dihydrate ($\text{CaCl}_2 \cdot 2\text{H}_2\text{O}$, Cat. No. BP510, 99.0 to 105.0%) and cobalt (II) chloride hexahydrate ($\text{Cl}_2\text{CoH}_{12}\text{O}_6$, Cat. No. A16346) were obtained from Fisher Scientific, Toronto, ON, Canada. Copper detection reagent (HI3847-100) was purchased from Hanna Instruments Canada, QC, Canada. 0.5 g silica gel packs (Wisesorb) were purchased from Amazon, Canada.

3.3 Auto-mixing tablet fabrication

The tablets used in this study were prepared following the procedure illustrated in Figure 11A. Each tablet was created separately, one by one, to ensure accuracy and minimize formulation errors during laboratory-scale preparation. First, the powdered tableting agents; 15.2 mg of PVP, 3.24 mg of PEG, 52.3 mg of mannitol, 80.2 mg of citric acid, and 80.2 mg of sodium bicarbonate are weighed individually into weighting paper. The powders were then thoroughly mixed using a spatula directly on the same paper. This manual method was chosen because it offers a simple, instrument-free, and reproducible approach that is particularly effective for preparing small quantities in the laboratory. Although this fabrication approach is suitable for laboratory-scale use to maintain uniform tablet composition, industrial-scale equipment is readily available for mass production [184,185]. PEG in the tablet formulation served as a lubricant, aiding in the easy removal of tablets from the die set, while PVP functioned as a binder, holding the components together. Mannitol acted as a bulking agent, providing volume and enhance the tablet's ability to form a solid, cohesive structure. The quantities of each component were adapted from previous studies on effervescent tablet formulations optimized for reagent delivery and stability [146]. Next, approximately 100 mg of the bicinchoninic acid reagent mixture (from the Hanna copper kit) was added and blended with the powder mixture. The final mixture was transferred into a powder

pressing die (13-mm from Specac, United Kingdom). In total, the tablet weighs an average of 350 mg. Each tablet was weighed individually after fabrication using an analytical balance, and the reported average mass was calculated based on measurements from 6 tablets. The tablets were compressed using a hydraulic press machine (Tianjin17, China) at an force of 2 t (19613.3 N) for 30 seconds. After compression, the tablets were removed from the die manually by carefully tapping the back of the die against the bench to avoid mechanical damage and stored in a glass vial along with a 0.5 g commercial silica gel pack to protect it from humidity damaging.

3.4 Detection Procedure

For copper detection, 5 mL of the water sample was collected in a glass vial. A single auto-mixing tablet was added, initiating effervescence and reagent release. The reaction was allowed to proceed for approximately 1.5–2 minutes which corresponding to fully dissolution of tablet. During this time, bicinchoninic acid in the tablet reacts with reduced Cu^{1+} ions, forming a purple-colored complex [182]. A 1 M nitrite stock solution was prepared in deionized (DI) water, and all diluted solutions were prepared in DI water at room temperature. To evaluate colourimetric intensity, pictures were taken by a smartphone camera (iPhone 13 with the *Vivid Cool* filter setting), and the grayscale color intensity of the solution was analyzed in by the open-source software *ImageJ*.

3.5 Result and Discussion

Our design integrates all necessary reagents into a single solid dose that dissolves upon contact with a small volume of water. The tablet incorporates an internal gas-generating system, based on the reaction between citric acid and sodium bicarbonate, that produces carbon dioxide (CO_2), creating convective mixing without the need for manual agitation or external devices. This self-mixing feature enables rapid and uniform reagent activation, facilitating a user-friendly and reproducible assay. The detection chemistry relies on 2,2'-biquinoline-4,4'-dicarboxylic acid (bicinchoninic acid, BCA), a chromogenic reagent, for the qualitative detection of Cu^{2+} ions by forming a purple-colored complex with Cu^{1+} , resulting in a visible color change (Figure 10). In the BCA method, Cu^{1+} ions react with two molecules of bicinchoninic acid to form a stable, water-soluble, purple-colored complex which allowing sensitive colourimetric detection. A constant 5.0 mL of water was used for all samples to keep the tablet-to-water ratio the same and allow reliable comparison. The tablet formulation integrates all the necessary components (including assay reagents, auto-mixing-agents, and stabilizers) into a compact, pre-measured dose. This ensures

consistent reagent dosing, minimizes the risk of contamination or spillage, and provides reliable performance in comparison to traditional powders and tablet formats.

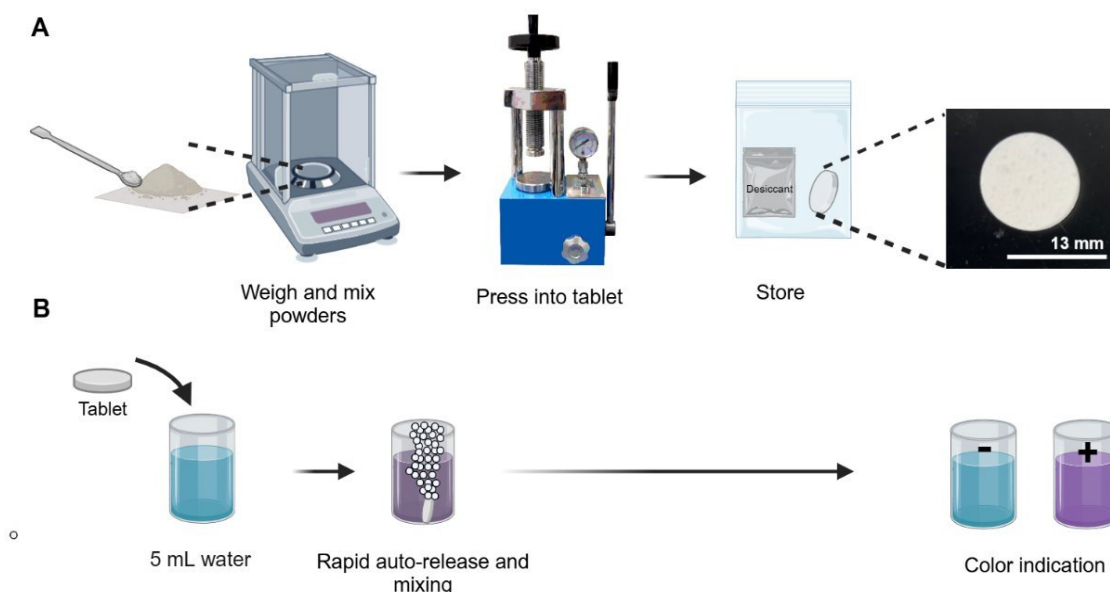


Figure 11. A. Fabrication tablet-based sensor for copper detection. Initially, all powders were measured and mixed in a weighting paper. Then, the mixture was transferred into tablet mold and pressed at force of 2 tf (19613.3 N) for 30 seconds, resulting in solid tablets. **B.** The detection procedure of copper in water samples. First, 5 ml of the water sample were collected, and a single eff-tablet is added to a glass vial. After 1.5-2 minutes of incubation, if the water sample contains copper, the purple-colored complex of bicinchoninic acid and Cu^{1+} is created. Then, the reaction between citric acid and bicarbonate will accelerate solution rate mixing.

3.5.1 Characterization

We evaluated the tablets in terms of their reagent dispersion efficiency, dissolution behaviour, weight stability, and CO_2 content to gain a better understanding of their performance. First, we assessed reagent dispersion during activation. As shown in Figure 12A (Video 2: [Link](#)), the powder-based kit exhibited material loss due to electrostatic dispersion. This was further supported by the quantitative data in Figure 12B; where three individual samples of tablets and powder packs were compared in terms of dispersion amount during activation. Tablet samples consistently

retained approximately 99% of their original weight, while powder samples showed significant material loss, with only 57.13%, 42.95%, and 78.95% of the reagent remaining. These results indicate that tablets are better suited for minimizing reagent waste and improving accuracy. Powdered reagents require careful handling and might dissolve quickly but need thorough mixing for full dissolution. To further evaluate mixing performance, we compared a traditional tablet and an auto-mixing tablet, both containing the same copper reagent concentration (2 ppm), as shown in Figure 12C (Video 1: [Link](#)). The auto-mixing tablet dissolved fully within 2 minutes, producing a uniform colourimetric response. In contrast, the traditional tablet remained partially undissolved even after 15 minutes and required vigorous shaking, making the process more labor-intensive and inconsistent.

Next step, we compared different forms of copper detection point-of-use methods; powder, traditional tablet and auto-mixing tablet, based on our own experimental data in Figure 12, as summarized in Figure 12D. Both tablets offer high dosage accuracy, ease of handling, user friendliness. However, regular tablets have lack of efficient dissolution in water and do not offer automatic mixing. Powders have the lowest dosage accuracy and variable dispersal amounts during assays. Overall, auto-mixing tablets excel in terms of convenience, accuracy, and efficiency.

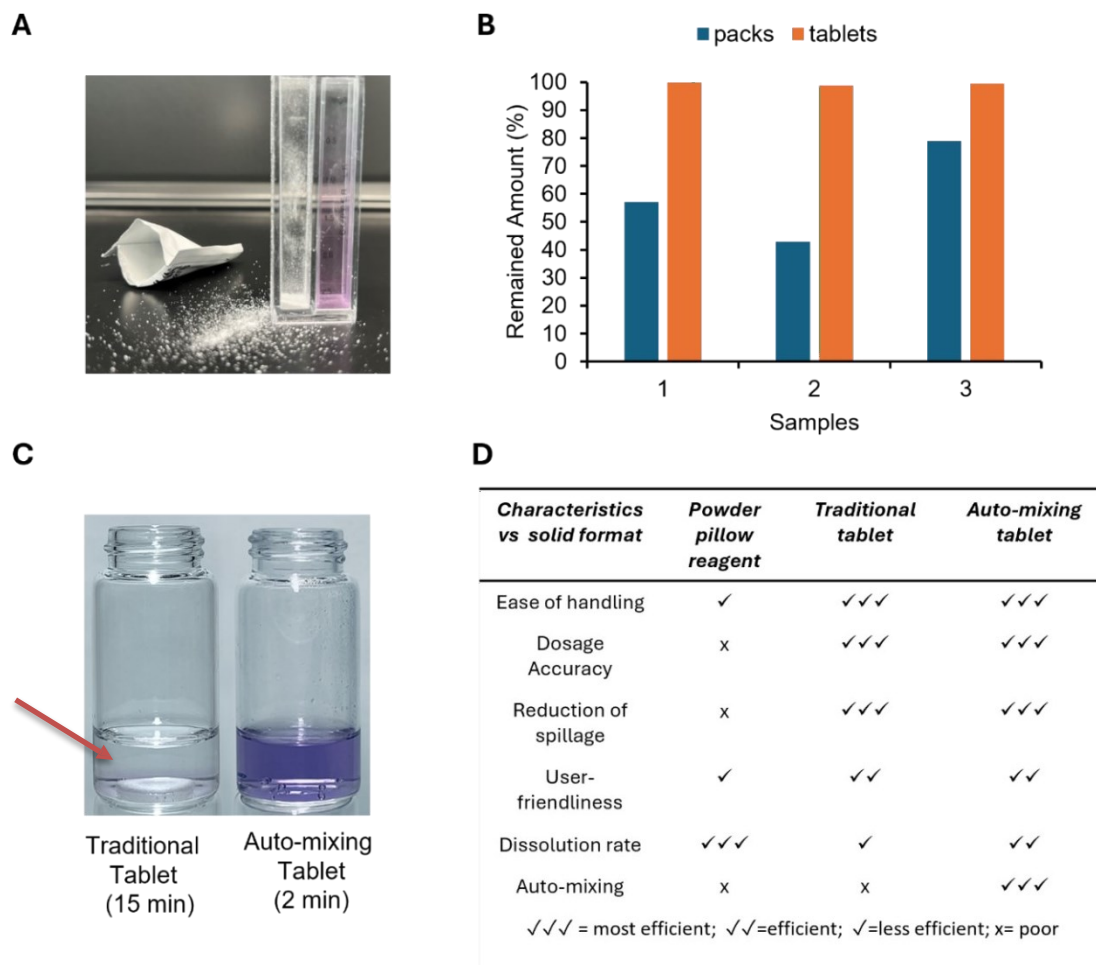


Figure 12. A. Tablet performance and dissolution behavior **A.** Image showing a powder-based kit during activation, where powder disperses due to electrostatic forces, leading to material loss despite careful handling. **B.** Comparison of the remained amount (%) between tablets and powder packs across three individual samples of tablets and powder packs. Tablets retained nearly their full initial mass with a mean of 99.36% (SD = 0.52%), while powder packs exhibited significant mass loss due to dispersion, with a lower mean of 59.68% (SD = 18.13%). The difference in retention between the two forms was statistically significant (unpaired t-test, $p\text{-value} \leq 0.05$) **C.** The performance of the auto-mixing tablets was compared with that of the traditional tablets in detecting copper (2 ppm). The auto-mixing tablet gave a uniform solution after 2 minutes, while the traditional tablet was not completely mixed even after 15 minutes. **D.** Comparison of premeasured unit dose reagents stored in different solid forms (auto-mixing tablets, traditional

tablets and powder pillow, and liquid solution) ready to use in detection assays: Performance across key aspects.

Additionally, to evaluate the structural integrity of the auto-mixing tablets, their weight was monitored over one month under room temperature storage. Tablets were periodically weighed at different time points to detect any changes. The initial average weight of 6 tablets on day 0 was 357.68 mg, with less than 2% variation observed throughout the testing period. These results confirm the tablets' structural stability over time, supporting their suitability for long-term practical use (Figure 13).

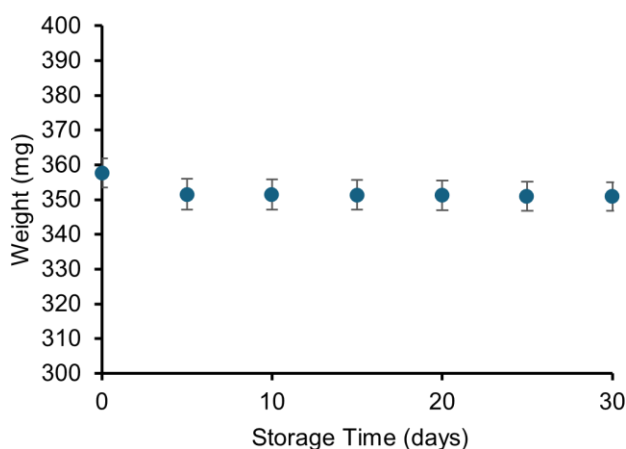


Figure 13. The stability of the weight of the tablets. Weight stability of tablets (n=6) over 30 days, with RSD less than 2%, indicating robust structural integrity. One-way ANOVA showed no statistically significant difference in weights over time (p-value > 0.09), supporting the structural stability and consistent formulation of the tablets.

Finally, the effervescence performance was also assessed by measuring carbon dioxide release, a key factor for ensuring rapid and efficient tablet dissolution. Tablets were stored in glass vials at room temperature. For each test, one tablet was reacted with 100 ml of 0.5 M sulfuric acid, and the weight change before and after dissolution was recorded. This difference was used to estimate the amount of carbon dioxide released, expressed as a percentage of the total tablet weight (~ 0.35 g). On day 0, the carbon dioxide content was ~ 0.03 g (n = 3), and remained stable over time, with

a similar value of ~ 0.04 g measured on day 30. This consistency confirms the tablets retained their effervescence capacity during storage (Figure 14).

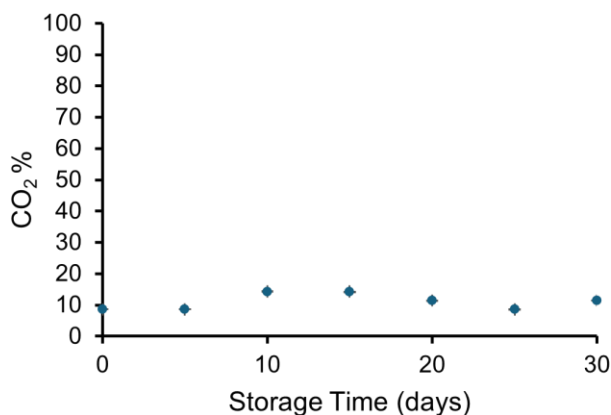


Figure 14. CO₂ content expressed as a percentage of total tablet weight over a 30-day storage period ($n = 3$). RSD remained below 0.1%, across all time points, demonstrating excellent consistency. One-way ANOVA confirmed no statistically significant difference in CO₂ content over time (p -value > 0.9), indicating chemical stability of the effervescent components throughout storage. Error bars are not visible in the plot as they are hidden by the size of the data markers due to minimal variation.

3.5.2 Detection of copper with tablets

First, 5.0 mL of the water sample was collected in a glass vial. DI water at room temperature was used as the source for all samples. Each condition was tested with three replicates ($n = 3$). The tablet was then added to the vial. The reagents are released into the solution and allow bicinchoninic acid to react with Cu¹⁺, to form a purple-colored complex with Cu¹⁺ (the reduced form of Cu²⁺), for less than 2 minutes. Bicinchoninate limited reactivity to the Cu²⁺. To determine Cu²⁺, it is first reduced to Cu¹⁺, enabling the complete assessment of both Cu¹⁺ and Cu²⁺ [182]. Meanwhile the reaction between citric acid and bicarbonate will accelerate solution rate and mixing of reagents. This process produces a uniform color development, suitable for quantification by image analysis. Figure 11B shows the detection assay of copper in water samples with auto-mixing tablets.

3.5.3 Analytical performance

Our study aims to develop a sensing device that eliminates the need for expensive laboratory instruments such as UV-Vis spectrophotometers for calibration curve generation. Instead, we employ a simplified, low-cost approach based on smartphone image capture and color intensity analysis, making the system accessible for field use and resource-limited settings. The analytical performance of the tablet colourimetric detection system was evaluated by generating a calibration curve by adding tablets to samples of known concentrations of copper. This approach allowed us to measure the correlation between the copper concentration and color intensity, which was proportional to the amount of copper present in the sample. The Michaelis–Menten equation [186], typically used to describe the kinetics of enzyme-catalyzed reactions, that adapted here to plot the relationship between the copper concentration in the samples and color intensity. The general form of the Michaelis–Menten equation is :

$$v = \frac{V_{\max} * [S]}{K_m + [S]}$$

where the v represents the reaction rate, V_{\max} is the maximum reaction rate, $[S]$ refers to the concentration of the substrate or analyte present, like copper ions in a sample. K_m , known as Michaelis constant. K_m is the amount of substrate needed for the reaction to reach half of its maximum rate. This resulted in a calibration curve with an R^2 value of 0.9953, with a linear range of 0.3-2 ppm, as presented in Figure 15A. The relative absorption intensity is linearly proportional to the concentration of copper at the first three concentrations, with a Limit of detection (LoD) of 0.3 ppm.

3.5.4 Real water sample

Next, we evaluated the utility of the auto-mixing tablet sensor in real-world conditions. Natural and treated water sources; tap and lake water samples were collected and analyzed using the auto-mixing tablets. Tap water samples from Loyola Campus, Côte-des-Neiges, and Downtown Montreal (Canada) contained copper concentrations of 2 ppm, 1 ppm, and 1.5 ppm, respectively. A lake water sample from the Marne River in Joinville-le-Pont (France), showed a concentration of 1 ppm. To assess detection accuracy and robustness, we conducted spiking tests by adding known concentrations of copper (0.5, 1, 1.5, and 1 ppm) to these samples, as shown in Figure 15B. Spiking enables validation of the tablet's ability to detect both native and added copper accurately,

ensuring reliable differentiation of the target analyte. Method validation was performed using the H13847 standard Hanna copper kit to determine total copper content. The concentrations measured with the auto-mixing tablets closely matched those obtained with the standard method, confirming the assay's accuracy and effectiveness for real-world copper detection. The standard method confirmed the assay's accuracy and effectiveness for real-world copper detection. As shown in the table, for all tested samples, both the semi-quantitative and quantitative results from the tablet-based method closely matched those from the standard method, demonstrating high accuracy and precision. In the semi-quantitative evaluation, naked-eye color comparisons showed that the color developed with the auto-mixing tablets was consistent with the standard method. For quantitative analysis, the color intensity of the real samples was captured using a smartphone and analyzed with ImageJ software. The calculated relative standard deviations (RSD) were 1.86% for samples from Loyola Campus, 6.86% from Côte-des-Neiges, 4.14% from Downtown Montreal, and 4.48% from the Marne River (Joinville-le-Pont, France), all below 6.9%. These values further confirm the precision and reliability of the tablet-based assay for practical copper detection.

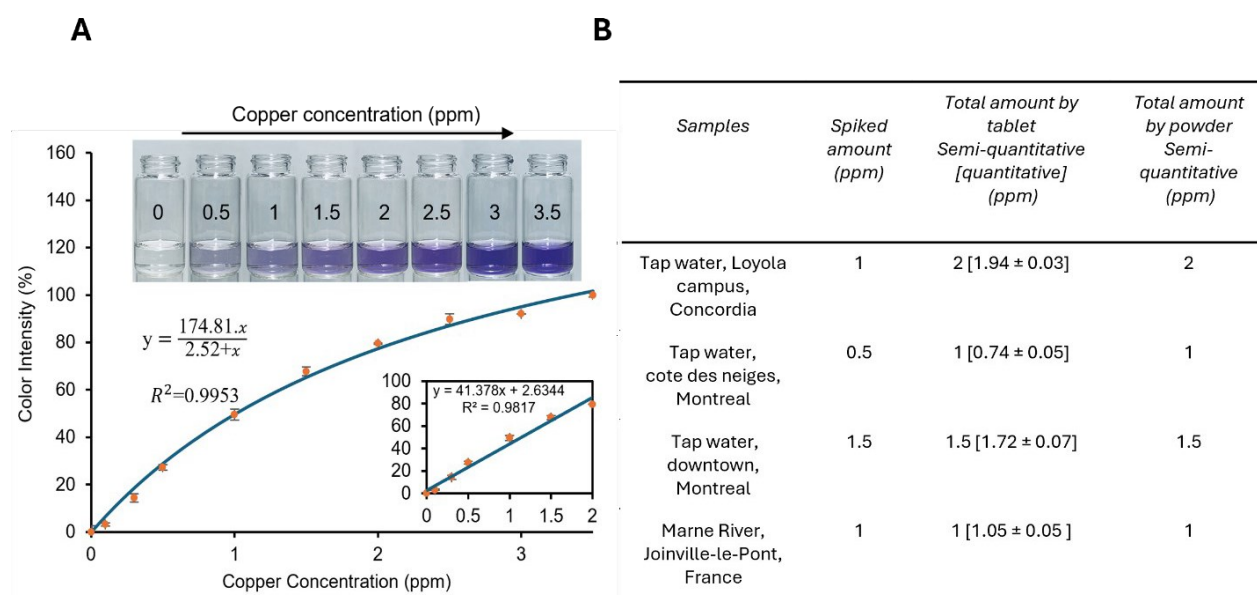


Figure 15. A. Analytical performance of the assay. The relationship between copper concentration and color intensity in the tablet colourimetric detection system, creates the calibration curve. The curve demonstrates a high degree of fit, with an R^2 value of 0.9953, with a linear range of 0.3-2 ppm. The LoD is marked at 0.3 ppm, and the working range of 0.3-3 ppm. **B.** Comparison between

the results of auto-mixing tablets and standard method for the different spiked amounts of copper in real water samples ($n=3$). The results obtained with our auto-mixing tablets were consistent with the total copper content determined using the standard method with RSD% less than 6.9, confirming the tablets' effectiveness in accurately detecting copper concentrations in real-world.

3.5.5 Selectivity analysis for copper detection with eff-tablets

To evaluate the selectivity of the sensor, we tested potential interferences commonly found in natural waters including magnesium (Mg^{2+}), calcium (Ca^{2+}), zinc (Zn^{2+}), cobalt (Co^{2+}), iron (Fe^{3+}) at 50 mg/l concentration. This concentration is significantly higher than the copper concentration in the spiked samples (1.5 ppm), which is a standard approach in interference studies. Testing at higher concentration ensures the sensor can detect even minor effects, thereby confirming the sensor's selectivity. To assess potential interference, we conducted detection experiments for spiked ion sample with adding one tablet to 5 mL of each solution. The results demonstrated a distinct color change only in the presence of copper, while the other ion samples maintained a colorless-grey appearance as illustrated in Figure 16.

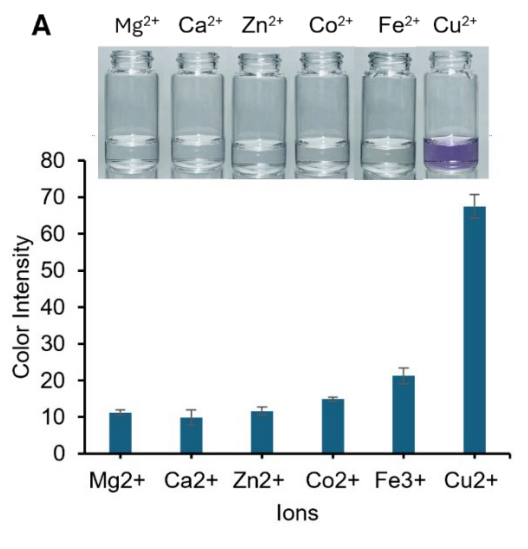


Figure 16. Potential Interference of copper was tested among common water ions Mg^{2+} , Ca^{2+} , Zn^{2+} , Co^{2+} , Fe^{3+} at 50 mg/l concentrations. While the working solution remained colorless for all other ions, a copper sample of 1.5 ppm was able to turn the solution purple, indicating the sensor's specificity for copper detection. One-way ANOVA, $p\text{-value} < 0.0001$, confirmed a statistically significant difference in color intensity among ions.

3.5.6 Stability tests: over period of time

The stability of the tablets was assessed over a period of three months by evaluating their performance and activity at 1, 4, and 8 weeks. Tablets were stored at room temperature in glass vials containing silica gel. Each month, samples spiked with 2 ppm of copper were analyzed to determine the copper content. In each experiment, one tablet was added to 5 mL of the sample, and the color intensity was measured in 2 minutes, after fully dissolving the tablet ($n=3$). This procedure was repeated three times to ensure the reliability of the results. The findings demonstrate that the developed tablets effectively maintain their functionality and sensitivity for up to three months at room temperature. The remarkable stability of these tablets ensures reliable performance, facilitating extended storage and transport to remote locations, as well as enabling cost-effective handling and use by non-experts. The data are presented in Figure 17, showing the stability profile of the tablets over the tested period.

In addition to evaluating stability, we compared our sensor system with several commercial copper detection kits to highlight the field-readiness and practical advantages of our proposed rapid auto-mixing tablets (Table 1). Compared to other kits, our auto-mixing tablet does not require crushing or manual force for dissolution due to its effervescent property, enabling quick automatic mixing. In contrast to powder-based kits, our tablet minimizes the risk of spillage and dispersal of powder during handling, ensures more precise reagent dosing, and eliminates the need for shaking or manual mixing. Furthermore, our system simplifies the detection process by eliminating the need for expensive and bulky laboratory instruments such as UV-Vis spectrophotometers or colorimeters, relying instead on straightforward image capture for quantification. These features make our tablets more user-friendly, portable, and highly suitable for field applications.

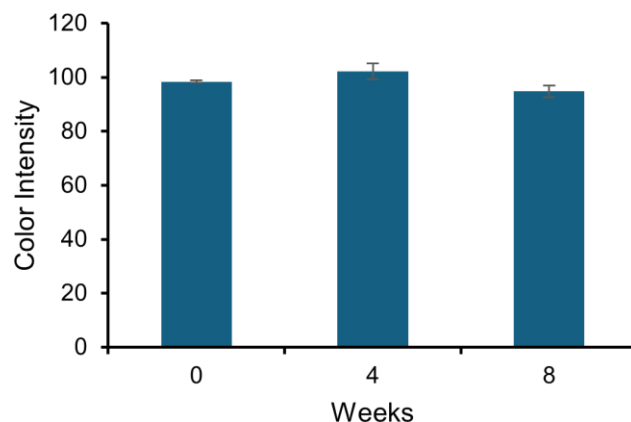


Figure 17. Stability of the auto-mixing tablets over an 8-week storage period ($n = 3$). The average color intensity at week 8 retained 96.29 ± 2.14 % of the original color intensity at week 1. RSD remained below 3%, confirming high reproducibility and consistent detection performance during storage.

Table 1. Comparison of the proposed auto-mixing tablet sensor with some commercial copper kits in terms of mixing efficiency and user-friendliness. A ✓ indicates the feature is present, while a ✗ indicates a challenge or limitation.

Product name/Ref	Format	Auto-mixing	Notes, Dissolving requirements	User-friendliness	Notes, Method of detection
Palintest Copper Reagent Tablets [172]	Tablet		✗, Crushing prior to dissolution		✗, Photometers
Lovibond Copper No. 1 Tablet Reagents [171]	Tablet		✗, Crushing prior to dissolution		✓, Visual
Thermo Scientific AC2029 Copper Reagent Tablets[187]	Tablet		✓, Rapid dissolution		✗, Colorimeter/spectrophotometers

Wilhelmsen Copper No.1 Tablets[188]	Tablet		N/A		✗, Photometers
Hanna Instruments Copper Test Kit[189]	Powder		✗, Shaking		✓, Visual
Hach Copper Reagent Set[190]	Powder		✗, Shaking		✗, Spectrophotometer
Merck Spectroquant® Copper Test (114767)[191]	Liquid		✗, Shaking		✗, Spectrophotometer
AquaPhoenix Copper Test Kit[192]	Liquid		✗, Shaking		✓, Visual
This work	Tablet		✓, Spontaneous rapid dissolution		✓, Visual or smartphone-based

3.7 Conclusion

This study showed the use of auto-mixing tablets for rapid, on-site copper detection in water, with combining bicinchoninate reagents with PEG, PVP, and mannitol in an effervescent base made of citric acid and sodium bicarbonate. The formulation was designed to promote quick release of reagents upon contact with water. The tablets were developed through a simple powder compression technique, offering consistent size and uniform composition. The tablet exhibited performance with high reproducibility (RSD < 3%). Also, tablet weight variation remained under 2%, and carbon dioxide remained consistent over one month at room temperature. The sensor covered a copper concentration range of 0–3 ppm, with a detection limit of 0.3 ppm, demonstrating strong selectivity, stability over eight weeks in glass vials at room temperature, and reliable performance in real water samples.

Chapter 4: Nitrite detection

This chapter describes the development of pullulan-based tablets for simple and user-friendly nitrite detection in soil using the Griess reaction. It details the fabrication of dual and all-in-one tablets with pullulan for reagent stabilization, optimized buffer conditions, and application to real soil samples. The tablets show high sensitivity, selectivity, and long-term stability at room temperature. This chapter is based on a submitted journal manuscript titled "User-friendly Detection of Nitrite in Soil Samples with Tablet-Based Sensor", Maryam Mansouri, Seyed Hamid Safiabadi Tali, Zubi Sadiq, and Sana Jahanshahi-Anbuhi. (revision requested, 2025)

Author Contributions: MM: conceptualization, investigation, methodology, formal analysis, validation, prepared figures, software, validation, visualization, writing – original draft, review and editing; SHST: conceptualization, methodology, validation, formal analysis; ZS: methodology; visualization, review and editing; SA: conceptualization, project administration, validation, supervision, reviewing & editing, funding acquisition, resources.

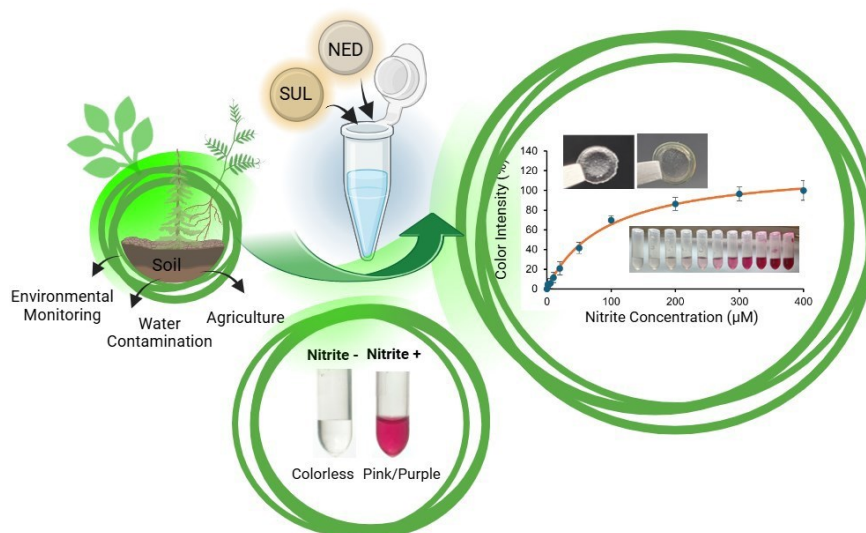


Figure 18. Graphical abstract illustrating a tablet-based sensor for user-friendly detection of nitrite in soil samples through a colourimetric reaction using SUL and NED reagents.

4.1 Introduction

Nitrite (NO_2^-) as a transitional compound within the broader nitrogen cycle, creating during the oxidation of ammonium (NH_4^+) and eventually converting to nitrate (NO_3^-) [63]. This conversion is fundamental to soil nutrient dynamics, especially for plant-accessible nitrogen. Increased agricultural demand has led to the overuse of inorganic fertilizers, which often contain nitrite as a component. This has exacerbated nitrogen leakage into the environment. The excessive accumulation of nitrite in soil can lead to significant environmental concerns such as eutrophication in water bodies and proliferation of harmful algal blooms. This phenomena reduce oxygen levels, disrupt biodiversity, and may produce toxins hazardous to humans and animals [64–67]. Additionally, nitrite contamination poses serious health risks, such as methemoglobinemia (blue baby syndrome) [37,69], central nervous system abnormalities [70], and an increased incidence of gastric and esophageal cancers due to the formation of carcinogenic nitrosamines in the stomach [36,68]. Given these risks, effective monitoring of nitrite levels in soil is a critical step in environmental pollution management and sustainable agriculture practice.

Establishing universal regulatory limits for nitrite concentrations in soil is challenging due to the variability in soil composition, regional agricultural practices, and environmental conditions. Based on our research, currently, there are no widely accepted international standards specifically for nitrite levels in soil [193]. While direct soil nitrite regulations are limited, it's important to consider the implications of nitrite levels in soil on environmental health. Elevated nitrite concentrations can leach into groundwater, potentially contaminating drinking water supplies, where standards are well-defined. For instance, the World Health Organization (WHO) guidelines specify a 3.0 mg/L (65.2 μM) limit for nitrite in drinking water and wildlife protection, while the U.S. Environmental Protection Agency (EPA) sets a Maximum Contaminant Level of 1 mg/L (21 μM) [71,72]. Although these regulations do not explicitly address soil, they highlight the potential risk of nitrite leaching into groundwater or nearby water sources. Consequently, reliable methods to detect and quantify nitrite in soil are critical for preventing adverse environmental and health impacts.

Nitrite can be detected using various methods, including chemiluminescence [194–196], capillary electrophoresis [197], chromatography [198], spectroscopy [94], fluorescence [199,200], electrochemical techniques [201,202] and colourimetric methods [107,203]. Among colourimetric

methods, the Griess reaction, first described in 1879 [106], remains one of the most widely used methods for nitrite analysis due to its simplicity, cost-effectiveness, specificity, sensitivity and practicality [94]. It continues to be extensively employed in numerous studies in recent years [41,204,205]. However, most traditional detection methods are costly, complex, and require specialized facilities and skilled operators, highlighting the need for point-of-use and point-of-care (POC) devices. These devices enable simple, portable, and user-friendly nitrite detection without requiring laboratory analysis. Research is ongoing on incorporating Griess assay in different POC platforms such as paper-based analytical devices, screen-printed electrode (SPE)-based, and polymer-based devices. However, these methods often suffer from limitations such as lack of stability at room temperature, complexity in fabrication, and insufficient sensitivity (Table 2).

Tablet-based sensors, provide a robust platform for on-site detection of analytes. These sensors enhance assay repeatability through pre-measured reagents, simplify handling, and improve reagent stability. Advances in polysaccharide encapsulation techniques, such as the use of pullulan, a polysaccharide readily dissolvable in water, have enabled the development of all-in-one bioassay tablets [137,138], while solving the complex fabrication process of other table-based methods used for nitrite detection [206]. Also, pullulan's ability to stabilize sensitive bioreagents at room temperature makes it a valuable material for POC applications, especially in regions with limited facilities [24,139].

Leveraging pullulan-based tablets to address the aforementioned challenges, this study focuses on the development of a novel tablet-based sensor for simplified detection of nitrite in soil. First, we demonstrate the applicability of the pullulan encapsulation method for Griess reagents to create highly stable sensors with high sensitivity. Then, using these tablets, we prepare a complete assay kit with an optimized buffer, ensuring reliable nitrite detection even under neutral and basic sample conditions and overcoming challenges posed by soil's varying pH levels. This approach combines the sensitivity and convenience of point-of-use and point-of-care (POC) devices with the stability and efficiency of polysaccharide encapsulation, offering a practical solution for nitrite monitoring in soil.

In the following sections, we demonstrate for the first time that the Griess reagents, including sulfanilamide (SUL) and N-(1-naphthyl)ethylenediamine (NED), can be successfully encapsulated in polysaccharides to form stable tablets for nitrite detection in soil. We systematically investigated

factors affecting tablet performance, including pullulan concentration and buffer conditions, while comparing the functionality of the dual-reagent system with the all-in-one reagent formulations. Further, we evaluated their practicality for real-world applications and assessed their stability over a six-week period. These tablets enable precise and affordable nitrite detection in soil samples. This tablet-based platform offers a practical, affordable, and scalable solution, enhancing soil monitoring and advancing environmental management.

4.2 Chemical and material

All reagents and chemicals were of analytical grade. Citric acid monohydrate (Cat. No. C1909), N-(1-naphthyl)ethylenediamine dihydrochloride (Cat. No. 33461, $\geq 98\%$), sulfanilamide (Cat. No. S9251, $\geq 98\%$), copper (II) sulfate pentahydrate ($\text{CuSO}_4 \cdot 5\text{H}_2\text{O}$, Cat. No. 209198, $\geq 98\%$), zinc sulfate heptahydrate ($\text{ZnSO}_4 \cdot 7\text{H}_2\text{O}$, Cat. No. Z4750), magnesium sulfate (MgO_4S , Cat. No. 208094, $\geq 97\%$), iron (III) chloride (FeCl_3 , Cat. No. 451649), Sodium nitrate (Cat. No. S5506, $\geq 99\%$), Mercury (II) chloride (HgCl_2 , Cat. No. 215465) were purchased from Sigma-Aldrich, USA. Pullulan (average Product. No. 21115, Mw: ~ 200 kDa), was obtained from Polyscience, Inc., USA. Sodium nitrite (Cat. No. 014244, $\geq 97.0\%$), Calcium chloride dihydrate ($\text{CaCl}_2 \cdot 2\text{H}_2\text{O}$, Cat. No. BP510) and cobalt (II) chloride hexahydrate ($\text{Cl}_2\text{CoH}_{12}\text{O}_6$, Cat. No. A16346), Lead (II) nitrate ($\text{Pb}(\text{NO}_3)_2$, Cat. No. A16345, 99%), were obtained from Fisher Scientific, Canada. 0.5 g silica gel packs (Wisesorb) were purchased from Amazon, Canada, and carbon steel trays (Betty Crocker) were purchased from a local store, Canada. Real soil samples were attained in Montreal, CA. Deionized water obtained from Sigma Aldrich, USA was used to prepare all solutions.

4.3 Tablet fabrication

First, N-(1-naphthyl)ethylenediamine dihydrochloride (NED) solution (0.5 mg/mL) was prepared in 10 mL of deionized water. Subsequently, sulfanilamide (SUL) solution (5 mg/mL) was prepared in 10 mL of a 0.05 M citric acid solution. The concentrations and volumes of NED and SUL used in this study were based on the standard Griess assay protocol [1]. For tablet fabrication, 100 μL of each solution was used per tablet. Pullulan-based encapsulation methods have previously been demonstrated by our research group for other reagents[24][139]. This work marks the first successful encapsulation of the Griess assay into pullulan-based tablets. The next step, percentage of pullulan was tested on shape and physical consistency of tablet formation, 3%, 4% and 5% w/v pullulan were added to each mixture solution of SUL and NED, followed by thoroughly

mixing using a vortex mixer (Model# 945FIA-LUS, 50/60 Hz, Fisherbrand, Waltham, MA USA) to ensure the complete dissolution of the chemical compounds. **Dual tablets creation:** A pipette drop-casting method was used to prepare the solid polysaccharide-encapsulated tablets, in which 100 μL of each individual SUL and NED solution was dispensed onto a flat carbon-steel tray. The liquids were then allowed to dry on the tray for 24 h at room temperature (22°C) in a dark environment, as the reagents are light sensitive. The tablets were formed by air drying at room temperature, producing solid discs. **All-in-one tablets creation:** Assay reagents of N-(1-naphthyl)ethylenediamine dihydrochloride (NED) solution (0.5 mg/mL) and sulfanilamide (SUL) solution (5 mg/mL), were pre-mixed and combined in a 1:1 ratio, and then 5% w/v pullulan was added to mixed solution. The volume of 200 μL of the all-in-one solution, equivalent to the total reagent volume used in the dual-tablet method, was dispensed onto a carbon-steel tray and led to dry for 24 h at room temperature in a dark environment. After drying, the resulting single integrated tablets were collected and stored in a glass vial with silica gel packs at room temperature for future use (Figure 19).

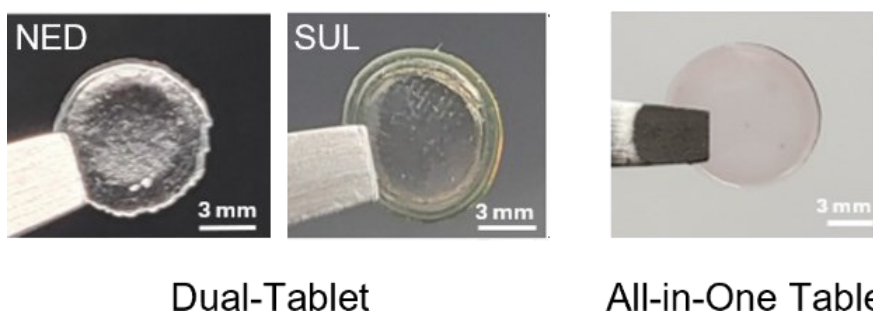


Figure 19. The actual images of the tablet systems used for nitrite detection: Dual-Tablet, and All-in-One Tablet. These tablets contain 5% w/v pullulan, giving uniform circular shape and a firm, easy-to-handle physical structure.

4.6 Detection of nitrite by tablets

The stock solution of nitrite (1 mM) was prepared by dissolving sodium nitrite in deionized water. Subsequently, various nitrite concentrations (1–400 μM) were prepared. Nitrite detection was carried out using the Griess assay reaction (Figure 20) specifically under acidic conditions, with a pH around 2.5 to 3 to facilitate the diazotization process [107,207]. For this aim we solved the tablets in citrate–phosphate buffer to have a consistence acidic condition for tests. For the next

step, we tested effect of buffer concentration on detection assay. For this purpose, different concentrations of citrate–phosphate buffer solution with a pH of 3 were prepared. Equal amounts of sodium phosphate dibasic and citric acid (1 M) were mixed, followed by the addition of citric acid for pH adjustment. With **Dual-Tablet** (NED and SUL): For each test, two tablets of NED tablet and SUL tablet, were dropped and mixed in a tube that contains 200 μL of citrate–phosphate buffer. Then, 300 μL of the different nitrite concentrations was added to the reagent mixture. With **All-In-One tablet**: One tablet containing both SUL and NED with same ratio was dissolved in 200 μL of water in a tube and 300 μL of the nitrite solution was added to it. For all tests after 2 minutes, pictures were taken by a smartphone camera (iPhone 13 with), and the grayscale color intensity of the solution was analyzed in by the open-source software *ImageJ*.

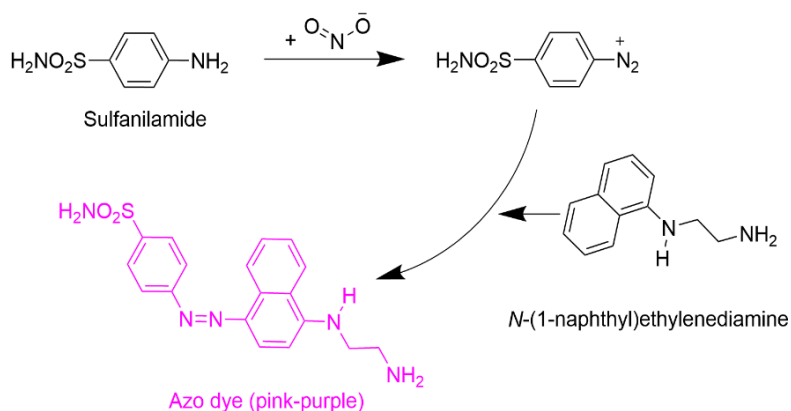


Figure 20. The schematic represents the Griess assay used for nitrite detection, which involves a two-step reaction. First, sulfanilamide reacts with nitrite ions, producing a diazonium cation. This cation then reacts with N-(1-naphthyl)ethylenediamine dihydrochloride, resulting in the formation of a purple-pink azo dye.

4.5 Real samples

A fixed volume of soil sample (equivalent to 5 mL in a compressed form) was taken from different areas in Downtown, Berri St and Notre-Dame-de-Grâce (NDG) in Montréal, and deionized water was added to reach a total volume of 15 mL. The mixture was thoroughly shaken by hand at room temperature until fully dispersed, then was left to settle for approximately 30 minutes. The supernatant solution was carefully extracted and centrifuged at 14,000 rpm for 3 minutes to

enhance the separation of water-soluble components (Figure 21A). The clear liquid supernatant was used as the test sample in citrate–phosphate buffer, following the same method as illustrated in Figure 21B.

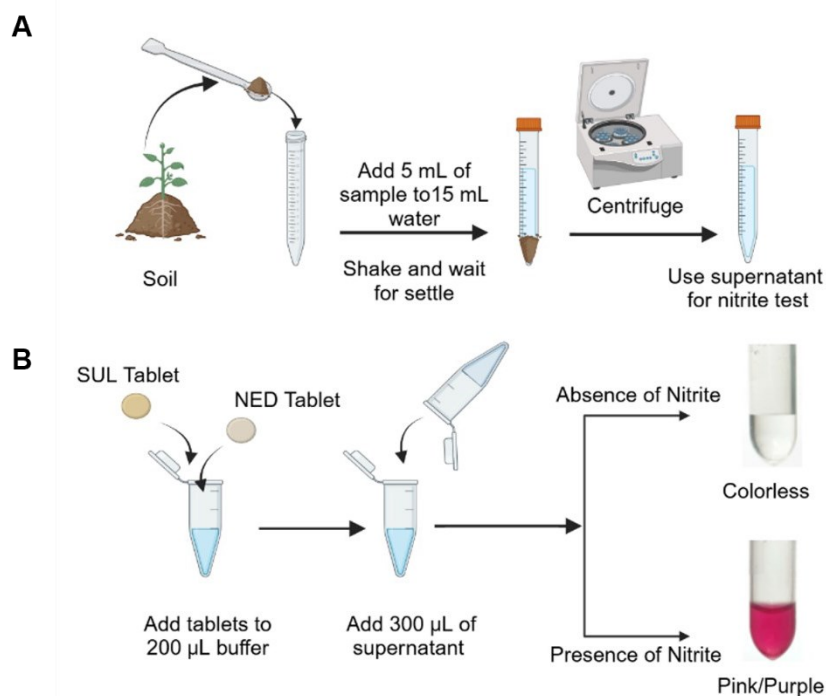


Figure 21. A. Sample preparation for detection of nitrite in soil samples: First, 5 mL of compressed soil samples were added to a tube and diluted with water to a total volume of 15 mL. The mixture was shaken thoroughly and allowed to settle. The supernatant was then collected and used as the test sample. **B.** Detection procedure of nitrite in soil samples: Two tablets (NED and SUL tablets) were added to a pre-loaded buffer test tube. Then the sample solution was added to the mixture. In the presence of nitrite, an azo dye forms, indicating the presence or absence of nitrite in the sample.

4.6 Results and discussion

The tablet-based sensors were designed to detect nitrite in soil samples through the chemical reaction between Griess reagents and nitrite. The initial studies focused on the percentage of pullulan required for formation of functional and easy-to-handle tablets to optimize the physical and functional properties of the tablets. According to our results, 5% w/v pullulan provides an optimal balance, ensuring both physical stability and adequate solubility in water for effective performance. Next, as the molarity of the buffer impacted the color intensity of the tests, the effect of buffer concentration on detection assays was studied. The Griess assay for nitrite detection is

only effective in acidic conditions, making it unreliable for nitrite detection in alkaline samples due to color variations. To overcome this, we optimized the buffer concentration to ensure consistent sensor performance across a wide pH range of samples (3–13), which is crucial for soil with varying pH levels. Different concentrations of citrate-phosphate buffer (0.2–1 M, pH 3) were tested using a 50 μ M nitrite solution, and results showed that 0.5–1 M buffers provided more reliable color intensity, comparable to standard test using deionized (DI) water without a buffer, as displayed in Figure 22A. To confirm the most effective buffer concentration for maintaining acidic conditions, we further tested its performance in nitrite-spiked solutions with different pH levels (3, 7, 13) to confirm its stability under varying soil sample pH conditions. Among the tested concentrations, 1 M citrate-phosphate buffer demonstrated the highest consistency in maintaining color across samples with pH 3, 7, 13. This ensures that the assay remains acidic regardless of the sample's pH, which is particularly important for soil analysis (Figure 22B).

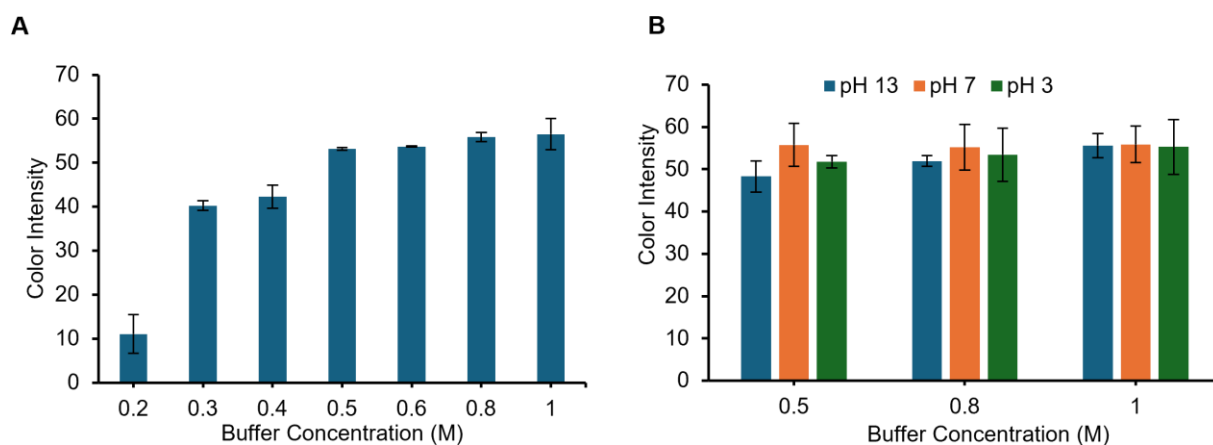


Figure 22. Color intensity increased with buffer concentration (0.2–1 M, $n = 3$). One-way ANOVA (p -value < 0.0001) indicated a highly significant effect of buffer concentration on color intensity. Tukey's HSD confirmed that 0.5–1 M buffers gave significantly higher and more consistent signals than concentrations ≤ 0.4 M (p -value < 0.001). **B.** Compatibility tests were conducted at 0.5 M, 0.8 M, and 1 M buffer concentrations ($n = 3$) under acidic, neutral, and basic pH.. Two-way ANOVA showed significant effects of buffer (p -value < 0.0001), pH (p -value < 0.05), and their interaction (p -value < 0.001). Among these, the 1 M buffer provided the most consistent results across all tested pH conditions. One-way ANOVA and Tukey's HSD, (p -value > 0.9).

Further, we performed a kinetic study with a concentration of 50 μM nitrite to evaluate the optimal time for reading the results as well as to compare the all-in-one tablet (Figure A1) activity with the condition where SUL and NED tablets were separately added to the solution. The time course of light absorbance was measured for nitrite samples spiked with nitrite using a UV-Vis spectrometer (BioTek, Cytation 5). In both readings, we included a control sample that did not contain nitrite to account for background color intensity. Kinetic behavior was studied over a period of 20 minutes, with absorbance measured at 548 nm at 15-second intervals. Within the first 20 seconds of reaction, the absorbance of the samples exhibited minimal variation, indicating that the reaction had reached completion, and the color intensity had stabilized. This suggests that the sensor response achieved saturation well before the 20-second mark, as shown in Figure 23. Although the detection reaction is completed less than 1 minute as tablets were pre-dissolve, a 2-minute period was selected for assay readings to allow sufficient time for complete tablet dissolution in the buffer solution.

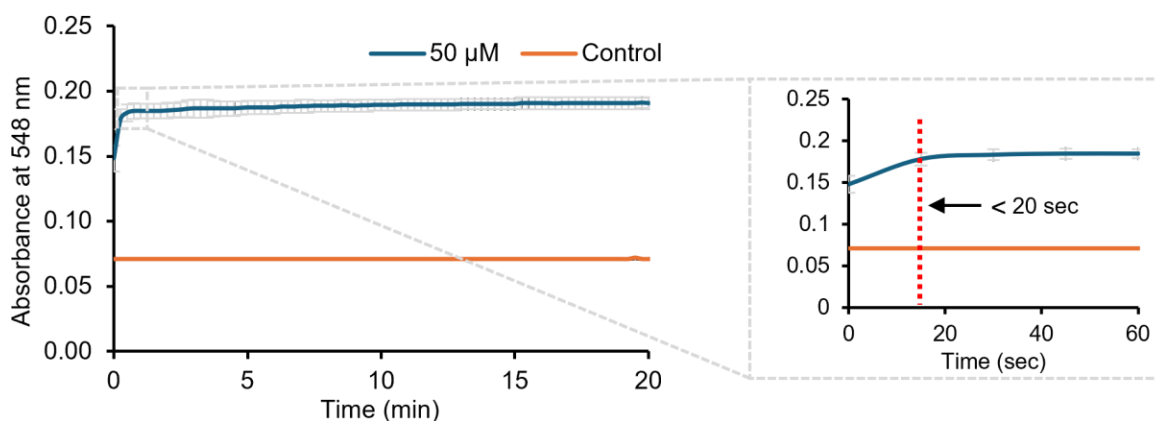


Figure 23. The kinetic study of nitrite detection using NED and SUL tablets at a concentration of 50 μM nitrite indicates that the reaction is complete in less than 20 seconds.

4.7.1 Analytical performance

To evaluate the analytical performance of the tablet-based colourimetric detection system, a calibration curve was generated by adding samples with varying nitrite concentrations. The color of the solution changed proportionally to the nitrite concentration, allowing for the correlation between nitrite concentration and color intensity to be measured. The Michaelis–Menten equation

was used to plot the relationship between nitrite concentration and color intensity. The Michaelis–Menten equation [186], typically used to describe the kinetics of enzyme-catalyzed reactions. The general form of the Michaelis–Menten equation is :

$$v = \frac{V_{\max} * [S]}{K_m + [S]}$$

where the v is a the reaction rate, V_{\max} represents the maximum reaction rate, $[S]$ is the concentration of the substrate or analyte, like nitrite ions in a sample. K_m , known as Michaelis constant, indicating the substrate concentration at which the reaction rate reaches half of V_{\max} . resulting in a calibration curve with an R^2 value of 0.9971, as shown in Figure 24. A LoD of 3 μM was calculated in a buffer medium. The same procedure was used to create the calibration curve for the all-in-one

tablets (Figure A2).

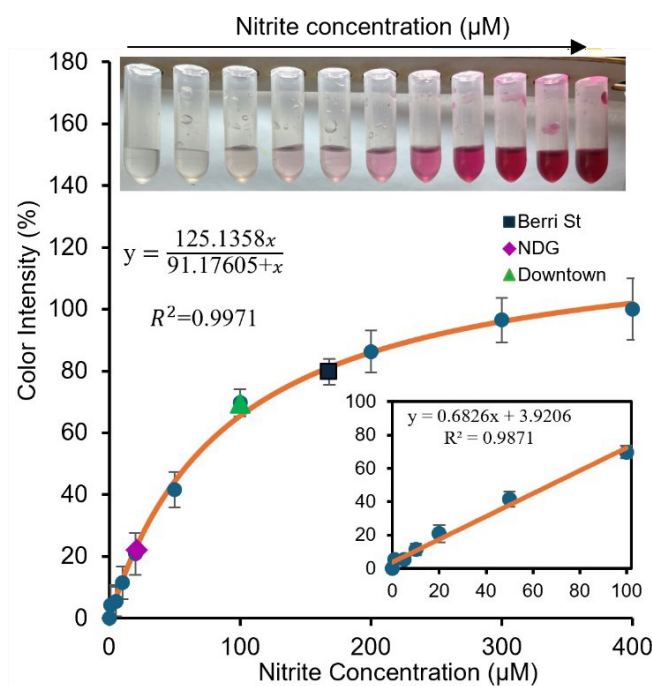


Figure 24. The calibration curve of nitrite detection with NED and SUL tablets. The calibration curve was found to follow the Michaelis–Menten equation with an R^2 value of 0.9971, confirming the compatibility of data with standard saturation model. The three samples of soil (Berri St. ■,

NDG ◆, and Downtown ▲) were collected in Montreal, Canada as specified in experimental Section and analyzed for their nitrite level. Each sample was tested with three replicates.

4.7.2 Real samples

To further evaluate the practical applicability of the nitrite tablet sensor, detection method was performed on three soil samples collected from different locations in Montreal, Quebec: sample 1 from Berri St (soil around tree roots), sample 2 from NDG (potted soil), and sample 3 from Downtown (planted area soil), Montreal, Canada. 5 mL of the sample was mixed with deionized water to make a total of 15 mL. The mixture was thoroughly shaken by hand at room temperature until fully dispersed, then allowed to settle. The supernatant was extracted and centrifuged at 14,000 rpm for 3 minutes. The clear liquid was used as the test sample in a citrate–phosphate buffer. These samples were compared with the calibration curve obtained from the buffer, with three test repetitions for each sample. The color intensity of the samples was recorded using a smartphone camera and analyzed with ImageJ software. The %R values were found to range from 83.57% to 111.33% for the soil sample 1, 80.40% to 104.24% for the soil sample 2, and 102.84% to 114.71% for the soil sample 3. The calculated RSD values were 5.28%, 5.54%, and 2.44%, respectively, all below 5.6% for all replicates, ensuring high precision and reproducibility of the results. The experimental data from the real-world soil samples aligned with the calibration curve, confirming that the tablets' effectiveness in detecting nitrite concentrations across all samples (Figure 25). This was further validated by comparing the results with the standard UV-Vis method, demonstrating the suitability of the tablets for practical applications (Figure A3).

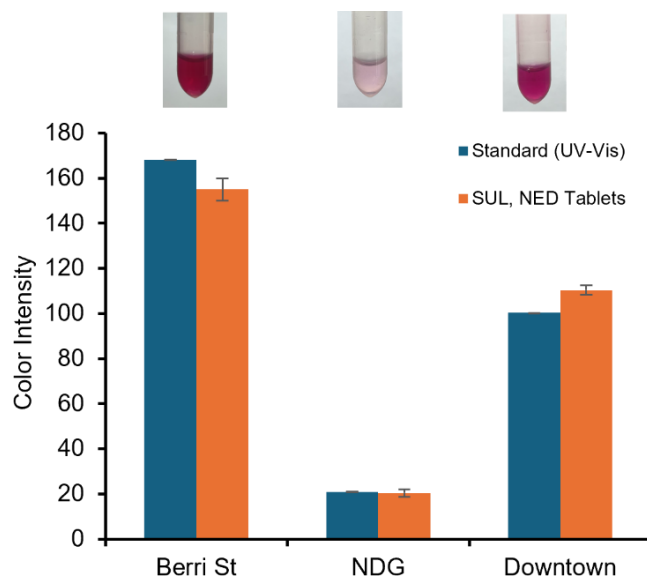


Figure 25. Comparison between the results of SUL, NED tablets and standard method for the nitrite detection in real soil samples (n=3). Paired t-tests showed no significant differences between methods (p-value > 0.05, p-value = 0.50 for Berri St., p-value = 0.54 for NDG, and p-value = 0.12 for Downtown), confirming that tablet results agree with UV-Vis measurements.

4.7.3 Selectivity tests

Potential interferants, including iron (Fe^{3+}), copper (Cu^{2+}), calcium (Ca^{2+}), cobalt (Co^{2+}), nitrate (NO_3^-), sodium (Na^+), mercury (Hg^{2+}), lead (Pb^{2+}), magnesium (Mg^{2+}), and zinc (Zn^{2+}) were evaluated for their impact on the proposed nitrite detection test. All interferents were tested at a concentration of 1mM in a 1M citrate-phosphate buffer, while nitrite (NO_2^-) was assessed at a concentration of 20 μM . For this study, 1 mM of each interfering ion was added to the test solutions separately, and the color intensity was measured and analyzed. No significant color changes were observed with the interfering agents, while the nitrite solution exhibited a distinct color change, as shown in Figure 26. These results confirm the selectivity of the tablet sensors for nitrite detection.

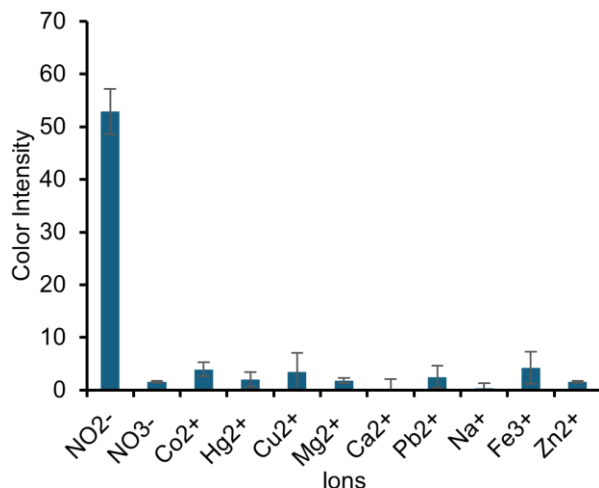


Figure 26. Potential interference of nitrite was tested with three replicates among common ions (nitrate, cobalt, mercury, copper, magnesium, calcium, lead, sodium, iron and zinc) at 1mM concentrations. While the working solution remained colorless for all three ions, a nitrite sample of 20 μ M was able to turn the solution purple, confirming the sensor's selectivity for nitrite detection. One-way ANOVA, p -value < 0.0001, confirmed a statistically significant difference in color intensity among ions.

4.7.4 Stability tests: over period of time

We assessed the stability of the tablets over a period of six weeks (Figure 27 Figure A4). Our tablets were stored at room temperature (RT) in a glass vial with a pack of silica gel, wrapped with aluminum foil. The tablets were tested in 50 μ M nitrite in citrate-phosphate buffer, and the results were normalized such that the percentage on day 0 represents the initial activity of the tablets, showing that the tablets were highly stable.

The results demonstrated that the tablets retained their functionality after six weeks, indicating their high stability in comparison with several reported POC testing devices for nitrite detection (Table 2). In addition, the tablet platform offers several advantages over liquid solutions for nitrite detection, including simplified transportation and storage. Each tablet contains a pre-measured amount of required reagents, eliminating the need for laboratory tools like weighing balances, pipettes, or the labor-intensive steps of calibration and solution preparation.

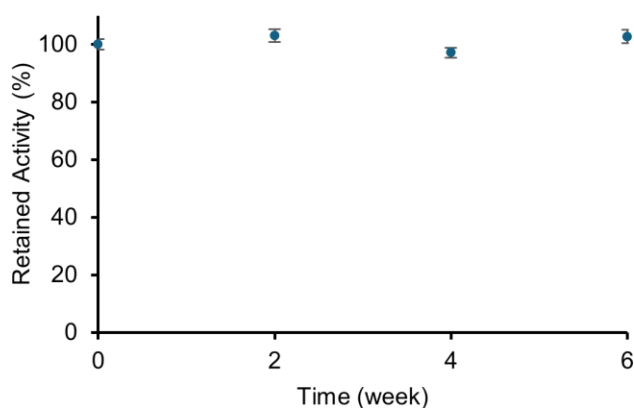


Figure 27. The stability of the tablets over six weeks (n=3). The average color intensity at week 6 recorded $102.3 \pm 1.81\%$ of the original color intensity recorded at week 1. RSD remained below 5.5%, confirming high reproducibility and consistent performance during storage.

Table 2. Comparison between the performance of the tablet sensors in this study with other reported POC assays.

Method/ref	Platform	Media	Working range	Stability	Fabrication process
Electrochemical [208]	Screen-printed electrode (SPE)-based	Soli	2.3 μM – 1.7 mM	7 days	Electrode modification with carbon allotropes, chitosan (CS), silver nanoparticles (AgNPs), and sol-gel (SG) matrix, Immobilization of – 1,8-Diaminonaphthalene (1,8-DAN)
Electrochemical [13]	Screen-printed electrode (SPE)-based	–	0.7–370 μM	20 days	Electrode modification with cytochrome c nitrite reductase, glucose oxidase (GOx) and catalase (Cat) enzymes were co-immobilized (ccNiR)
Surface-Enhanced Raman Spectroscopy (SERS) [209]	Silicon -based	Water, food, and biological samples	1 μM <	–	Nanostructured preparation, Surface functionalization with nitrite-selective ligand, Integration into a portable raman system
Photometric and fluorescence [199]	Solution-based	Water and soil	2.17 – 65.2 μM	–	Microwave-assisted synthesis of nanoparticles, neutral red (NR) functionalization, 3D-printed smartphone platform
Griess assay [210]	Paper-based	Water	6.81-144.9 μM	~1-3 days	Fabrication of ionogel matrix, the ionogel was impregnated with griess reagents, integration with paper-based device, Combined PMMA polymer
Griess assay [211]	PDMS-based	Water	4.35 – 97.80 μM	2 weeks	Fabrication of PDMS microfluidic chip with 3D printing and CO ₂ laser ablation, integration with a microfluidic platform, embedding photometric system, sample injection system incorporation
Griess assay [212]	PMMA-based	Water	0.36–3.57 μM	–	fabrication of PMMA microfluidic channels by laser cutter, integration with PDMS layer, sample injection system incorporation, fabrication of LED-PT detection system
Griess assay [26]	Tablet-based	–	0.4 μM <	4 weeks at RT	Fabrication of core tablet by microcrystalline cellulose (MCC), sodium bicarbonate and citric acid, and lyophilized assay reagents, fabrication of barrier layer by hydroxypropyl

					cellulose (HPC) and microcrystalline cellulose, fabrication of top layer by microcrystalline cellulose, poly(vinylpyrrolidone) (PVP), and lyophilized assay reagents, compression and molding
Griess assay [213]	Paper-based	Human saliva	22–520 μ M	4 weeks at 4°C	Wax printing on cellulose paper, heat treatment, reagent deposition, cutting into strips
Griess assay [214]	Paper-based	Human saliva, preservative water, ham, sausage, and river water	0–25 μ M	12 hours at 5°C	Fabrication of paraffin-coated filter paper, stamping of hydrophobic barriers, reagent deposition, cutting
Griess assay [215]	Paper-based	Meat (pork)	0.014–3.62 mM	~1 week at 4°C	Wax printing on filter paper, heat treatment at 120°C, reagent deposition, coffee-ring enhancement, cutting
Griess assay (this work)	Tablet-based (Dual)	Soil	3–400 μ M	6 weeks at RT	Solution preparation, mixing with pullulan, pipetting, drying
Griess assay (this work)	Tablet-based (All-in-one)	Soil	5–400 μ M	6 weeks at RT	Solution preparation, mixing with pullulan, pipetting, drying

4.7 Conclusion

Tablet-based sensors were developed for user-friendly nitrite detection in soil by encapsulating Griess reagents N-(1-naphthyl)ethylenediamine (NED) and sulfanilamide (SUL) into pullulan-based polysaccharide tablets. A simple mixing and drying method produced firm, uniform tablets with pre-measured reagents, removing the need for lab instruments or complex preparation. Two tablet types were made: Dual-tablet (SUL and NED separately) and All-in-one, showing the method's versatility. To support detection in soils with varying pH, an optimized citrate-phosphate buffer was included, maintaining necessary acidic conditions. The real sample assays showed high accuracy and precision of RSD less than 5.6% for all replicates (as mentioned in 4.7.2 section). The tablets showed detection range of 3–400 μ M with a LoD of 3 μ M. Additionally, the tablets remained stable for at least six weeks at room temperature.

Chapter 5: Conclusions and future direction

This thesis highlights the development of tablet-based sensors for user-friendly, rapid detection of (1) copper in water and (2) nitrite in soil, offering significant advantages over traditional methods, by eliminating the need for complex and bulky equipment, expert handling, transportation, storage, and financial resources. This approach enables quick and easy detection through simple and rapid colourimetric analysis.

In the first study presented in Chapter 3, a rapid auto-mixing tablet sensor designed for on-site detection of copper in water. For the first time, we integrated bicinchoninate mixture reagents, PEG, PVP and mannitol into an effervescence base composited of citric acid and sodium bicarbonate, enabling rapid release and automatic dispersion of reagents upon contact with the solution, ensuring consistent and homogeneous reactions. The tablets were produced using a simple powder compression method, resulting in a uniform size and composition, with less than 2% variation in average weight over one month. Pre-measured reagent quantities enhance reproducibility while reducing user error and preparation time. The embedded carbon dioxide generation maintained consistently in CO₂ release over four weeks, ensuring rapid dissolution and uniform color development. The tablets demonstrated colourimetric a copper detection range of 0-3 ppm, with a detection limit (LoD) as low as 0.3 ppm. Interference studies confirmed high selectivity for copper ions in the presence of potential interfering ions. Real water sample tests showed excellent recovery rates and validated the sensor's performance in real world applications. The tablets retained 99% reagent integrity during storage, with no significant degradation observed for at least one month at room temperature. Overall, this simple, stable, and portable tablet platform provides an accessible and reliable solution for copper monitoring in water, without the need for lab equipment or trained personnel.

In the second study, presented in Chapter 4, portable tablet-based sensors were developed by encapsulating the Griess reagents, N-(1-naphthyl)ethylenediamine dihydrochloride and sulfanilamide, into polysaccharides. This approach results in stable, simple tablets designed for point-of-use and rapid nitrite detection in soil. By using 5% w/v pullulan, employed a simple encapsulation method of mixing and drying in a tray, producing firm and uniform circular tablets. These tablets contain pre-measured quantities of reagents, eliminating the need for repetitive weighing and labor-intensive reagent optimization and laboratory instruments. The tablets were

produced in two forms: Dual-tablet (SUL and NED tablets), as well as All-in-one tablets, demonstrating the flexibility of this method for nitrite detection in soil samples. While the Griess assay traditionally requires acidic conditions, incorporating an optimized citrate-phosphate buffer in our tablets ensured stable detection and maintained the necessary acidic conditions across samples with a wide pH range, making the tablets compatible with soil samples with different pH conditions. The outcomes of real-sample tests reinforce the potential of these tablets for practical, real-world applications. The assay demonstrated excellent precision, with a RSD% value of less than 5.6% for all samples. The recovery percentage (%R) values of 83.57% to 111.33%, 80.40% to 104.24%, and 102.84% to 114.71% further validated the assay's accuracy. The tablets were effective in detecting nitrite in the range of 3–400 μM , with a LoD of 3 μM . The tablets exhibited excellent stability for extended periods (up to six weeks), making them suitable for long-term use at room temperature. In conclusion, the design of these tablets makes them ideal not only for soil monitoring but also for a wide range of applications in water and food testing. This simple yet innovative sensing platform offers a reliable, reproducible, and user-friendly detection, opening new possibilities for environmental monitoring and agricultural evaluation.

In conclusion, the design of these two types of tablets makes them ideal not only for environmental monitoring for a wide range of applications in water and soil. This simple yet innovative sensing platform for point-of-use and POC devices and under ASSURED criteria, offers a reliable, inexpensive, and user-friendly alternative to traditional methods, opening new possibilities for environmental monitoring and agricultural evaluation.

Future direction

To continue develop these findings and enhancing the user experience, it is valuable to investigate innovative approaches. Further research can be expanded by exploring additional aspects that involve:

- Making dual-detection tablets by integrating the detection of two analytes using colourimetric and fluorescence methods within a single tablet. This could enhance efficiency for environmental testing, facilitating the simultaneous detection of multiple analytes through a single, user-friendly platform.
- Investigating paper-based fluorescent/ colourimetric platforms for enabling the easy and simultaneous monitoring of multiple contaminants through an inexpensive, user-friendly platform.
- Investigating 96-well paper plates with pre-loaded reagents to analyze multiple analytes in one platform by incorporating various colourimetric assays or even integrating fluorescence and colourimetric techniques
- The sensor can be further advanced through the integration of a mobile phone application that analyzes color, enabling copper or nitrite monitoring by taking photos and automatically analyzing results.
- Expanding the use of nitrite tablets in other media, such as food testing, broadening the scope of environmental and health monitoring.
- Expanding the use of auto-mixing tablets for detecting other analytes.
- The recyclability of the tablets can be further examined.
- In the nitrite tablet preparation for real samples, the samples were prepared using the centrifugation method. Further investigations could focus on replacing this step with other user-friendly methods.
- Portable centrifuges could be used for nitrite tablet detection assays to facilitate on-site detection applications.

References

- [1] P. Information, Griess Reagent Kit for Nitrite Determination (G-7921), Mol. Probes (2003) 1–3.
- [2] A.K. Yetisen, M.S. Akram, C.R. Lowe, Paper-based microfluidic point-of-care diagnostic devices, *Lab Chip* 13 (2013) 2210–2251. <https://doi.org/10.1039/c3lc50169h>.
- [3] W. Yang, D. Yang, S. Gong, X. Dong, L. Liu, S. Yu, X. Zhang, S. Ge, D. Wang, N. Xia, D. Yu, X. Qiu, An immunoassay cassette with a handheld reader for HIV urine testing in point-of-care diagnostics, *Biomed. Microdevices* 22 (2020). <https://doi.org/10.1007/s10544-020-00494-4>.
- [4] D. Unold, J.H. Nichols, Point-of-Care Testing: Needs, Opportunity, and Innovation, 3rd Edition, by Christopher P. Price, Andrew St John, and Larry J. Kricka, eds., *Clin. Chem.* 56 (2010) 1893–1894. <https://doi.org/10.1373/clinchem.2010.154872>.
- [5] Z. Li, Y. Bai, M. You, J. Hu, C. Yao, L. Cao, F. Xu, Fully integrated microfluidic devices for qualitative, quantitative and digital nucleic acids testing at point of care, *Biosens. Bioelectron.* 177 (2021) 112952. <https://doi.org/10.1016/j.bios.2020.112952>.
- [6] P. Wu, D.G. Castner, D.W. Grainger, Diagnostic devices as biomaterials: A review of nucleic acid and protein microarray surface performance issues, *J. Biomater. Sci. Polym. Ed.* 19 (2008) 725–753. <https://doi.org/10.1163/156856208784522092>.
- [7] L. Basabe-Desmonts, S. Ramstrom, G. Meade, S. O'Neill, A. Riaz, L.P. Lee, A.J. Ricco, D. Kenny, Single-step separation of platelets from whole blood coupled with digital quantification by interfacial platelet cytometry (iPC), *Langmuir* 26 (2010) 14700–14706. <https://doi.org/10.1021/la9039682>.
- [8] A.H. Becerra, M.G. Flores, J.P. Palma-Nicolas, G. Ramírez-García, L.M. López-Marín, Mycosome-Coated Gold Nanoparticles for Plasmonic Detection of Tuberculosis-Associated Antibodies, *ACS Appl. Nano Mater.* 7 (2024) 11203–11213. <https://doi.org/10.1021/acsanm.4c00706>.
- [9] A.C. Hurt, C. Baas, Y. Deng, S. Roberts, A. Kelso, I.G. Barr, Performance of influenza

- rapid point-of-care tests in the detection of swine lineage A(H1N1) influenza viruses, *Influenza Other Respi. Viruses* 3 (2009) 171–176. <https://doi.org/10.1111/j.1750-2659.2009.00086.x>.
- [10] P.B. Luppá, C. Müller, A. Schlichtiger, H. Schlebusch, Point-of-care testing (POCT): Current techniques and future perspectives, *TrAC - Trends Anal. Chem.* 30 (2011) 887–898. <https://doi.org/10.1016/j.trac.2011.01.019>.
- [11] E.C. Okpara, T.O. Ajiboye, D.C. Onwudiwe, O.B. Wojuola, Optical and electrochemical techniques for Point-of-Care water quality monitoring: A review, *Results Chem.* 5 (2023) 100710. <https://doi.org/10.1016/j.rechem.2022.100710>.
- [12] M.M. Bordbar, A. Sheini, P. Hashemi, A. Hajian, H. Bagheri, Disposable paper-based biosensors for the point-of-care detection of hazardous contaminations—a review, *Biosensors* 11 (2021) 1–51. <https://doi.org/10.3390/bios11090316>.
- [13] T. Monteiro, S. Gomes, E. Jubete, L. Añorga, C.M. Silveira, M.G. Almeida, A quasi-reagentless point-of-care test for nitrite and unaffected by oxygen and cyanide, *Sci. Rep.* 9 (2019) 1–10. <https://doi.org/10.1038/s41598-019-39209-y>.
- [14] G. Zhao, G. Liu, A Portable Electrochemical System for the On-Site Detection of Heavy Metals in Farmland Soil Based on Electrochemical Sensors, *IEEE Sens. J.* 18 (2018) 5645–5655. <https://doi.org/10.1109/JSEN.2018.2845306>.
- [15] K. Chauhan, P. Singh, B. Kumari, R.K. Singhal, Synthesis of new benzothiazole Schiff base as selective and sensitive colorimetric sensor for arsenic on-site detection at ppb level, *Anal. Methods* 9 (2017) 1779–1785. <https://doi.org/10.1039/C6AY03302D>.
- [16] J. Guo, M. Zhou, C. Yang, Fluorescent hydrogel waveguide for on-site detection of heavy metal ions, *Sci. Rep.* 7 (2017) 7902. <https://doi.org/10.1038/s41598-017-08353-8>.
- [17] S. Sachdeva, R.W. Davis, A.K. Saha, Microfluidic Point-of-Care Testing: Commercial Landscape and Future Directions, *Front. Bioeng. Biotechnol.* 8 (2021). <https://doi.org/10.3389/fbioe.2020.602659>.
- [18] A.T. Singh, D. Lantigua, A. Meka, S. Taing, M. Pandher, G. Camci-Unal, Paper-Based Sensors: Emerging Themes and Applications, *Sensors* 18 (2018) 2838.

- <https://doi.org/10.3390/s18092838>.
- [19] G.G. Morbioli, T. Mazzu-Nascimento, A.M. Stockton, E. Carrilho, Technical aspects and challenges of colorimetric detection with microfluidic paper-based analytical devices (μ PADs) - A review, *Anal. Chim. Acta* 970 (2017) 1–22.
<https://doi.org/10.1016/j.aca.2017.03.037>.
 - [20] X. Qin, J. Liu, Z. Zhang, J. Li, L. Yuan, Z. Zhang, L. Chen, Microfluidic paper-based chips in rapid detection: Current status, challenges, and perspectives, *TrAC Trends Anal. Chem.* 143 (2021) 116371. <https://doi.org/10.1016/j.trac.2021.116371>.
 - [21] World Health Organization (WHO), Point-of-Care Tests for Sexually Transmitted Infections: Target Product Profiles, (2023).
<https://iris.who.int/bitstream/handle/10665/371294/9789240077102-eng.pdf?sequence=1>.
 - [22] K. Yamada, H. Shibata, K. Suzuki, D. Citterio, Toward practical application of paper-based microfluidics for medical diagnostics: state-of-the-art and challenges, *Lab Chip* 17 (2017) 1206–1249. <https://doi.org/10.1039/c6lc01577h>.
 - [23] M. Naseri, Z.M. Ziora, G.P. Simon, W. Batchelor, ASSURED-compliant point-of-care diagnostics for the detection of human viral infections, *Rev. Med. Virol.* 32 (2022).
<https://doi.org/10.1002/rmv.2263>.
 - [24] M. Al-Kassawneh, Z. Sadiq, S. Jahanshahi-Anbuhi, Pullulan-stabilized gold nanoparticles tablet as a nanozyme sensor for point-of-care applications, *Sens. Bio-Sensing Res.* 38 (2022) 100526. <https://doi.org/10.1016/j.sbsr.2022.100526>.
 - [25] A.R. Esfahani, Z. Sadiq, O.D. Oyewunmi, S.H. Safiabadi Tali, N. Usen, D.C. Boffito, S. Jahanshahi-Anbuhi, Portable, stable, and sensitive assay to detect phosphate in water with gold nanoparticles (AuNPs) and dextran tablet, *Analyst* 146 (2021) 3697–3708.
<https://doi.org/10.1039/D0AN02063J>.
 - [26] V.Y.C. Li, B. Udugama, P. Kadhiresan, W.C.W. Chan, Sequential Reagent Release from a Layered Tablet for Multistep Diagnostic Assays, *Anal. Chem. TA - TT - 94* (2022) 17102–17111. <https://doi.org/10.1021/acs.analchem.2c03315> LK -
<https://concordiauniversity.on.worldcat.org/oclc/9696896835>.

- [27] C. Vulpe, B. Levinson, S. Whitney, S. Packman, J. Gitschier, Isolation of a candidate gene for Menkes disease and evidence that it encodes a copper-transporting ATPase, *Nat. Genet.* 3 (1993) 7–13. <https://doi.org/10.1038/ng0193-7>.
- [28] P.C. Bull, G.R. Thomas, J.M. Rommens, J.R. Forbes, D.W. Cox, The Wilson disease gene is a putative copper transporting P-type ATPase similar to the Menkes gene, *Nat. Genet.* 5 (1993) 327–337. <https://doi.org/10.1038/ng1293-327>.
- [29] Y.H. Hung, A.I. Bush, R.A. Cherny, Copper in the brain and Alzheimer's disease, *J. Biol. Inorg. Chem.* 15 (2010) 61–76. <https://doi.org/10.1007/s00775-009-0600-y>.
- [30] L. Liu, Z. Fang, X. Zheng, D. Xi, Nanopore-Based Strategy for Sensing of Copper(II) Ion and Real-Time Monitoring of a Click Reaction, *ACS Sensors* 4 (2019) 1323–1328. <https://doi.org/10.1021/acssensors.9b00236>.
- [31] G.-L. Xie, H. Yu, M.-H. Deng, X.-L. Zhao, P. Yu, A colorimetric microfluidic sensor made by a simple instrumental-free prototyping process for sensitive quantitation of copper, *Chem. Pap. TA - TT - 73* (2019) 1509–1517. <https://doi.org/10.1007/s11696-019-00702-3> LK - <https://concordiauniversity.on.worldcat.org/oclc/8078806718>.
- [32] S. Cinti, V. Mazzaracchio, G. Öztürk, D. Moscone, F. Arduini, A lab-on-a-tip approach to make electroanalysis user-friendly and de-centralized: Detection of copper ions in river water, *Anal. Chim. Acta* 1029 (2018) 1–7. <https://doi.org/10.1016/j.aca.2018.04.065>.
- [33] B.K. Vinay, P. ArchanaRaj, A. Nambiar, B.M. Vivek, Biosensors for copper ions determination in water: a step up progression from conventional techniques to state of art, *Int. J. Environ. Anal. Chem.* 00 (2024) 1–27. <https://doi.org/10.1080/03067319.2024.2331032>.
- [34] Z. Gerdan, Y. Saylan, A. Denizli, Recent Advances of Optical Sensors for Copper Ion Detection, *Micromachines* 13 (2022) 1298. <https://doi.org/10.3390/mi13081298>.
- [35] K.J. Rader, R.F. Carbonaro, E.D. van Hullebusch, S. Baken, K. Delbeke, The Fate of Copper Added to Surface Water: Field, Laboratory, and Modeling Studies, *Environ. Toxicol. Chem.* 38 (2019) 1386–1399. <https://doi.org/10.1002/etc.4440>.
- [36] Z. Liu, V.S. Manikandan, A. Chen, Recent advances in nanomaterial-based

- electrochemical sensing of nitric oxide and nitrite for biomedical and food research, *Curr. Opin. Electrochem.* 16 (2019) 127–133. <https://doi.org/10.1016/j.coelec.2019.05.013>.
- [37] D.H.K. Lee, Nitrates, nitrites, and methemoglobinemia, *Environ. Res.* 3 (1970) 484–511. [https://doi.org/10.1016/0013-9351\(70\)90042-3](https://doi.org/10.1016/0013-9351(70)90042-3).
- [38] H. Li, Y. Song, B. Zhou, H. Xu, Nitrite: From Application to Detection and Development, *Appl. Sci.* 14 (2024). <https://doi.org/10.3390/app14199027>.
- [39] J.F. Tan, A. Anastasi, S. Chandra, Electrochemical detection of nitrate, nitrite and ammonium for on-site water quality monitoring, *Curr. Opin. Electrochem.* 32 (2022) 100926. <https://doi.org/10.1016/j.coelec.2021.100926>.
- [40] J. Zhang, C. Yue, Y. Ke, H. Qu, L. Zeng, Fluorescent probes for the detection of biogenic amines, nitrite and sulfite in food: Progress, challenges and perspective, *Adv. Agrochem* 2 (2023) 127–141. <https://doi.org/10.1016/j.aac.2023.03.001>.
- [41] A. Kumar, N. Dey, Recent Advances in Designing Colorimetric Probes for Nitrite Ions, *Asian J. Org. Chem.* 13 (2024). <https://doi.org/10.1002/ajoc.202300453>.
- [42] H. Ali, E. Khan, What are heavy metals? Long-standing controversy over the scientific use of the term ‘heavy metals’ – proposal of a comprehensive definition, *Toxicol. Environ. Chem.* 100 (2018) 6–19. <https://doi.org/10.1080/02772248.2017.1413652>.
- [43] V. Masindi, K.L. Muedi, Environmental contamination by heavy metals, *Heavy Met.* 10 (2018) 115–133.
- [44] R. Dixit, Wasiullah, D. Malaviya, K. Pandiyan, U. Singh, A. Sahu, R. Shukla, B. Singh, J. Rai, P. Sharma, H. Lade, D. Paul, Bioremediation of Heavy Metals from Soil and Aquatic Environment: An Overview of Principles and Criteria of Fundamental Processes, *Sustainability* 7 (2015) 2189–2212. <https://doi.org/10.3390/su7022189>.
- [45] G.L. Turdean, Design and Development of Biosensors for the Detection of Heavy Metal Toxicity, *Int. J. Electrochem.* 2011 (2011) 1–15. <https://doi.org/10.4061/2011/343125>.
- [46] K. Tag, K. Riedel, H.-J. Bauer, G. Hanke, K.H.R. Baronian, G. Kunze, Amperometric detection of Cu²⁺ by yeast biosensors using flow injection analysis (FIA), *Sensors*

- Actuators B Chem. 122 (2007) 403–409. <https://doi.org/10.1016/j.snb.2006.06.007>.
- [47] M.B. Gumpu, S. Sethuraman, U.M. Krishnan, J.B.B. Rayappan, A review on detection of heavy metal ions in water – An electrochemical approach, *Sensors Actuators B Chem.* 213 (2015) 515–533. <https://doi.org/10.1016/j.snb.2015.02.122>.
- [48] V. Rajaganapa, F. Xavier, D. Sreekumar, P.K. Mandal, Heavy Metal Contamination in Soil, Water and Fodder and their Presence in Livestock and Products : A Review, *J. Environ. Sci. Technol.* 4 (2011) 234–249. <https://doi.org/10.3923/jest.2011.234.249>.
- [49] M. Valko, H. Morris, M. Cronin, Metals, Toxicity and Oxidative Stress, *Curr. Med. Chem.* 12 (2005) 1161–1208. <https://doi.org/10.2174/0929867053764635>.
- [50] L. Patrick, Lead toxicity part II: The role of free radical damage and the use of antioxidants in the pathology and treatment of lead toxicity, *Altern. Med. Rev.* 11 (2006) 114–127.
- [51] D. Bagal-Kestwal, M.S. Karve, B. Kakade, V.K. Pillai, Invertase inhibition based electrochemical sensor for the detection of heavy metal ions in aqueous system: Application of ultra-microelectrode to enhance sucrose biosensor's sensitivity, *Biosens. Bioelectron.* 24 (2008) 657–664. <https://doi.org/10.1016/j.bios.2008.06.027>.
- [52] C.A. Flemming, J.T. Trevors, Copper toxicity and chemistry in the environment: a review, *Water. Air. Soil Pollut.* 44 (1989) 143–158. <https://doi.org/10.1007/BF00228784>.
- [53] J.Y. Uriu-Adams, C.L. Keen, Copper, oxidative stress, and human health, *Mol. Aspects Med.* 26 (2005) 268–298. <https://doi.org/10.1016/j.mam.2005.07.015>.
- [54] B.-E. Kim, T. Nevitt, D.J. Thiele, Mechanisms for copper acquisition, distribution and regulation, *Nat. Chem. Biol.* 4 (2008) 176–185. <https://doi.org/10.1038/nchembio.72>.
- [55] R. V Timoshenko, A.N. Vaneev, N.A. Savin, N.L. Klyachko, Y.N. Parkhomenko, S. V Salikhov, A.G. Majouga, P. V Gorelkin, A.S. Erofeev, Promising Approaches for Determination of Copper Ions in Biological Systems, *Nanotechnologies Russ.* 15 (2020) 121–134. <https://doi.org/10.1134/S1995078020020196> LK - <https://concordiauniversity.on.worldcat.org/oclc/8773832036>.

- [56] C. Isarankura-Na-Ayudhya, T. Tantimongcolwat, H.J. Galla, V. Prachayasittikul, Fluorescent protein-based optical biosensor for copper ion quantitation, *Biol. Trace Elem. Res.* 134 (2010) 352–363. <https://doi.org/10.1007/s12011-009-8476-9>.
- [57] M. Wołowiec, M. Komorowska-Kaufman, A. Pruss, G. Rzepa, T. Bajda, Removal of Heavy Metals and Metalloids from Water Using Drinking Water Treatment Residuals as Adsorbents: A Review, *Minerals* 9 (2019) 487. <https://doi.org/10.3390/min9080487>.
- [58] N. Aksuner, E. Henden, I. Yilmaz, A. Cukurovali, A highly sensitive and selective fluorescent sensor for the determination of copper(II) based on a schiff base, *Dye. Pigment.* 83 (2009) 211–217. <https://doi.org/10.1016/j.dyepig.2009.04.012>.
- [59] Q. Gao, L. Ji, Q. Wang, K. Yin, J. Li, L. Chen, Colorimetric sensor for highly sensitive and selective detection of copper ion, *Anal. Methods* 9 (2017) 5094–5100. <https://doi.org/10.1039/c7ay01335c>.
- [60] WHO, Guidelines for Drinking-water Quality: Second addendum, World Heal. Organ. Press 1 (2008) 17–19. http://www.who.int/water_sanitation_health/dwq/secondaddendum20081119.pdf.
- [61] Q.-H. Wang, L.-J. Yu, Y. Liu, L. Lin, R. Lu, J. Zhu, L. He, Z.-L. Lu, Methods for the detection and determination of nitrite and nitrate: A review, *Talanta* 165 (2017) 709–720. <https://doi.org/10.1016/j.talanta.2016.12.044>.
- [62] W. Bedale, J.J. Sindelar, A.L. Milkowski, Dietary nitrate and nitrite: Benefits, risks, and evolving perceptions, *Meat Sci.* 120 (2016) 85–92. <https://doi.org/10.1016/j.meatsci.2016.03.009>.
- [63] H. Abdolmohammad-Zadeh, E. Rahimpour, Utilizing of Ag@AgCl@graphene oxide@Fe₃O₄ nanocomposite as a magnetic plasmonic nanophotocatalyst in light-initiated H₂O₂ generation and chemiluminescence detection of nitrite, *Talanta* 144 (2015) 769–777. <https://doi.org/10.1016/j.talanta.2015.07.030>.
- [64] C.L. Walters, The Exposure of Humans to Nitrite, *Oncology* 37 (1980) 289–296. <https://doi.org/10.1159/000225455>.
- [65] F. Beeckman, H. Motte, T. Beeckman, Nitrification in agricultural soils: impact, actors

- and mitigation, *Curr. Opin. Biotechnol.* 50 (2018) 166–173.
<https://doi.org/10.1016/j.copbio.2018.01.014>.
- [66] P.F. Swann, The toxicology of nitrate, nitrite and n-nitroso compounds, *J. Sci. Food Agric.* 26 (1975) 1761–1770. <https://doi.org/10.1002/jsfa.2740261119>.
- [67] W.E.J. Phillips, Naturally occurring nitrate and nitrite in foods in relation to infant methaemoglobinaemia, *Food Cosmet. Toxicol.* 9 (1971) 219–228.
[https://doi.org/10.1016/0015-6264\(71\)90307-5](https://doi.org/10.1016/0015-6264(71)90307-5).
- [68] P. Jakszyn, Nitrosamine and related food intake and gastric and oesophageal cancer risk: A systematic review of the epidemiological evidence, *World J. Gastroenterol.* 12 (2006) 4296. <https://doi.org/10.3748/wjg.v12.i27.4296>.
- [69] V.Y. Titov, Y.M. Petrenko, Proposed Mechanism of Nitrite-Induced Methemoglobinemia, *Biochem.* 70 (2005) 473–483. <https://doi.org/10.1007/s10541-005-0139-7>.
- [70] J.D. Brender, P.J. Weyer, P.A. Romitti, B.P. Mohanty, M.U. Shinde, A.M. Vuong, J.R. Sharkey, D. Dwivedi, S.A. Horel, J. Kantamneni, J.C. Huber, Q. Zheng, M.M. Werler, K.E. Kelley, J.S. Griesenbeck, F.B. Zhan, P.H. Langlois, L. Suarez, M.A. Canfield, Prenatal Nitrate Intake from Drinking Water and Selected Birth Defects in Offspring of Participants in the National Birth Defects Prevention Study, *Environ. Health Perspect.* 121 (2013) 1083–1089. <https://doi.org/10.1289/ehp.1206249>.
- [71] WHO, Nitrate and nitrite in Drinking-water Background document for development of, *Drink. Water* 2 (2016) 21.
- [72] United States Environmental Protection Agency (EPA), National Primary Drinking Water Regulations, (n.d.). <https://www.epa.gov/ground-water-and-drinking-water/national-primary-drinking-water-regulations> (accessed March 3, 2025).
- [73] C.H. Lu, S.L. Wang, S.L. Ye, G.N. Chen, H.H. Yang, Ultrasensitive detection of Cu²⁺ with the naked eye and application in immunoassays, *NPG Asia Mater.* 4 (2012).
<https://doi.org/10.1038/am.2012.18>.
- [74] Y. Wang, T. Ma, J. Brake, Z. Sun, J. Huang, J. Li, X. Wu, A novel method of rapid detection for heavy metal copper ion via a specific copper chelator

- bathocuproinedisulfonic acid disodium salt, *Sci. Rep.* 13 (2023) 1–13.
<https://doi.org/10.1038/s41598-023-37838-y>.
- [75] Y. Liu, Q. Xue, C. Chang, R. Wang, Z. Liu, L. He, Recent progress regarding electrochemical sensors for the detection of typical pollutants in water environments, *Anal. Sci.* 38 (2022) 55–70. <https://doi.org/10.2116/analsci.21SAR12>.
- [76] D. Pan, Y. Wang, Z. Chen, T. Lou, W. Qin, Nanomaterial/Ionophore-Based Electrode for Anodic Stripping Voltammetric Determination of Lead: An Electrochemical Sensing Platform toward Heavy Metals, *Anal. Chem.* 81 (2009) 5088–5094.
<https://doi.org/10.1021/ac900417e>.
- [77] F. Ejeian, P. Etedali, H.-A. Mansouri-Tehrani, A. Soozanipour, Z.-X. Low, M. Asadnia, A. Taheri-Kafrani, A. Razmjou, Biosensors for wastewater monitoring: A review, *Biosens. Bioelectron.* TA - TT - 118 (2018) 66–79.
<https://doi.org/10.1016/j.bios.2018.07.019> LK -
<https://concordiauniversity.on.worldcat.org/oclc/7813192161>.
- [78] L.A. Romero-Cano, A.I. Zárate-Guzmán, F. Carrasco-Marín, L. V. González-Gutiérrez, Electrochemical detection of copper in water using carbon paste electrodes prepared from bio-template (grapefruit peels) functionalized with carboxyl groups, *J. Electroanal. Chem.* 837 (2019) 22–29. <https://doi.org/10.1016/j.jelechem.2019.02.005>.
- [79] R. V Timoshenko, P. V Gorelkin, A.N. Vaneev, O.O. Krasnovskaya, R.A. Akasov, A.S. Garanina, D.A. Khochenkov, T.M. Iakimova, N.L. Klyachko, T.O. Abakumova, V.S. Shashkovskaya, K.D. Chaprov, A.A. Makarov, V.A. Mitkevich, Y. Takahashi, C.R.W. Edwards, Y.E. Korchev, A.S. Erofeev, Electrochemical Nanopipette Sensor for In Vitro/In Vivo Detection of Cu ²⁺ Ions, (2024). <https://doi.org/10.1021/acs.analchem.3c03337>.
- [80] L. Cui, J. Wu, H. Ju, Electrochemical sensing of heavy metal ions with inorganic, organic and bio-materials, *Biosens. Bioelectron.* 63 (2015) 276–286.
<https://doi.org/10.1016/j.bios.2014.07.052>.
- [81] M.N. Velasco-Garcia, Optical biosensors for probing at the cellular level: A review of recent progress and future prospects, *Semin. Cell Dev. Biol.* 20 (2009) 27–33.

<https://doi.org/10.1016/j.semcd.2009.01.013>.

- [82] H.N. Kim, W.X. Ren, J.S. Kim, J. Yoon, Fluorescent and colorimetric sensors for detection of lead, cadmium, and mercury ions, *Chem. Soc. Rev.* TA - TT - 41 (2012) 3210–3244. <https://doi.org/10.1039/c1cs15245a> LK - <https://concordiauniversity.on.worldcat.org/oclc/781866606>.
- [83] A. Ramdass, V. Sathish, E. Babu, M. Velayudham, P. Thanasekaran, S. Rajagopal, Recent developments on optical and electrochemical sensing of copper(II) ion based on transition metal complexes, *Coord. Chem. Rev.* 343 (2017) 278–307. <https://doi.org/10.1016/j.ccr.2017.06.002>.
- [84] Z.-C. Liu, J.-W. Qi, C. Hu, L. Zhang, W. Song, R.-P. Liang, J.-D. Qiu, Cu nanoclusters-based ratiometric fluorescence probe for ratiometric and visualization detection of copper ions, *Anal. Chim. Acta* 895 (2015) 95–103. <https://doi.org/10.1016/j.aca.2015.09.002>.
- [85] Y. Niu, T. Ding, J. Liu, G. Zhang, L. Tong, X. Cheng, Y. Yang, Z. Chen, B. Tang, Fluorescence switch of gold nanoclusters stabilized with bovine serum albumin for efficient and sensitive detection of cysteine and copper ion in mice with Alzheimer's disease, *Talanta* 223 (2021) 121745. <https://doi.org/10.1016/j.talanta.2020.121745>.
- [86] K. Patir, S.K. Gogoi, Nitrogen-doped carbon dots as fluorescence ON-OFF-ON sensor for parallel detection of copper(ii) and mercury(ii) ions in solutions as well as in filter paper-based microfluidic device, *Nanoscale Adv.* 1 (2019) 592–601. <https://doi.org/10.1039/c8na00080h>.
- [87] B. Kaur, N. Kaur, S. Kumar, Colorimetric metal ion sensors - A comprehensive review of the years 2011-2016, *Coord. Chem. Rev.* TA - TT - 358 (2018) 13–69. <https://doi.org/10.1016/j.ccr.2017.12.002> LK - <https://concordiauniversity.on.worldcat.org/oclc/7285099252>.
- [88] D. Zhu, B. Liu, G. Wei, Two-Dimensional Material-Based Colorimetric Biosensors: A Review, *Biosensors* 11 (2021) 259. <https://doi.org/10.3390/bios11080259> LK - <https://concordiauniversity.on.worldcat.org/oclc/9456337867>.
- [89] B.R. Gangapuram, R. Bandi, R. Dadigala, G.M. Kotu, V. Guttana, Facile Green Synthesis

- of Gold Nanoparticles with Carboxymethyl Gum Karaya, Selective and Sensitive Colorimetric Detection of Copper (II) Ions, *J. Clust. Sci. Incl. Nanoclusters Nanoparticles* TA - TT - 28 (2017) 2873–2890. <https://doi.org/10.1007/s10876-017-1264-3> LK - <https://concordiauniversity.on.worldcat.org/oclc/7127939472>.
- [90] Y. Ma, H. Niu, X. Zhang, Y. Cai, Colorimetric detection of copper ions in tap water during the synthesis of silver/dopamine nanoparticles, *Chem. Commun. (Cambridge, England)* TA - TT - 47 (2011) 12643–12645. <https://doi.org/10.1039/c1cc15048k> LK - <https://concordiauniversity.on.worldcat.org/oclc/762175160>.
- [91] G.J. Park, I.H. Hwang, E.J. Song, H. Kim, C. Kim, A colorimetric and fluorescent sensor for sequential detection of copper ion and cyanide, *Tetrahedron* TA - TT - 70 (n.d.) 2822–2828. <https://doi.org/10.1016/j.tet.2014.02.055> LK - <https://concordiauniversity.on.worldcat.org/oclc/5539271645>.
- [92] H.-H. Deng, G.-W. Li, A.-L. Liu, W. Chen, X.-H. Lin, X.-H. Xia, Thermally treated bare gold nanoparticles for colorimetric sensing of copper ions, *Microchim. Acta Anal. Sci. Based Micro- Nanomater.* TA - TT - 181 (2014) 911–916. <https://doi.org/10.1007/s00604-014-1184-y> LK - <https://concordiauniversity.on.worldcat.org/oclc/5679128287>.
- [93] T. Lou, L. Chen, Z. Chen, Y. Wang, L. Chen, J. Li, Colorimetric detection of trace copper ions based on catalytic leaching of silver-coated gold nanoparticles, *ACS Appl. Mater. Interfaces* TA - TT - 3 (2011) 4215–4220. <https://doi.org/10.1021/am2008486> LK - <https://concordiauniversity.on.worldcat.org/oclc/762475591>.
- [94] P. Singh, M.K. Singh, Y.R. Beg, G.R. Nishad, A review on spectroscopic methods for determination of nitrite and nitrate in environmental samples, *Talanta* 191 (2019) 364–381. <https://doi.org/10.1016/j.talanta.2018.08.028>.
- [95] A.T. Mubarak, A.A. Mohamed, K.F. Fawy, A.S. Al-Shihry, A novel kinetic determination of nitrite based on the perphenazine-bromate redox reaction, *Microchim. Acta* 157 (2007) 99–105. <https://doi.org/10.1007/s00604-006-0661-3>.
- [96] X.F. Yue, Z.Q. Zhang, H.T. Yan, Flow injection catalytic spectrophotometric

- simultaneous determination of nitrite and nitrate, *Talanta* 62 (2004) 97–101.
[https://doi.org/10.1016/S0039-9140\(03\)00421-1](https://doi.org/10.1016/S0039-9140(03)00421-1).
- [97] Z. Moldovan, Kinetic spectrophotometric determination of nitrite with tropaeolin 00-bromate system, *Anal. Lett.* 43 (2010) 1344–1354.
<https://doi.org/10.1080/00032710903518757>.
- [98] T. Tomiyasu, S. Aikou, K. Anazawa, H. Sakamoto, A kinetic method for the determination of copper(II) by Its catalytic effect on the oxidation of 3-methyl-2-benzothiazolinone hydrazone with hydrogen peroxide: A mechanistic study, *Anal. Sci.* 21 (2005) 917–922. <https://doi.org/10.2116/analsci.21.917>.
- [99] A.A. Ensafi, A. Kazemzadeh, Simultaneous determination of nitrite and nitrate in various samples using flow injection with spectrophotometric detection, *Anal. Chim. Acta* 382 (1999) 15–21. [https://doi.org/10.1016/S0003-2670\(98\)00755-7](https://doi.org/10.1016/S0003-2670(98)00755-7).
- [100] I.A. Pettas, S.I. Lafis, M.I. Karayannis, Reaction rate method for determination of nitrite by applying a stopped-flow technique, *Anal. Chim. Acta* 376 (1998) 331–337.
[https://doi.org/10.1016/S0003-2670\(98\)00553-4](https://doi.org/10.1016/S0003-2670(98)00553-4).
- [101] M.I.H. Helaleh, T. Korenaga, Ion chromatographic method for simultaneous determination of nitrate and nitrite in human saliva, *J. Chromatogr. B Biomed. Sci. Appl.* 744 (2000) 433–437. [https://doi.org/10.1016/S0378-4347\(00\)00264-4](https://doi.org/10.1016/S0378-4347(00)00264-4).
- [102] H. Li, C.J. Meininger, G. Wu, Rapid determination of nitrite by reversed-phase high-performance liquid chromatography with fluorescence detection, *J. Chromatogr. B Biomed. Sci. Appl.* 746 (2000) 199–207. [https://doi.org/10.1016/S0378-4347\(00\)00328-5](https://doi.org/10.1016/S0378-4347(00)00328-5).
- [103] K. Zhu, M. Kerry, B. Serr, M. Mintert, Parts per billion of nitrite in microcrystalline cellulose by ion chromatography mass spectrometry with isotope labeled internal standard, *J. Pharm. Biomed. Anal.* 235 (2023) 115648.
<https://doi.org/10.1016/j.jpba.2023.115648>.
- [104] M.D. Croitoru, Nitrite and nitrate can be accurately measured in samples of vegetal and animal origin using an HPLC-UV/VIS technique, *J. Chromatogr. B Anal. Technol. Biomed. Life Sci.* 911 (2012) 154–161. <https://doi.org/10.1016/j.jchromb.2012.11.006>.

- [105] J. Lei, H. Zheng, L. Liu, W. Li, [Simultaneous determination of six nitroaromatic compounds and three anions in environmental matrices using a liquid chromatography-ion chromatography coupled system], *Se Pu = Chinese J. Chromatogr.* 42 (2024) 92—98. <https://doi.org/10.3724/sp.j.1123.2023.10027>.
- [106] G. v. Bechi, Ueber Succinylverbindungen der Toluidine, *Berichte Der Dtsch. Chem. Gesellschaft* 12 (1879) 25–26. <https://doi.org/10.1002/cber.18790120111>.
- [107] J.B. Fox, Kinetics and Mechanisms of the Griess Reaction, *Anal. Chem.* 51 (1979) 1493–1502. <https://doi.org/10.1021/ac50045a032>.
- [108] D. Tsikas, Analysis of nitrite and nitrate in biological fluids by assays based on the Griess reaction: Appraisal of the Griess reaction in the l-arginine/nitric oxide area of research, *J. Chromatogr. B* 851 (2007) 51–70. <https://doi.org/10.1016/j.jchromb.2006.07.054>.
- [109] A.C. Bratton, E.K. Marshall, A NEW COUPLING COMPONENT FOR SULFANILAMIDE DETERMINATION, *J. Biol. Chem.* 128 (1939) 537–550. [https://doi.org/10.1016/S0021-9258\(18\)73708-3](https://doi.org/10.1016/S0021-9258(18)73708-3).
- [110] J.P. Singh, A rapid method for determination of nitrate in soil and plant extracts, *Plant Soil* 110 (1988) 137–139. <https://doi.org/10.1007/BF02143549>.
- [111] G. Wang, Spectrophotometric determination of nitrate and nitrite in water and some fruit samples using column preconcentration, *Talanta* 46 (1998) 671–678. [https://doi.org/10.1016/S0039-9140\(97\)00325-1](https://doi.org/10.1016/S0039-9140(97)00325-1).
- [112] H. Wu, X. Shen, D. Huo, Y. Ma, M. Bian, C. Shen, C. Hou, Fluorescent and colorimetric dual-readout sensor based on Griess assay for nitrite detection, *Spectrochim. Acta - Part A Mol. Biomol. Spectrosc.* 225 (2020). <https://doi.org/10.1016/j.saa.2019.117470>.
- [113] N. Ishio, K. Fukushi, K. Michiba, S. Takeda, S.I. Wakida, Optimum conditions for effective use of the terminating ion in transient isotachophoresis for capillary zone electrophoretic determination of nitrite and nitrate in seawater, with artificial seawater as background electrolyte, *Anal. Bioanal. Chem.* 374 (2002) 1165–1169. <https://doi.org/10.1007/s00216-002-1583-5>.
- [114] X. Wang, E. Masschelein, P. Hespel, E. Adams, A. van Schepdael, Simultaneous

- determination of nitrite and nitrate in human plasma by on-capillary preconcentration with field-amplified sample stacking, *Electrophoresis* 33 (2012) 402–405.
<https://doi.org/10.1002/elps.201100285>.
- [115] A. Gáspár, P. Juhász, K. Bágyi, Application of capillary zone electrophoresis to the analysis and to a stability study of nitrite and nitrate in saliva, *J. Chromatogr. A* 1065 (2005) 327–331. <https://doi.org/10.1016/j.chroma.2004.12.085>.
- [116] T. Miyado, Y. Tanaka, H. Nagai, S. Takeda, K. Saito, K. Fukushi, Y. Yoshida, S.I. Wakida, E. Niki, Simultaneous determination of nitrate and nitrite in biological fluids by capillary electrophoresis and preliminary study on their determination by microchip capillary electrophoresis, *J. Chromatogr. A* 1051 (2004) 185–191.
<https://doi.org/10.1016/j.chroma.2004.08.037>.
- [117] Y. Zhang, L. Yang, X. Tian, Y. Guo, W. Tang, A. Yu, W. Zhang, B. Sun, S. Zhang, Determination of trace nitrites and nitrates in human urine and plasma by field-amplified sample stacking open-tubular capillary electrochromatography in a nano-latex coated capillary, *J. Anal. Chem.* 70 (2015) 885–891.
<https://doi.org/10.1134/S1061934815070199>.
- [118] P.K. Rastogi, V. Ganesan, S. Krishnamoorthi, A promising electrochemical sensing platform based on a silver nanoparticles decorated copolymer for sensitive nitrite determination, *J. Mater. Chem. A* 2 (2014) 933–943. <https://doi.org/10.1039/c3ta13794e>.
- [119] D. Zhang, H. Ma, Y. Chen, H. Pang, Y. Yu, Amperometric detection of nitrite based on Dawson-type vanadotungstophosphate and carbon nanotubes, *Anal. Chim. Acta* 792 (2013) 35–44. <https://doi.org/10.1016/j.aca.2013.07.010>.
- [120] M. Pietrzak, M.E. Meyerhoff, Polymeric Membrane Electrodes with High Nitrite Selectivity Based on Rhodium(III) Porphyrins and Salophens as Ionophores, *Anal. Chem.* 81 (2009) 3637–3644. <https://doi.org/10.1021/ac900092f>.
- [121] S. Yang, M.E. Meyerhoff, Study of cobalt(III) corrole as the neutral ionophore for nitrite and nitrate detection via polymeric membrane electrodes, *Electroanalysis* 25 (2013) 2579–2585. <https://doi.org/10.1002/elan.201300400>.

- [122] C. Deng, J. Chen, Z. Nie, M. Yang, S. Si, Electrochemical detection of nitrite based on the polythionine/carbon nanotube modified electrode, *Thin Solid Films* 520 (2012) 7026–7029. <https://doi.org/10.1016/j.tsf.2012.07.010>.
- [123] Z. Wang, X. Liu, M. Yang, S. An, X. Han, W. Zhao, Z. Ji, X. Zhao, N. Xia, X. Yang, M. Zhong, Electrochemical detection of nitrite based on difference of surface charge of self-assembled monolayers, *Int. J. Electrochem. Sci.* 9 (2014) 1139–1145. [https://doi.org/10.1016/s1452-3981\(23\)07784-2](https://doi.org/10.1016/s1452-3981(23)07784-2).
- [124] Z. Yilong, Z. Dean, L. Daoliang, Electrochemical and Other Methods for Detection and Determination of Dissolved Nitrite: A Review, *Int. J. Electrochem. Sci.* 10 (2015) 1144–1168. [https://doi.org/10.1016/S1452-3981\(23\)05062-9](https://doi.org/10.1016/S1452-3981(23)05062-9).
- [125] M. Moorcroft, Detection and determination of nitrate and nitrite: a review, *Talanta* 54 (2001) 785–803. [https://doi.org/10.1016/S0039-9140\(01\)00323-X](https://doi.org/10.1016/S0039-9140(01)00323-X).
- [126] G. Manjari, S. Saran, S. Radhakrishanan, P. Rameshkumar, A. Pandikumar, S.P. Devipriya, Facile green synthesis of Ag–Cu decorated ZnO nanocomposite for effective removal of toxic organic compounds and an efficient detection of nitrite ions, *J. Environ. Manage.* 262 (2020) 110282. <https://doi.org/10.1016/j.jenvman.2020.110282>.
- [127] D. Manoj, R. Saravanan, J. Santhanalakshmi, S. Agarwal, V.K. Gupta, R. Boukherroub, Towards green synthesis of monodisperse Cu nanoparticles: An efficient and high sensitive electrochemical nitrite sensor, *Sensors Actuators, B Chem.* 266 (2018) 873–882. <https://doi.org/10.1016/j.snb.2018.03.141>.
- [128] W. Zhu, Y. Zhang, J. Gong, Y. Ma, J. Sun, T. Li, J. Wang, Surface Engineering of Carbon Fiber Paper toward Exceptionally High-Performance and Stable Electrochemical Nitrite Sensing, *ACS Sensors* 4 (2019) 2980–2987. <https://doi.org/10.1021/acssensors.9b01474>.
- [129] A. Baciú, F. Manea, A. Pop, R. Pode, J. Schoonman, Simultaneous voltammetric detection of ammonium and nitrite from groundwater at silver-electrodecorated carbon nanotube electrode, *Process Saf. Environ. Prot.* 108 (2017) 18–25. <https://doi.org/10.1016/j.psep.2016.05.006>.
- [130] Y. Zhang, J. Nie, H. Wei, H. Xu, Q. Wang, Y. Cong, J. Tao, Y. Zhang, L. Chu, Y. Zhou,

- X. Wu, Electrochemical detection of nitrite ions using Ag/Cu/MWNT nanoclusters electrodeposited on a glassy carbon electrode, *Sensors Actuators, B Chem.* 258 (2018) 1107–1116. <https://doi.org/10.1016/j.snb.2017.12.001>.
- [131] Q. Zhang, Y. Wang, A. Song, X. Yang, D. Yin, L. Shen, Advancements in fluorescent probes for nitrite sensing: A review, *J. Mol. Struct.* 1296 (2024) 136926. <https://doi.org/10.1016/j.molstruc.2023.136926>.
- [132] K. Wu, W. Yang, Z. Yan, H. Wang, Z. Zheng, A. Jiang, X. Wang, Z. Tang, Accurate quantification, naked eyes detection and bioimaging of nitrite using a colorimetric and near-infrared fluorescent probe in food samples and *Escherichia coli*, *Spectrochim. Acta Part A Mol. Biomol. Spectrosc.* 282 (2022) 121692. <https://doi.org/10.1016/j.saa.2022.121692>.
- [133] A.K. Nussler, M. Glanemann, A. Schirmeier, L. Liu, N.C. Nüssler, Fluorometric measurement of nitrite/nitrate by 2,3-diaminonaphthalene, *Nat. Protoc.* 1 (2006) 2223–2226. <https://doi.org/10.1038/nprot.2006.341>.
- [134] J. Wu, L. Jiang, P. Verwilt, J. An, H. Zeng, L. Zeng, G. Niu, J.S. Kim, A colorimetric and fluorescent lighting-up sensor based on ICT coupled with PET for rapid, specific and sensitive detection of nitrite in food, *Chem. Commun.* 55 (2019) 9947–9950. <https://doi.org/10.1039/c9cc05048e>.
- [135] Q. Wang, S. Ma, H. Huang, A. Cao, M. Li, L. He, Highly sensitive and selective spectrofluorimetric determination of nitrite in food products with a novel fluorogenic probe, *Food Control* 63 (2016) 117–121. <https://doi.org/10.1016/j.foodcont.2015.11.023>.
- [136] H.M. Free, The Development of Diagnostic Test Strips “ He [Al Free] said , ‘ Well , instead of doing it that way , we could get rid of the dropper if we just dipped the paper into the urine .’ That ’ s what started it .”, (2010).
- [137] S. Jahanshahi-Anbuhi, K. Pennings, V. Leung, M. Liu, C. Carrasquilla, B. Kannan, Y. Li, R. Pelton, J.D. Brennan, C.D.M. Filipe, Pullulan Encapsulation of Labile Biomolecules to Give Stable Bioassay Tablets, *Angew. Chemie Int. Ed.* 53 (2014) 6155–6158. <https://doi.org/10.1002/anie.201403222>.

- [138] S. Jahanshahi-Anbuhi, B. Kannan, V. Leung, K. Pennings, M. Liu, C. Carrasquilla, D. White, Y. Li, R.H. Pelton, J.D. Brennan, C.D.M. Filipe, Simple and ultrastable all-inclusive pullulan tablets for challenging bioassays, *Chem. Sci.* 7 (2016) 2342–2346. <https://doi.org/10.1039/C5SC04184H>.
- [139] H. Hajimiri, S.H. Safiabadi Tali, M. Al-Kassawneh, Z. Sadiq, S. Jahanshahi-Anbuhi, Tablet-Based Sensor: A Stable and User-Friendly Tool for Point-of-Care Detection of Glucose in Urine, *Biosensors* 13 (2023) 893. <https://doi.org/10.3390/bios13090893>.
- [140] Z. Sadiq, M. Al-Kassawneh, S.H. Safiabadi Tali, S. Jahanshahi-Anbuhi, Tailoring plasmonic sensing strategies for the rapid and sensitive detection of hypochlorite in swimming water samples, *Microchim. Acta* 191 (2024). <https://doi.org/10.1007/s00604-024-06246-y>.
- [141] M. Al-Kassawneh, Z. Sadiq, S. Jahanshahi-Anbuhi, User-friendly and ultra-stable all-inclusive gold tablets for cysteamine detection, *RSC Adv.* 13 (2023) 19638–19650. <https://doi.org/10.1039/D3RA03073C>.
- [142] B. Udugama, P. Kadhiresan, A. Samarakoon, W.C.W. Chan, Simplifying Assays by Tableting Reagents, *J. Am. Chem. Soc.* 139 (2017) 17341–17349. <https://doi.org/10.1021/jacs.7b07055>.
- [143] S.G. Patel, M. Siddaiah, Formulation and evaluation of effervescent tablets: a review, *J. Drug Deliv. Ther.* 8 (2018) 296–303. <https://doi.org/10.22270/jddt.v8i6.2021>.
- [144] A. Aslani, H. Jahangiri, Formulation, characterization and physicochemical evaluation of ranitidine effervescent tablets, *Adv. Pharm. Bull.* 3 (2013) 315–322. <https://doi.org/10.5681/apb.2013.051>.
- [145] A. Aslani, T. Sharifian, Formulation, characterization and physicochemical evaluation of amoxicillin effervescent tablets, *Adv. Biomed. Res.* 3 (2014) 209. <https://doi.org/10.4103/2277-9175.143252>.
- [146] S.H. Safiabadi Tali, M. Al-Kassawneh, M. Mansouri, Z. Sadiq, S. Jahanshahi-Anbuhi, All-Inclusive Sensing Tablet with Integrated Passive Mixer for Ultraviscous Solutions, *ACS Sensors* (2025). <https://doi.org/10.1021/acssensors.4c03726>.

- [147] T. Gong, J. Liu, X. Liu, J. Liu, J. Xiang, Y. Wu, A sensitive and selective sensing platform based on CdTe QDs in the presence of l -cysteine for detection of silver, mercury and copper ions in water and various drinks, *Food Chem.* 213 (2016) 306–312. <https://doi.org/10.1016/j.foodchem.2016.06.091>.
- [148] V.L. Dressler, D. Pozebon, A.J. Curtius, Determination of heavy metals by inductively coupled plasma mass spectrometry after on-line separation and preconcentration, *Spectrochim. Acta Part B At. Spectrosc.* 53 (1998) 1527–1539. [https://doi.org/10.1016/S0584-8547\(98\)00180-3](https://doi.org/10.1016/S0584-8547(98)00180-3).
- [149] A.S.N. Trindade, A.F. Dantas, D.C. Lima, S.L.C. Ferreira, L.S.G. Teixeira, Multivariate optimization of ultrasound-assisted extraction for determination of Cu, Fe, Ni and Zn in vegetable oils by high-resolution continuum source atomic absorption spectrometry, *Food Chem.* 185 (2015) 145–150. <https://doi.org/10.1016/j.foodchem.2015.03.118>.
- [150] E.S. Forzani, H. Zhang, W. Chen, N. Tao, Detection of Heavy Metal Ions in Drinking Water Using a High-Resolution Differential Surface Plasmon Resonance Sensor, *Environ. Sci. Technol.* 39 (2005) 1257–1262. <https://doi.org/10.1021/es049234z>.
- [151] S. Wang, E.S. Forzani, N. Tao, Detection of Heavy Metal Ions in Water by High-Resolution Surface Plasmon Resonance Spectroscopy Combined with Anodic Stripping Voltammetry, *Anal. Chem.* 79 (2007) 4427–4432. <https://doi.org/10.1021/ac0621773>.
- [152] R. Sitko, P. Janik, B. Zawisza, E. Talik, E. Margui, I. Queralt, Green Approach for Ultratrace Determination of Divalent Metal Ions and Arsenic Species Using Total-Reflection X-ray Fluorescence Spectrometry and Mercapto-Modified Graphene Oxide Nanosheets as a Novel Adsorbent, *Anal. Chem.* 87 (2015) 3535–3542. <https://doi.org/10.1021/acs.analchem.5b00283>.
- [153] R. Van Grieken, A. Speecke, J. Hoste, The determination of copper in iron and steel by 14-Mev neutron activation analysis, *Anal. Chim. Acta* 51 (1970) 151–162. [https://doi.org/10.1016/S0003-2670\(01\)95703-4](https://doi.org/10.1016/S0003-2670(01)95703-4).
- [154] M.F. Reis, M. Abdulla, R.M. Parr, A. Chatt, H.S. Dang, A.A.S.C. Machado, Trace element contents in food determined by neutron activation analysis and other techniques,

- Biol. Trace Elem. Res. 43–45 (1994) 481–487. <https://doi.org/10.1007/BF02917350>.
- [155] V.N. Losev, O. V. Buyko, A.K. Trofimchuk, O.N. Zuy, Silica sequentially modified with polyhexamethylene guanidine and Arsenazo I for preconcentration and ICP–OES determination of metals in natural waters, *Microchem. J.* 123 (2015) 84–89. <https://doi.org/10.1016/j.microc.2015.05.022>.
- [156] K.M. Dimpe, J.C. Ngila, N. Mabuba, P.N. Nomngongo, Evaluation of sample preparation methods for the detection of total metal content using inductively coupled plasma optical emission spectrometry (ICP–OES) in wastewater and sludge, *Phys. Chem. Earth, Parts A/B/C* 76–78 (2014) 42–48. <https://doi.org/10.1016/j.pce.2014.11.006>.
- [157] G.L. Donati, R.S. Amais, C.B. Williams, Recent advances in inductively coupled plasma optical emission spectrometry, *J. Anal. At. Spectrom.* 32 (2017) 1283–1296. <https://doi.org/10.1039/C7JA00103G>.
- [158] J. Feldmann, P. Salaün, E. Lombi, Critical review perspective: elemental speciation analysis methods in environmental chemistry - moving towards methodological integration, *Environ. Chem.* 6 (2009) 275. <https://doi.org/10.1071/EN09018>.
- [159] J.F. Zhang, Y. Zhou, J. Yoon, J.S. Kim, Recent progress in fluorescent and colorimetric chemosensors for detection of precious metal ions (silver, gold and platinum ions), *Chem. Soc. Rev.* 40 (2011) 3416. <https://doi.org/10.1039/c1cs15028f>.
- [160] Z. Gerdan, Y. Saylan, A. Denizli, Recent Advances of Optical Sensors for Copper Ion Detection, *Micromachines* 13 (2022) 1298. <https://doi.org/10.3390/mi13081298>.
- [161] A.W. Martinez, S.T. Phillips, E. Carrilho, S.W. Thomas, H. Sindi, G.M. Whitesides, Simple telemedicine for developing regions: Camera phones and paper-based microfluidic devices for real-time, off-site diagnosis, *Anal. Chem.* 80 (2008) 3699–3707. <https://doi.org/10.1021/ac800112r>.
- [162] N. Bagheri, V. Mazzaracchio, S. Cinti, N. Colozza, C. Di Natale, P.A. Netti, M. Saraji, S. Roggero, D. Moscone, F. Arduini, Electroanalytical Sensor Based on Gold-Nanoparticle-Decorated Paper for Sensitive Detection of Copper Ions in Sweat and Serum, *Anal. Chem.* 93 (2021) 5225–5233. <https://doi.org/10.1021/acs.analchem.0c05469>.

- [163] H.N. Nayan Kumar, D.H. Nagaraju, Z. Yhobu, P. Shivakumar, K.S. Manjunatha Kumara, S. Budagumpi, B.M. Praveen, Recent advances in on-site monitoring of heavy metal ions in the environment, *Microchem. J.* 182 (2022) 107894. <https://doi.org/10.1016/j.microc.2022.107894>.
- [164] Y.D. Li, H.H. Chai, S.J. Zhang, Z.S. Lu, C.M. Li, L. Yu, Sensitive and portable colorimetric detection of copper in water by cotton thread based pre-concentration, *Microchem. J.* 148 (2019) 735–742. <https://doi.org/10.1016/j.microc.2019.05.056>.
- [165] M. Pérez-Rodríguez, M. del P. Cañizares-Macías, A prototype microfluidic paper-based chromatic device for simultaneous determination of copper(II) and zinc(II) in urine, *Talanta Open* 7 (2023) 100178. <https://doi.org/10.1016/j.talo.2022.100178>.
- [166] O.D. Oyewunmi, S.H. Safiabadi-Tali, S. Jahanshahi-Anbuhi, Dual-Modal Assay Kit for the Qualitative and Quantitative Determination of the Total Water Hardness Using a Permanent Marker Fabricated Microfluidic Paper-Based Analytical Device, *Chemosensors* 8 (2020) 97. <https://doi.org/10.3390/chemosensors8040097>.
- [167] M.M. Mentele, J. Cunningham, K. Koehler, J. Volckens, C.S. Henry, Microfluidic Paper-Based Analytical Device for Particulate Metals, *Anal. Chem.* 84 (2012) 4474–4480. <https://doi.org/10.1021/ac300309c>.
- [168] A. Radwan, I.M. El-Sewify, H.M.E.-S. Azzazy, Monitoring of Cobalt and Cadmium in Daily Cosmetics Using Powder and Paper Optical Chemosensors, *ACS Omega* 7 (2022) 15739–15750. <https://doi.org/10.1021/acsomega.2c00730>.
- [169] Hach Company, FerroVer Iron Reagent Powder Pillows (pk/100), Hatch (2025). Industrial Test Systems – Heavy Metals Check (accessed March 30, 2025).
- [170] C.-P. Canada, Lovibond RP009-0 Powder Pillow DPD Free Chlorine Reagent, 5 mL, 100 Tests, Cole-Parmer (2025). <https://www.coleparmer.ca/i/lovibond-rp009-0-powder-pillow-dpd-free-chlorine-reagent-5-ml-100-tests/9956052> (accessed March 30, 2025).
- [171] Lovibond, Copper No.1 Tablet Reagents, 250 pack, (n.d.). <https://www.lovibond.com/usa-en/PW/Water-Testing/Products/Reagents/Tablet-Reagents/Copper-No.-1/Copper-No.1-Tablet-Reagents-250-pack> (accessed April 4, 2025).

- [172] Palintest Ltd., Palintest total copper, 250 tests, (n.d).
<https://www.lincolnaquatics.com/palintest-reagents/25-765/product/25-765> (accessed April 4, 2025).
- [173] M. Al-Kassawneh, Z. Sadiq, S. Jahanshahi-Anbuhi, User-friendly and ultra-stable all-inclusive gold tablets for cysteamine detection, *RSC Adv.* 13 (2023) 19638–19650.
<https://doi.org/10.1039/d3ra03073c>.
- [174] Z. Sadiq, S.H. Safiabadi Tali, S. Jahanshahi-Anbuhi, Gold Tablets: Gold Nanoparticles Encapsulated into Dextran Tablets and Their pH-Responsive Behavior as an Easy-to-Use Platform for Multipurpose Applications, *ACS Omega* 7 (2022) 11177–11189.
<https://doi.org/10.1021/acsomega.1c07393>.
- [175] Z. Sadiq, S.H. Safiabadi Tali, M. Mansouri, S. Jahanshahi-Anbuhi, A dual-functional nanogold tablet as a plasmonic and nanozyme sensor for point-of-care applications, *Nanoscale Adv.* (2025). <https://doi.org/10.1039/D5NA00082C>.
- [176] M. Rahamathulla, S.M. Alshahrani, A. Al Saqr, A. Alshetaili, F. Shakeel, Effervescent floating matrix tablets of a novel anti-cancer drug neratinib for breast cancer treatment, *J. Drug Deliv. Sci. Technol.* 66 (2021) 102788. <https://doi.org/10.1016/j.jddst.2021.102788>.
- [177] S. Jadhav, A. Gangurde, A Bird Eye View on Effervescent Drug Delivery System, *Int. J. Drug Deliv. Technol.* 13 (2023) 1046–1058. <https://doi.org/10.25258/ijddt.13.3.45>.
- [178] I. Diane, J. Burt, N. Windsor, (12) United States Patent, 2 (2006).
- [179] Y. Sun, X. Yang, J. Hu, F. Ji, H. Chi, Y. Liu, K. Hu, F. Hao, X. Wen, Portable one-step effervescence tablet-based microextraction combined with smartphone digital image colorimetry: Toward field and rapid detection of trace nickel ion, *Talanta* 274 (2024) 126036. <https://doi.org/10.1016/j.talanta.2024.126036>.
- [180] P. Zhou, R. Zheng, W. Zhang, W. Liu, Y. Li, H. Wang, X. Wang, Development of an effervescent tablet microextraction method using NiFe₂O₄-based magnetic nanoparticles for preconcentration/extraction of heavy metals prior to ICP-MS analysis of seafood, *J. Anal. At. Spectrom.* 34 (2019) 598–606. <https://doi.org/10.1039/C8JA00331A>.
- [181] Y. Sun, X. Yang, R. Zhang, T. Xia, K. Hu, F. Hao, Y. Liu, Q. Deng, S. Yang, X. Wen,

- One-step effervescence tablet-assisted switchable hydrophilic solvent microextraction combined with micro spectrophotometry for the determination of copper in *Salvia yunnanensis* and environmental samples, *Microchem. J.* 187 (2023) 108372.
<https://doi.org/10.1016/j.microc.2022.108372>.
- [182] S. Webzell, Chemical reactions, *Machinery* 176 (2018) 15–18.
<https://doi.org/10.4324/9781003234357-12>.
- [183] No Title, (n.d.). <https://doi.org/>.
- [184] N.O. Sierra-Vega, R.J. Romañach, R. Méndez, Feed frame: The last processing step before the tablet compaction in pharmaceutical manufacturing, *Int. J. Pharm.* 572 (2019) 118728. <https://doi.org/10.1016/j.ijpharm.2019.118728>.
- [185] D.J. Goodwin, S. van den Ban, M. Denham, I. Barylski, Real time release testing of tablet content and content uniformity, *Int. J. Pharm.* 537 (2018) 183–192.
<https://doi.org/10.1016/j.ijpharm.2017.12.011>.
- [186] K.A. Johnson, R.S. Goody, The original Michaelis constant: Translation of the 1913 Michaelis-Menten Paper, *Biochemistry* 50 (2011) 8264–8269.
<https://doi.org/10.1021/bi201284u>.
- [187] Thermo Scientific, Thermo Scientific AC2029 Copper (Free, Total) Reagent Tablets, 50 Tests, (n.d.). <https://www.tequipment.net/Thermo-Scientific/AC2029/Lab-Accessories/> (accessed April 4, 2025).
- [188] Wilhelmsen, Copper No.1 Tablets (100), (n.d.). <https://www.wilhelmsen.com/product-catalogue/products/marine-chemicals/test-kits-and-reagents/water-test-kit---spares-and-consumables/copper-no.1-tablets100> (accessed April 4, 2025).
- [189] Hanna Instruments, Copper Chemical Test Kit – HI3847, (n.d.).
<https://hannacan.com/product/copper-chemical-test-kit-hi3847/> (accessed April 4, 2025).
- [190] Hach Company, Copper Reagent Set, Porphyrin, 10 mL, (n.d.).
https://ca.hach.com/copper-reagent-set-porphyrin-10-ml/product?id=14533947376&utm_source=chatgpt.com (accessed April 4, 2025).

- [191] Merck KGaA / Sigma-Aldrich, Copper Test, photometric, (n.d.).
<https://www.sigmaaldrich.com/CA/en/product/mm/114767> (accessed April 4, 2025).
- [192] AquaPhoenix Scientific, K-3510 Copper Test Kit, (n.d.).
<https://catalog.aquaphoenixsci.com/products/testing-supplies/test-kits/k-3510-copper>
 (accessed April 4, 2025).
- [193] <https://ccme.ca/en/results/143ch1,2,3,4,5,6.pdf>, (n.d.).
- [194] H. Zhang, L. Zhang, C. Lu, L. Zhao, Z. Zheng, CdTe nanocrystals-enhanced chemiluminescence from peroxyxynitrous acid–carbonate and its application to the direct determination of nitrite, *Spectrochim. Acta Part A Mol. Biomol. Spectrosc.* 85 (2012) 217–222. <https://doi.org/10.1016/j.saa.2011.09.063>.
- [195] Z. Lin, W. Xue, H. Chen, J.-M. Lin, Peroxyxynitrous-Acid-Induced Chemiluminescence of Fluorescent Carbon Dots for Nitrite Sensing, *Anal. Chem.* 83 (2011) 8245–8251.
<https://doi.org/10.1021/ac202039h>.
- [196] M. Yaqoob, B. Folgado Biot, A. Nabi, P.J. Worsfold, Determination of nitrate and nitrite in freshwaters using flow-injection with luminol chemiluminescence detection, *Luminescence* 27 (2012) 419–425. <https://doi.org/10.1002/bio.1366>.
- [197] X. Wang, E. Adams, A. Van Schepdael, A fast and sensitive method for the determination of nitrite in human plasma by capillary electrophoresis with fluorescence detection, *Talanta* 97 (2012) 142–144. <https://doi.org/10.1016/j.talanta.2012.04.008>.
- [198] L. He, K. Zhang, C. Wang, X. Luo, S. Zhang, Effective indirect enrichment and determination of nitrite ion in water and biological samples using ionic liquid-dispersive liquid–liquid microextraction combined with high-performance liquid chromatography, *J. Chromatogr. A* 1218 (2011) 3595–3600. <https://doi.org/10.1016/j.chroma.2011.04.014>.
- [199] P. Das, S. Biswas, S.S. Bhattacharya, P. Nath, Carbon Nanodot–Neutral Red-Based Photometric and Fluorescence Sensing for Trace Detection of Nitrite in Water and Soil Using Smartphone, *ACS Appl. Nano Mater.* 5 (2022) 3265–3274.
<https://doi.org/10.1021/acsanm.1c03702>.
- [200] Z. Huang, T. Korenaga, M.I.H. Helaleh, Kinetic Spectrofluorimetric Determination of

- Nitrite in Water Samples and Nitrogen Dioxide in the Atmosphere Sampled by the Liquid Droplet Method, *Microchim. Acta* 134 (2000) 179–183.
<https://doi.org/10.1007/s006040050064>.
- [201] M. Ghanei-Motlagh, M.A. Taher, A novel electrochemical sensor based on silver/halloysite nanotube/molybdenum disulfide nanocomposite for efficient nitrite sensing, *Biosens. Bioelectron.* 109 (2018) 279–285.
<https://doi.org/10.1016/j.bios.2018.02.057>.
- [202] D. Ning, H. Zhang, J. Zheng, Electrochemical sensor for sensitive determination of nitrite based on the PAMAM dendrimer-stabilized silver nanoparticles, *J. Electroanal. Chem.* 717–718 (2014) 29–33. <https://doi.org/10.1016/j.jelechem.2013.12.011>.
- [203] J. Nam, I.-B. Jung, B. Kim, S.-M. Lee, S.-E. Kim, K.-N. Lee, D.-S. Shin, A colorimetric hydrogel biosensor for rapid detection of nitrite ions, *Sensors Actuators B Chem.* 270 (2018) 112–118. <https://doi.org/10.1016/j.snb.2018.04.171>.
- [204] J. Sun, T. Long, Z. Chen, H. Luo, J. Cao, D. Xu, Z. Yuan, Rapid and dual-mode nitrite detection with improved sensitivity by nanointerface-regulated ultrafast Griess assay, *Anal. Chim. Acta* 1336 (2025) 343524. <https://doi.org/10.1016/j.aca.2024.343524>.
- [205] O.R. Chanu, R. Savitha, A. Kapoor, S. Gopalakrishnan, V. Karthik, S. Pushpavanam, A Facile Colorimetric Sensor for Sensitive Detection of Nitrite in the Simulated Saliva, *Sens. Imaging* 25 (2024) 1–20. <https://doi.org/10.1007/s11220-024-00458-5>.
- [206] V.Y.C. Li, B. Udugama, P. Kadhiresan, W.C.W. Chan, Sequential Reagent Release from a Layered Tablet for Multistep Diagnostic Assays, *Anal. Chem.* 94 (2022) 17102–17111. <https://doi.org/10.1021/acs.analchem.2c03315>.
- [207] D. Giustarini, R. Rossi, A. Milzani, I. Dalle-Donne, Nitrite and Nitrate Measurement by Griess Reagent in Human Plasma: Evaluation of Interferences and Standardization, *Methods Enzymol.* 440 (2008) 361–380. [https://doi.org/10.1016/S0076-6879\(07\)00823-3](https://doi.org/10.1016/S0076-6879(07)00823-3).
- [208] A.M. Gurban, L.G. Zamfir, P. Epure, I.R. Șuică-Bunghez, R.M. Senin, M.L. Jecu, M.L. Jinga, M. Doni, Flexible Miniaturized Electrochemical Sensors Based on Multiwalled Carbon Nanotube-Chitosan Nanomaterial for Determination of Nitrite in Soil Solutions,

- Chemosensors 11 (2023). <https://doi.org/10.3390/chemosensors11040224>.
- [209] D. Yang, B. Youden, N. Yu, A.J. Carrier, M.R. Servos, K.D. Oakes, Surface-Enhanced Raman Spectroscopy for Nitrite Detection, (2025). <https://doi.org/10.1021/acs.jafc.4c09391>.
- [210] R. Catalan-Carrio, J. Saez, L.Á. Fernández Cuadrado, G. Arana, L. Basabe-Desmonts, F. Benito-Lopez, Ionogel-based hybrid polymer-paper handheld platform for nitrite and nitrate determination in water samples, *Anal. Chim. Acta* 1205 (2022) 1–8. <https://doi.org/10.1016/j.aca.2022.339753>.
- [211] S. Dudala, S.K. Dubey, S. Goel, Fully Integrated, Automated, and Smartphone Enabled Point-of-Source Portable Platform With Microfluidic Device for Nitrite Detection, *IEEE Trans. Biomed. Circuits Syst.* 13 (2019) 1518–1524. <https://doi.org/10.1109/TBCAS.2019.2939658>.
- [212] W. Khongpet, P. Yanu, S. Pencharee, C. Puangpila, S. Kradtap Hartwell, S. Lapanantnoppakhun, Y. Yodthongdee, A. Paukpol, J. Jakmunee, A compact multi-parameter detection system based on hydrodynamic sequential injection for sensitive determination of phosphate, nitrite, and nitrate in water samples, *Anal. Methods* 12 (2020) 855–864. <https://doi.org/10.1039/c9ay02327e>.
- [213] J. Noiphung, M.P. Nguyen, C. Punyadeera, Y. Wan, W. Laiwattanapaisa, C.S. Henry, Development of paper-based analytical devices for minimizing the viscosity effect in human saliva, *Theranostics* 8 (2018) 3797–3807. <https://doi.org/10.7150/thno.24941>.
- [214] T.M.G. Cardoso, P.T. Garcia, W.K.T. Coltro, Colorimetric determination of nitrite in clinical, food and environmental samples using microfluidic devices stamped in paper platforms, *Anal. Methods* 7 (2015) 7311–7317. <https://doi.org/10.1039/c5ay00466g>.
- [215] E. Trofimchuk, Y. Hu, A. Nilghaz, M.Z. Hua, S. Sun, X. Lu, Development of paper-based microfluidic device for the determination of nitrite in meat, *Food Chem.* 316 (2020). <https://doi.org/10.1016/j.foodchem.2020.126396>.
- [216] S.N. Baker, G.A. Baker, Luminescent carbon nanodots: Emergent nanolights, *Angew. Chemie - Int. Ed.* 49 (2010) 6726–6744. <https://doi.org/10.1002/anie.200906623>.

- [217] Z. Yang, Z. Li, M. Xu, L. Zhang, J. Zhang, Y. Su, F. Gao, H. Wei, Controllable Synthesis of Fluorescent Carbon, *Micro Nano Lett.* 5 (2013) 247–259.
- [218] A. Khayal, V. Dawane, M.A. Amin, V. Tirth, V.K. Yadav, A. Algahtani, S.H. Khan, S. Islam, K.K. Yadav, B.H. Jeon, Advances in the methods for the synthesis of carbon dots and their emerging applications, *Polymers (Basel)*. 13 (2021) 1–31.
<https://doi.org/10.3390/polym13183190>.
- [219] M. Tuerhong, Y. XU, X.B. YIN, Review on Carbon Dots and Their Applications, *Chinese J. Anal. Chem.* 45 (2017) 139–150. [https://doi.org/10.1016/S1872-2040\(16\)60990-8](https://doi.org/10.1016/S1872-2040(16)60990-8).
- [220] Z. Kang, S.T. Lee, Carbon dots: Advances in nanocarbon applications, *Nanoscale* 11 (2019) 19214–19224. <https://doi.org/10.1039/c9nr05647e>.
- [221] L. Bao, Z.L. Zhang, Z.Q. Tian, L. Zhang, C. Liu, Y. Lin, B. Qi, D.W. Pang, Electrochemical tuning of luminescent carbon nanodots: From preparation to luminescence mechanism, *Adv. Mater.* 23 (2011) 5801–5806.
<https://doi.org/10.1002/adma.201102866>.
- [222] P.-C. Hsu, P.-C. Chen, C.-M. Ou, H.-Y. Chang, H.-T. Chang, Extremely high inhibition activity of photoluminescent carbon nanodots toward cancer cells, *J. Mater. Chem. B* 1 (2013) 1774. <https://doi.org/10.1039/c3tb00545c>.
- [223] Y. Dong, R. Wang, W. Tian, Y. Chi, G. Chen, “Turn-on” fluorescent detection of cyanide based on polyamine-functionalized carbon quantum dots, *RSC Adv.* 4 (2014) 3685–3689. <https://doi.org/10.1039/C3RA45893H>.
- [224] X. Hou, F. Zeng, F. Du, S. Wu, Carbon-dot-based fluorescent turn-on sensor for selectively detecting sulfide anions in totally aqueous media and imaging inside live cells, *Nanotechnology* 24 (2013) 335502. <https://doi.org/10.1088/0957-4484/24/33/335502>.
- [225] S.D. Torres Landa, N.K. Reddy Bogireddy, I. Kaur, V. Batra, V. Agarwal, Heavy metal ion detection using green precursor derived carbon dots, *IScience* 25 (2022) 103816. <https://doi.org/10.1016/j.isci.2022.103816>.
- [226] Y. Dong, R. Wang, G. Li, C. Chen, Y. Chi, G. Chen, Polyamine-Functionalized Carbon Quantum Dots as Fluorescent Probes for Selective and Sensitive Detection of Copper

- Ions, *Anal. Chem.* 84 (2012) 6220–6224. <https://doi.org/10.1021/ac3012126>.
- [227] Z. Sun, Y. Zhou, W. Zhou, J. Luo, R. Liu, X. Zhang, L. Zhou, Q. Pang, Pb(II) detection and versatile bio-imaging of green-emitting carbon dots with excellent stability and bright fluorescence, *Nanoscale* 13 (2021) 2472–2480. <https://doi.org/10.1039/D0NR07245A>.
- [228] S. Barman, M. Sadhukhan, Facile bulk production of highly blue fluorescent graphitic carbon nitride quantum dots and their application as highly selective and sensitive sensors for the detection of mercuric and iodide ions in aqueous media, *J. Mater. Chem.* 22 (2012) 21832. <https://doi.org/10.1039/c2jm35501a>.
- [229] Z.-X. Wang, X.-H. Yu, F. Li, F.-Y. Kong, W.-X. Lv, D.-H. Fan, W. Wang, Preparation of boron-doped carbon dots for fluorometric determination of Pb(II), Cu(II) and pyrophosphate ions, *Microchim. Acta* 184 (2017) 4775–4783. <https://doi.org/10.1007/s00604-017-2526-3>.
- [230] S. Mohapatra, S. Sahu, N. Sinha, S.K. Bhutia, Synthesis of a carbon-dot-based photoluminescent probe for selective and ultrasensitive detection of Hg²⁺ in water and living cells, *Analyst* 140 (2015) 1221–1228. <https://doi.org/10.1039/C4AN01386G>.
- [231] A. Clermont-Paquette, K. Larocque, A. Piekny, R. Naccache, Shining a light on cells: amine-passivated fluorescent carbon dots as bioimaging nanoprobe, *Mater. Adv.* 5 (2024) 3662–3674. <https://doi.org/10.1039/d3ma00702b>.

Appendices

The part contains three sections focused on sensor development. **APPENDIX A** presents supplementary information for Chapter 3. **APPENDIX B** presents supplementary information for Chapter 4. **APPENDIX C** reports on the early-stage attempts involving the synthesis, characterization, and application of carbon dots (CDs) for detecting heavy metals in water, with a focus on their potential use in portable platforms. Although these efforts did not yield successful outcomes, they are documented here for the sake of record-keeping. The section includes an introduction to carbon dots, their synthesis methods, and initial fluorescence-based tests for detecting metals such as Cu^{2+} and Pb^{3+} . Additionally, it covers attempts to develop quantum dot (QD) tablets and paper-based platforms. Despite the challenges faced and the inability to achieve reliable results in these tests, the documentation serves as a foundation for future improvements and further research.

APPENDIX A. Supplementary information for Chapter 3

Here are links to two videos providing supporting information: 1- A comparison of the format of traditional and auto-mixing tablets. [Video 1: [Link](#)]. 2-A demonstration of the challenges encountered with the powder formulation. [Video 2: [Link](#)]

APPENDIX B. Supplementary information for Chapter 4

In this section the development and optimization of tablet-based sensors for nitrite detection has been examined. It covers experiments for tablet formation. Also includes stability, kinetics, and calibration curve of all-in-one tablets. Additionally, the sensor's real soil sample results for nitrite detection were compared with standard UV-Vis methods.

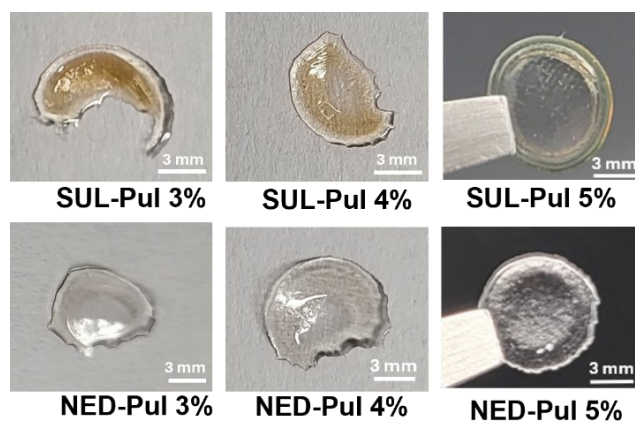


Figure A 4. Different percentages of pullulan (3%, 4%, and 5% w/v) were tested for preparing solid tablets. The solutions were pipetted to prepare polysaccharide-encapsulated tablets. Each N-(1-naphthyl)ethylenediamine dihydrochloride (NED) and sulfanilamide (SUL) solution was dispensed onto a carbon-steel tray and dried at room temperature in a dark environment for 24 hours. Compared to 5% tablets, lower percentages were not physically stable and did not maintain a spherical shape. Conversely, increasing the pullulan percentage prolonged the dissolving time during tests. Thus, the 5% composition was optimized and chosen for subsequent experiments. With regard to the concentrations of SUL and NED, we formulated the tablets and determined the concentrations and volumes of NED and SUL according to the standard Griess assay protocol [1]. In both methods, 100 μ L of NED solution (1 mg/mL) and 100 μ L of SUL solution (10 mg/mL) was used to cast the tablets.

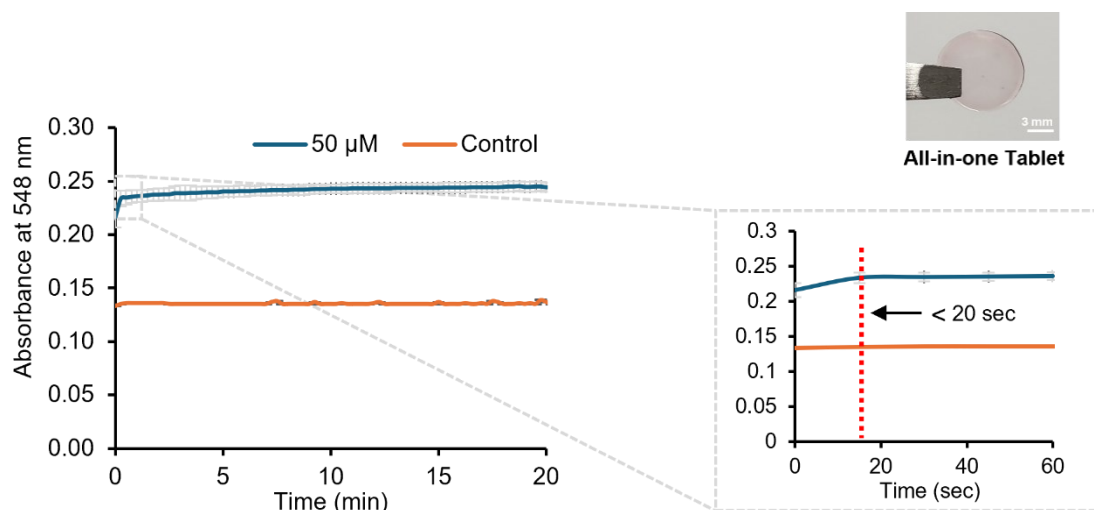


Figure A5. The kinetic study of all-in-one tablets in concentration of 50 μM nitrite ($n=3$). The time-dependent light absorbance of the nitrite samples was measured using a UV-Vis spectrometer. To account for background color intensity, in readings we added a control sample which did not contain the nitrite. The absorbance at 548 nm was recorded at 15-seconds intervals over a total time duration of 20 minutes. The results showed that, similar to the kinetics of SUL and NED tablets the sensor had rapid increase in absorbance response, stabilizing and saturating within the first minutes. Since the all-in-one tablet has a pinkish color due to the reaction between the reagents during the drying process, it showed a higher absorbance level in both 50 μM nitrite and background color intensity compared to the SUL and NED tablets.

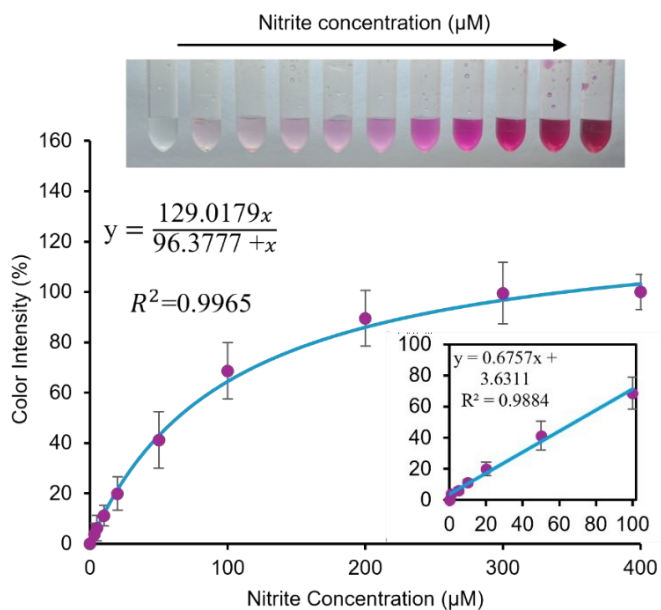


Figure A6. The calibration curve for nitrite detection using all-in-one tablets was developed. The color intensity of the solution correlated with nitrite concentration, and the Michaelis–Menten equation was used to plot the relationship. The calibration curve had an R^2 value of 0.9965, and a LoD of 5 μM was calculated in the buffer medium ($n=3$).

Analytical performance comparison

The SUL, NED tablet and all-in-one tablet showed similar performance and sensitivity across the parameters. LoD is lower for SUL, NED (3 μM) compared to 5 μM (due to a background color) for All-in-one, making it more effective for detecting lower concentrations. In terms of accuracy,

both figures showed a strong correlation ($R^2 > 0.98$) in both the linear curve and the Michaelis-Menten curve. While UV-Vis range detection is 1-200 μM , the tablet-based method covers a broader working range of 3-400 μM , as well as offering pre-measured quantities, ease of use, portability and stability (Table A1).

Table A1. Analytical Performance Comparison of Dual (SUL, NED) Tablet, All-in-One Tablet, and UV-Vis Method.

Parameter	Dual tablet	All-in-one tablet
Working range (μM)	3-400	5-400
Linear range (μM)	0-100	0-100
Sensitivity (slope of linear curve)	0.6826	0.6757
R^2 (linear curve)	0.9871	0.9884
R^2 (Michaelis-Menten curve)	0.9971	0.9965

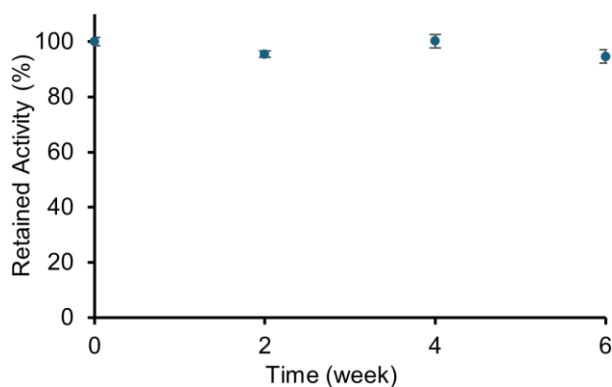


Figure A7. The stability of all-in-one tablets was assessed over six weeks. Tablets were stored at room temperature (22°C) in a glass vial containing silica gel pack and wrapped in aluminum foil. Tablets were tested in 50 μM nitrite solution in citrate-phosphate buffer. Results were normalized such that the percentage on day 0 represented 100% activity. According to the standard Griess assay protocol [1], liquid reagent mixtures have limited stability, requiring use within 8 hours due

to NED's sensitivity to air and light. In contrast, the tablets exhibited high stability, comparable to SUL and NED tablets (n=3).

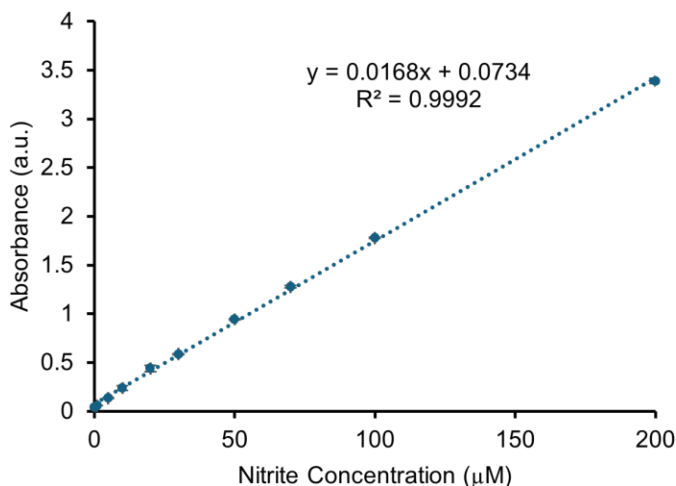


Figure A8. Nitrite detection was performed using standard UV-Vis tests following the ThermoFisher Scientific protocol (n=3) [1]. The reagent solutions we prepared by dissolving 1 mg/ml of NED in deionized water and 10 mg/ml of SUL in 5% phosphoric acid. In the next step, a mixture of 1:1 ratio of the NED and SUL solutions was prepared for use in the tests before measurements. For the test, 20 μL of the Griess reagent mixture was added to one well of a 96-well plate, followed by the addition of 150 μL of the sample and 130 μL of deionized water. After that, the solution was shaken for 30 minutes on a microplate vortex mixer (Fisherbrand, USA) before reading the results at room temperature with a UV-Vis instrument at 540 nm (Cytation 5, Agilent Technologies, USA). Nitrite concentrations of 1-200 μM were prepared in deionized water and tested with the UV-Vis method to obtain the calibration curve.

APPENDIX C. Development of portable fluorescent sensors for heavy metal detection in water

C.1 Introduction to carbon dots

Carbon dots (CDs) such as fullerenes, carbon nanotubes, and graphene are a novel class of materials known by their small size, with a diameter of less than 10 nm, composed from carbon. Because of their optical and chemical properties and biocompatibility they are becoming a promising alternative to metal-based quantum [216]. CDs are synthesized through two main

approaches. One is "top-down", which involve breaking down larger carbon materials like graphite or carbon nanotubes into small pieces through techniques like laser ablation, electrochemical oxidation and arc discharge. The other approaches is "bottom-up" that build CDs nanomaterials from smaller organic molecules through chemical reactions such as pyrolysis, microwave synthesis, and hydrothermal methods [217,218]. CDs are strong fluorescence materials with excellent stability. They have gained many attentions these days because of their unique properties including; excellent biocompatibility, low toxicity, and tunable fluorescence, which means that they can emit light in various colors based on their size or surface modifications [219,220]. Different functional groups (e.g., amino, carboxyl, hydroxyl) could be used to modify the surface of these materials and enhance their properties, such as fluorescence, solubility, and reactivity [221]. It is thought that the number of conjugated π bonds significantly affects the optical properties of these materials, particularly lead to the red shift, longer wavelength, in the photoluminescence emission. CDs could have anticancer activity as they can induce reactive oxygen species (ROS) generation within cancer cells leading to their apoptosis even without light exposure [222].

C.2 Detection heavy metals by CDs

As discussed earlier, heavy metal pollution is one of the most harmful threats to human health and the environment, with the potential to impact global sustainability over the long time. Therefore, develop practical and effective sensors is necessary for detecting these elements and reduce water pollution. CDs have chosen as desire materials for detection of heavy metal ions, due to the excellent fluorescence properties. CDs are not commonly utilized for detecting anions in compared with metal ion. When anions are added they can recover the fluorescence that was quenched by the cations, as the anions form stable complexes with the metal ions. Typically, in anion assays cations are used as controlling agents [223,224]. Many CDs have been used for fluorometric metal ion sensing. As an example, green synthesized and simple CDs were used for fluorescence sensing, specially targeting Iron (III) and Escherichia coli (E. coli) [225]. Dong et al. developed branched polyamine-functionalized carbon quantum dots for detect trace amounts of Cu^{2+} with a detection limit of 6 nM. The quenching happened through an IFE. They tested Cu concentrations ranging from 0 to 9 μM in real river water samples [226]. Sun and co-workers developed green-emitting carbon dots for measuring lead ions and bioimaging. the detection limit was 3.0174 μM for Pb^{2+} . They tested imaging ability in zebrafish embryos which showed both biological and

environmental applications of particles [227]. In the other study, highly blue fluorescent graphitic carbon nitride QDs (g-CNQDs) applied as sensor for measuring mercuric and iodide ions. The detection was based on by ON-OFF-ON" mechanism, as the fluorescence is quenched by Hg^{2+} ions (OFF) and restored by the addition of I^- ions (ON) and iodide binds to the Hg^{2+} to form HgI_2 [228]. In 2017, Wang et al. synthesised boron-doped carbon dots (B-C-dots) with blue light fluorescence for quenching by Pb^{2+} and Cu^{2+} ions. After that, the addition of pyrophosphate (PPi) restores the fluorescence by binding with the Cu^{2+} ions. The study has done with detection limits of 8.47 nM for Pb^{2+} and 13.56 nM for Cu^{2+} . [229] Mohapatra et al. developed nitrogen-sulfur co-doped carbon dots (NSCDs) with quantum yield of 69%. These NSCDs serve as highly sensitive photoluminescent sensors for detecting mercury ions, with limit of detection of 0.05 nM. The fluorescence quenching occurred because of the interaction between the sulfur in the NSCDs and Hg^{2+} ions [230].

C.3 Synthesis of graphene quantum dots

One gram of citric acid was placed in a crucible and heated at a temperature of 180–200°C until it melted completely. After five minutes, one gram of thiourea was introduced into the molten citric acid. The color of the mixture gradually changed from pale yellow to orange over a period of 20 minutes, indicating the formation of functionalized graphene quantum dots. Subsequently, the orange-colored liquid was added dropwise into 100 mL of a 10 mg/mL NaOH aqueous solution under vigorous stirring. This process resulted in the formation of functionalized graphene quantum dots.

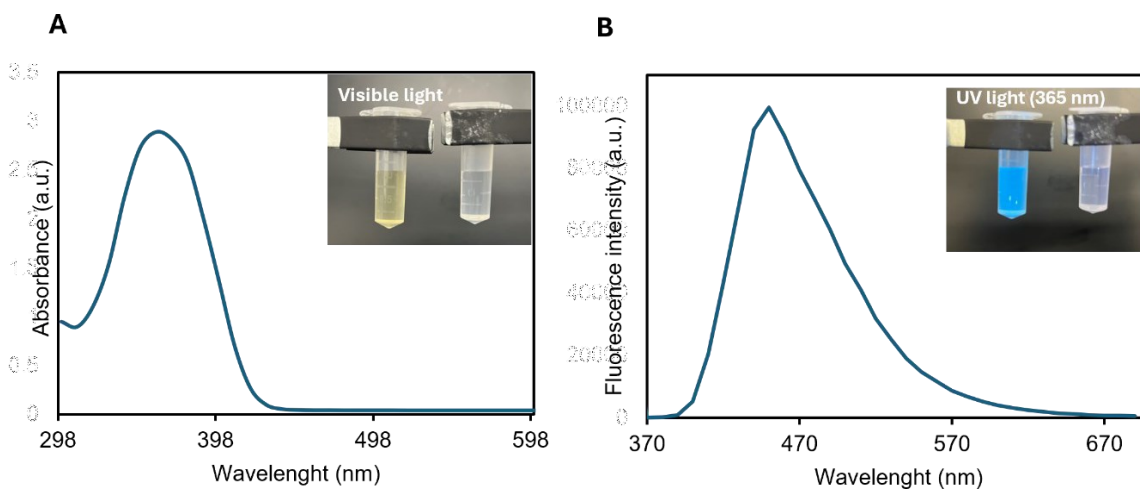
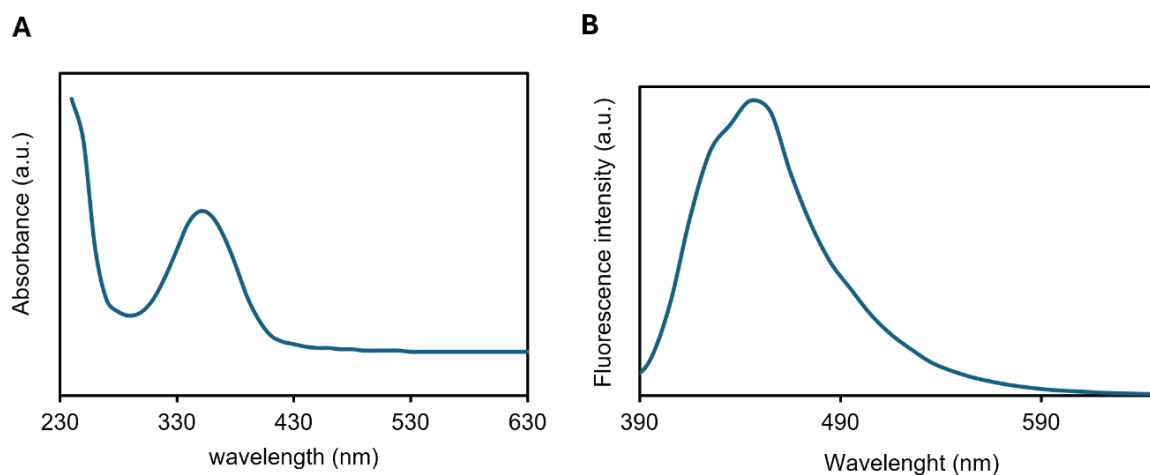


Figure A9. Optical properties of functionalized graphene quantum dots. **A.** The UV-Vis absorbance was measured using a UV-Vis spectrophotometer (BioTek Cytation 5, imaging reader) with a 1 cm quartz cuvette. The absorption spectra were recorded over a range of 298–800 nm. **B.** Fluorescence spectra. All fluorescence data were collected at an excitation wavelength (λ_{ex}) of 365 nm, with emissions measured from 230 to 800 nm at 1 nm intervals. Data were processed using Excel

C.4 Synthesis of pentaethylenhexamine (PH6-CDs)

The CDs were synthesized using [231] a CEM Discover SP microwave reactor. First, for CDs, 0.384 g (500 mM) of citric acid was added to 4 mL of distilled water and 375 mM of the amine passivating agent in a microwave reaction tube. The amine passivating agents used were ethylenediamine (ED2), diethyltriamine (DT3), tetraethylenetriamine (TT4), tetraethylenepentamine (TP5), and pentaethylenhexamine (PH6). The solutions were sonicated for 15 minutes, or until a homogenous solution was observed. The mixed solutions were then heated to 210 °C for 10 minutes. After the reactions were complete, they were dialyzed in Milli-Q water using a cellulose dialysis membrane (molecular weight cut-off = 3.5–5.0 kDa) to remove excess material. The samples were dialyzed for 5 days, and the water was changed twice per day. A decrease in colour



correlated with the removal of unwanted products. The samples were then purified by washing twice with acetone and twice with ethanol. After each wash, the precipitate was collected by centrifugation at 10 000 rpm \times for 10 minutes, and the supernatant was discarded. The remaining precipitate was left to dry for 12 to 24 hours in an oven at 80 °C, then crushed into a fine powder

and resuspend in ultrapure water. Finally, for biological purposes and to prevent contamination, the resuspended materials were filtered through a 0.22 μm nylon filter.

Figure A10. Optical properties of amine-passivated CDs. **A.** The UV-Vis absorbance of the PH6-CDs was measured using a UV-Vis spectrophotometer (BioTek Cytation 5, imaging reader) with a 1 cm quartz cuvette. The absorption spectra were recorded over a range of 230–800 nm. **B.** Fluorescence spectra of the PH6-CDs were obtained by setting the excitation wavelength (λ_{ex}) to 350 nm, with emissions measured from 230 to 800 nm at 1 nm intervals. Data was processed using Excel.

C.5 Heavy metal quenching assays

1 mg of CDs were measured into a 20 mL vial and diluted to create a 10 $\mu\text{g/mL}$ dispersion of PH6-CDs. This solution was vortexed for 30 seconds and sonicated for 2 minutes to prevent aggregation. 100 nM concentration of heavy metal ions (Pb^{+3} , Cu^{+2} , Fe^{+3} , Co^{+2} , Hg^{+2} and Ca^{+2}) were added to the cuvette. This solution was stirred for 20 seconds prior to acquiring fluorescence measurements and the fluorescence intensity (Figure A8. A). Endpoint fluorescence was collected at an excitation wavelength of 350 nm and emission wavelength of 455 nm. The metals showed a potential ability for quenching the CDs. Pre-mixed solutions of two metal ions, Pb^{+3} , Cu^{+2} , showed higher quenching abilities among other metals. The results were demonstrated in Figure A8 B.

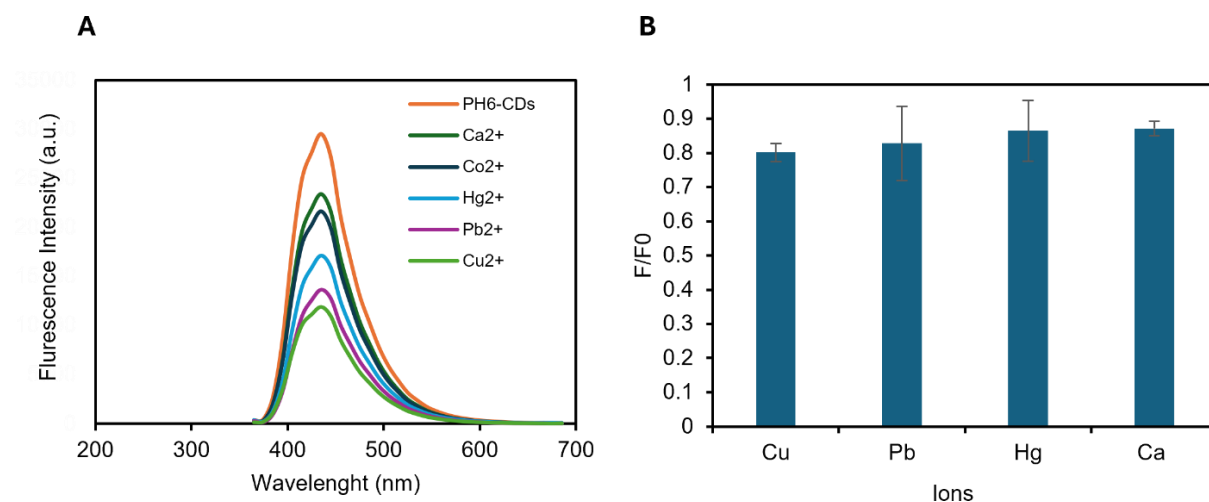
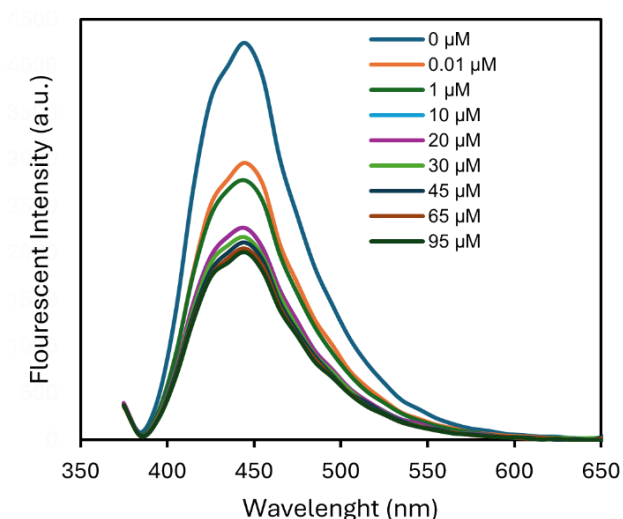


Figure A11. Heavy metal monitoring using 10 $\mu\text{g/mL}$ dispersion of PH6-CDs. **A.** A concentration of 100 nM of Pb^{3+} , Cu^{2+} , Fe^{3+} , Co^{2+} , Hg^{2+} , and Ca^{2+} was added to the cuvette and measured for



fluorescence intensity. Fluorescence data were collected at an excitation wavelength (λ_{ex}) of 350 nm at 1 nm intervals. **B.** Endpoint fluorescence results were recorded for Pb^{3+} , Cu^{2+} , Hg^{2+} , and Ca^{2+} (100 nM) at $\lambda_{\text{ex}} = 350$ nm and $\lambda_{\text{em}} = 455$ nm.

Figure A12. Quantitation of Cu^{+2} through fluorescence spectroscopy in the range 0-95 μM using a 10 $\mu\text{g/mL}$ dispersion of PH6-CDs. Fluorescence data were collected at an excitation wavelength (λ_{ex}) of 350 nm at 1 nm intervals.

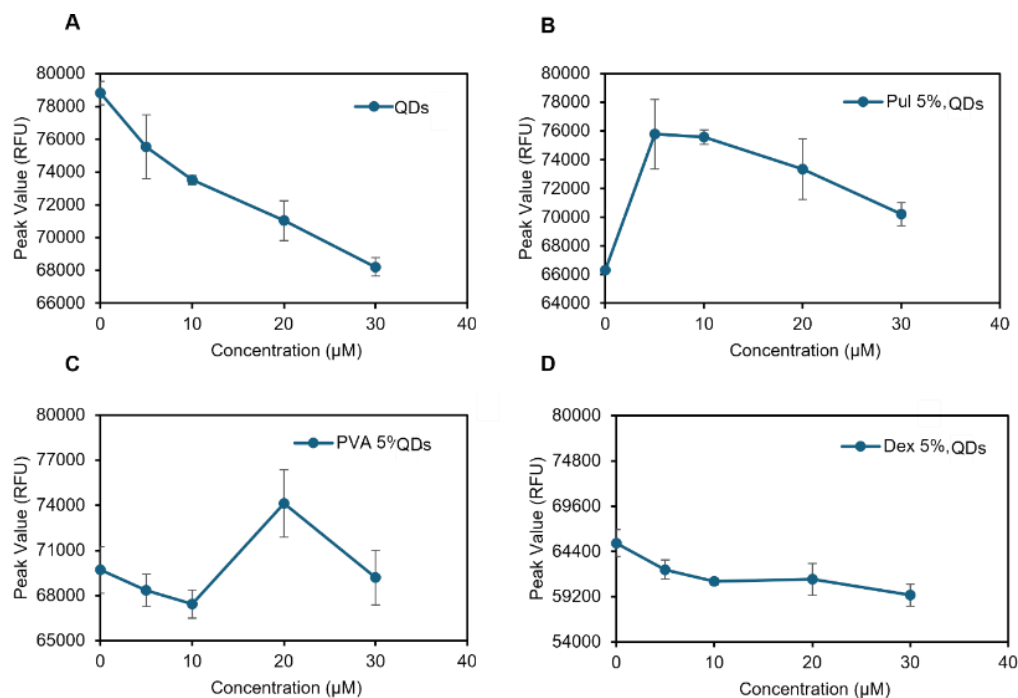


Figure A13. The figures compare the effect of adding different types of polymers on heavy metal detection using functionalized graphene quantum dots (A). Polymers, including dextran(B) pullulan(C), and polyvinyl alcohol (PVA) (D), were added at a concentration of 5% w/v to the quantum dot solution. The solutions were then added to the cuvette, and fluorescence intensity was

measured. Fluorescence data were collected at an λ_{ex} of 365 nm at 1 nm intervals. Data was processed using Excel. As shown, the addition of polymers interfered with metal ion detection.

C.6 Fluorescence portable platforms; QDs paper-based plate and QDs tablet-based

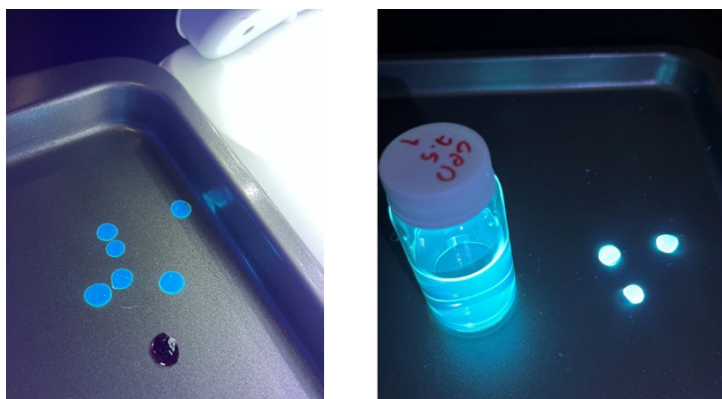


Figure A14. 2% pullulan solution was used to mix with QDs and investigate their physical characteristics on a tablet platform containing QDs. The polysaccharide was freshly mixed with a CD solution. The mixture was then thoroughly mixed, and 100 μL was pipetted onto the tray and left to dry at room temperature.

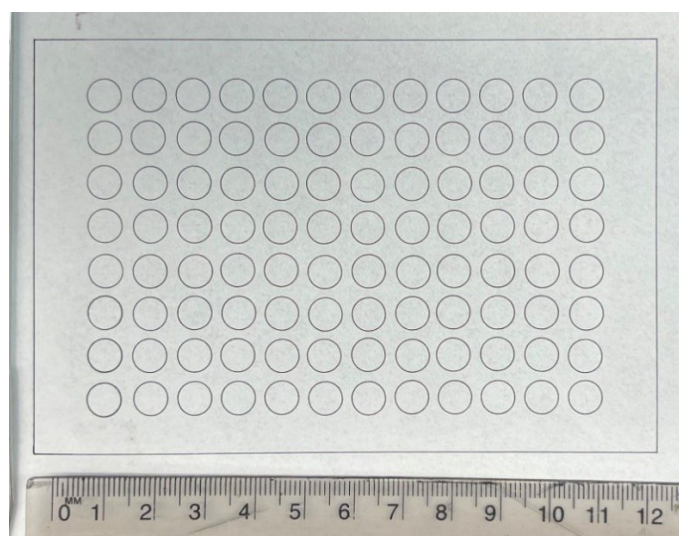


Figure A15. Creating paper-plate. To analyze the potential of using carbon dots (CDs) in a paper-plate platform sensor, the platform was first designed using inkscape software then they were fabricated via the PHLC method by first laminating the filter papers by thermal bonding of Parafilm in an oven and then laser ablation of the patterns on the paper side. In order to get a robust bonding and uniform lamination, we optimized the process in terms of temperature (80–140 °C), duration of heating (5–60 minutes), and cooling (at room temperature or slow cooling in the oven). We found 90 °C and 30 minutes with cooling at room temperature (~2 minutes) gave proper lamination.

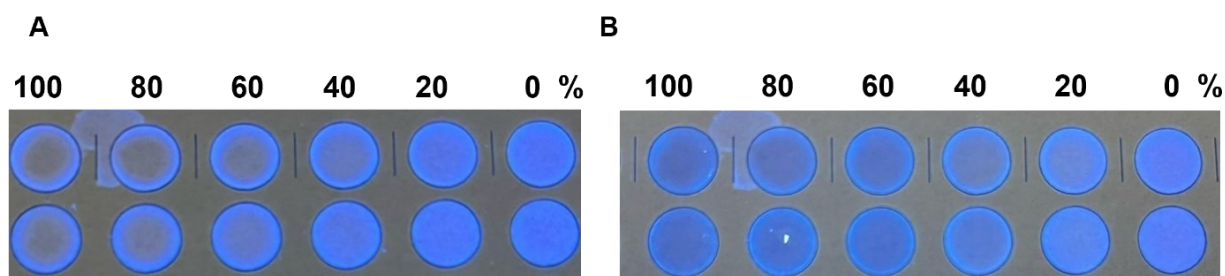


Figure A16. Testing acetone percentages on paper-based plate embedded with dried QDs on paper. (A) 10 μ L of solution was added to each well and left to dry at room temperature. Different percentages of acetone (0-100%) were added to the dried QDs on paper, and the photo was captured immediately, before drying (A) and after acetone dried (B).